Fall 2020

Therapeutic DNA: Delivery and as a delivery vehicle

Natalie J. Holl

Department:

THERAPEUTIC DNA: DELIVERY AND AS A DELIVERY VEHICLE

by

NATALIE JORDAN HOLL

A THESIS

Presented to the Graduate Faculty of the

MISSOURI UNIVERSITY OF SCIENCE AND TECHNOLOGY

In Partial Fulfillment of the Requirements for the Degree

MASTER OF SCIENCE IN APPLIED AND ENVIRONMENTAL BIOLOGY

2020

Approved by:

Yue-Wern Huang, Advisor
Risheng Wang
Katie B. Shannon

PUBLICATION THESIS OPTION

This thesis consists of the following two articles, formatted in the style used by the Missouri University of Science and Technology:

Paper I, Evolutionary Timeline of Genetic Delivery and Gene Therapy, found on pages 4–64, has been submitted to *Current Gene Therapy*.

Paper II, DOX-loaded DNA Origami Triangle Uptake and Cytotoxic Effects in Triple Negative Breast Cancer Cell Lines, found on pages 65–109, is intended for submission to *Cells*.

ABSTRACT

A review of gene delivery methods and gene editing methods, as well as original research utilizing DNA as a delivery vehicle is presented in the following thesis. Thousands of diseases have been linked to genes. Gene therapy, either delivering therapeutic genes or editing DNA bases, has arisen as a treatment option with the potential to cure diseases, rather than just ease symptoms. Genes and editing tools need to be delivered to cells for these therapies to be effective and many techniques have been developed to address the issue of delivery. Nonviral and viral methods have been used to deliver nucleic acids and several different protein systems have been employed to edit genes. Gene therapy will continue to evolve as delivery are improved. Along with being delivered as a therapeutic molecule, DNA has been investigated as a carrier itself. DNA origami, have been utilized to deliver chemotherapies to breast cancer. Globally, millions of women are affected by breast cancer each year. DNA origami was analyzed as a carrier for the chemotherapy Doxorubicin (DOX) in two triple negative breast cancer (TNBC) cell lines, a type of breast cancer with few treatments. The killing efficiency and uptake of DOX loaded into a model DNA origami triangle (DOX-DNA-T) were elucidated. Inhibition of various pathways revealed DOX-DNA-T was internalization by multiple energy-dependent pathways. DOX-DNA-T altered the subcellular localization of DOX and increased the concentration of DOX inside cells. A delayed killing was observed with DOX-DNA-T compared to free DOX, but the carrier was able to modulate the toxicity between cell lines. Overall, DNA delivery is able to treat various disease conditions and DNA origami is an interesting carrier for therapeutics.

ACKNOWLEDGMENTS

I would would like to acknowledge the support received from all the individuals I worked with during my master's, my department, and grants. I'm especially appreciative of Dr. Yue-Wern Huang, my advisor, for his support and mentorship, as well as my other committee members Dr. Katie Shannon and Dr. Risheng Wang.

I'd like to thank Dr. Katie Shannon and Brad Bromley whose help and guidance allowed me complete experiments using confocal micrscopy. To all of the undergraduate students who helped perform experiments and offered moral support, namely Chandler Mossman, Milan Chandra, Taryn Dewey, and Rachel Nixon, thank you for volunterring your time and efforts. I'm also thankful for Dr. Matt Thimgan, who was always able to encourage me, and the experimental advice from Dr. Han-Jung Lee and Dr. Stephen Hou.

Missouri S&T Biological Sciences Department provided two semesters of academic support through a graduate teaching assistanceship in the Cell Biology Laboratory course. I am appreciateive of this support as well as the time I was able to spend with Mrs. Terry Wilson, who was a source of guidance as a teacher and leader. The Biological Sciences Department also supplied a $500 award for research funding, which was appreciated. Two semesters of my master's were supported finicially through graduate research assistanceships. I'm grateful for the opportunity to receive support from a Missouri S&T Center for Research in Energy and Environment internal seed grant and the National Science Foundation.

Finally, I'd like to acknowledge the unending support and encouragement I've received from my mom, Kim Holl, who's always been there when I needed her.

TABLE OF CONTENTS

LIST OF ILLUSTRATIONS

PAPER I Page

PAPER II

LIST OF TABLES

NOMENCLATURE

Symbol	Description
CPPs	cell-penetrating peptides
ZFNs	zinc finger nucleases
TALENs	transcription activator-like effector nucleases
CRISPR	clustered regularly interspaced short palindromic repeats
Cas	CRISPR-associated protein
DOPE	dioleoylphosphatidylethanolamine
PEG	polyethylene glycol
PTDs	protein transduction domains
CPT	covalent protein transduction
NPT	noncovalent protein transduction
siRNA	small interfering RNA
sgRNA	single-guide RNA
AV	adenovirus
AAV	adeno-associated virus
cDNA	complementary DNA
LTR	long terminal repeat
SIN	self-inactivating
LV	lentivirus
HSC	hematopoietic stem cells
DSB	double strand break

HDR	homology-directed repair
NHEJ	non-homologous end joining
BE	base editor
RNAi	RNA interference
TNBC	triple negative breast cancer
DOX	Doxorubicin
DNA-T	triangle DNA origami
DOX-DNA-T	DOX-loaded DNA-T

SECTION

1. INTRODUCTION

Here, a review of DNA delivery and genome editing techniques are presented, as well as original research over the uptake and cytotoxicity of DNA nanostructures, also known as DNA origami. The original research has the potential to improve the therapeutic efficacy of DNA origami as a carrier system.

Predisposition to and development of certain diseases have been linked with specific genes [1]. Many genetic diseases are due to simple mutations in one gene, such as sickle cell anemia, cystic fibrosis, and Huntington's disease [2-4]. Historically, genetic diseases have not been able to be cured, with symptoms only being able to be modulated with drugs. Traditional protein and small molecule drugs used to treat genetic diseases often have pharmacokinetic issues [1]. However, with current technology, these diseases can be cured by supplying diseased cells with functional genes or correcting a mutated gene.

DNA, the material encoding all of instructions required for life, has been utilized as a therapeutic molecule and more recently to deliver other therapies to cells. Delivery of compounds across target cell membranes is essential for function inside cells. Nucleic acid and therapeutic molecule delivery have been achieved using a variety of different methods. However, delivery methods are constantly improving and the optimal carriers for different systems are still sought.

Many methods have been developed in an attempt to deliver therapeutic nucleic acids or genome editing tools for genome correcting, each with varying effectivity, cytotoxicity, immunogenicity, and sustainable effects [1, 5]. Delivery strategies fall into two main categories: viral and nonviral. Nonviral methods rely on physical (microinjection, bioballistics, hydrodynamic force, ultrasonic nebulization, and electroporation) or chemical (calcium phosphate co-precipitation, lipofection, and cell-penetrating peptides) cell membrane infiltration [5-13]. A variety of viruses have also been used for delivery and to overcome the cell membrane, including adenoviruses, adeno-associated viruses, and retroviruses [14]. Zinc finger nucleases (ZFNs), transcription activator-like effector nucleases (TALENs), and CRISPR-Cas systems have been utilized to target and correct defective genes after delivery into cells [1]. These subjects are further reviewed in Paper I.

Our understanding of DNA has allowed us to develop methods to reprogram cells, including technologies that can edit genes. Our ability to program DNA also gave rise to a method to fold the nucleic acid into new and accurate shapes in 2006 [15, 16]. Most nanostructures and nanoparticles used for delivery are not programmable; it can be difficult to control their size uniformly and their shapes are often limited to spheres [17]. The geometry of nanostructures can affect their biodistribution, their movement through fluids, and their cellular internalization [17]. The use of DNA allows for high precision design of geometry and easy functionalization [15, 18]. The design and flexibility of DNA nanostructures, or DNA origami, is optimal for a drug carrier system. However, degradation in vivo by endogenous endonucleases is a large concern [16].

DNA origami has been utilized for chemotherapy delivery and cancer treatment. Millions of women are diagnosed each year with breast cancer [19]. Triple negative breast cancers (TNBCs), a particularly devastating form of breast cancer [20, 21], lack treatment options because they do not respond to frequently used cancer therapies [22]. Often, harsh nonspecific chemotherapies are used in combination with surgery [21, 23, 24]. One such chemotherapy is Doxorubicin (DOX) [25]. DNA origami has been used to delivery DOX to cancer cells, as DOX intercalates into the DNA double helix [25, 26]. These nanostructures have been shown to have high passive accumulation within tumors and increase drug delivery to the tumor site [18, 27]. Using nanocarriers to directly deliver drugs to tumors can increase retention time to combat drug resistance and can reduce overall toxicity in patients [15, 28, 29].

Although DNA origami have been used for the delivery of chemotherapeutic drugs, their exact uptake mechanism is not entirely understood, an important aspect which influences drug delivery efficacy. Paper II discusses original research utilizing DNA origami to deliver DOX to breast cancer cells. The killing efficiency, uptake mechanism, and subcellular localization of a model DNA origami triangle were determined in two TNBC cell lines. It was found that DNA nanostructures facilitate drug entry, have delayed toxicity and release of drugs, and are internalized by energy-dependent pathways. Localization was time- and concentration-dependent.

PAPER

I. EVOLUTIONARY TIMELINE OF GENETIC DELIVERY AND GENE THERAPY

Natalie J. Holl[a], Han-Jung Lee[b], and Yue-Wern Huang[a,*]

[a]Department of Biological Sciences, College of Arts, Sciences, and Business, Missouri University of Science and Technology, Rolla, MO 65409, USA;

[b]Department of Natural Resources and Environmental Studies, College of Environmental Studies, National Dong Hwa University, Hualien 97401, Taiwan

ABSTRACT

There are more than 3,500 genes that are being linked to hereditary diseases or correlated with elevated risk of certain illnesses. As an alternative to conventional treatments with small molecule drugs, gene therapy has arisen as an effective treatment with the potential to not just alleviate disease conditions but also to possibly cure them completely. In order for these treatment regimens to work, genes or editing tools intended to correct diseased genetic material must be efficiently delivered to target sites. There have been many techniques developed to achieve such a goal. In this article, we systematically review a variety of gene delivery and therapy methods that include physical methods, chemical and biochemical methods, viral methods, and genome editing. We discuss their historical discovery, mechanisms, advantages, limitations, safety, and perspective.

1. INTRODUCTION

Hereditary diseases and disease predisposition have been associated with particular genes. Over 3,000 genes have been linked to hereditary illnesses and around 500 have been identified that increase risk for certain diseases [1]. For example, cystic fibrosis is a recessive illness occurring in individuals carrying two copies of a mutant CFTR (cystic fibrosis transmembrane conductance regulator) gene [2]. Patients carrying two recessive β-globin genes with a single base substitution present with sickle cell anemia [3] and patients with one copy of a dominant mutation in the huntingtin (HTT) gene develop Huntington's disease [4]. Historically, these diseases are not curable and symptoms can only be managed. Some treatments, such as proteins and small molecules, are difficult to apply due to bioavailability, stability, specific targeting, and other pharmacokinetics issues [1].

The idea of gene therapy first arose in the 1970s [5]. Initial applications focused on gene replacement therapy to treat inherited disorders by supplying target cells with a copy of a normal gene. In the last fifty years, these delivered treatments have advanced to include protein-coding cDNA sequences and non-coding small nucleic acids that regulate a broad spectrum of cellular behaviors and functions. Both of which are becoming mainstream therapies and hold tremendous potential in revolutionizing medicine. In addition to replacing a target gene, protein-coding cDNAs are being widely used to manipulate neurotrophic factors in neurodegenerative diseases such as Parkinson's and Alzheimer's diseases, modulate regulatory proteins that involve cell survival and apoptosis of cancer, produce angiogenic factors in cardiac ischemia, and immune-

modulate HIV and other immune diseases [6]. In the past decade, non-coding small nucleic acids represent a new shift of paradigm in gene therapy. Non-coding nucleic acids include oligonucleotides, catalytic RNAs or DNAs, antisense RNAs, and aptamers. These non-coding nucleic acids have been used to completely silence or partially regulate functions of certain genes to mitigate disease severity or progression in cancer, neurodegenerative diseases, and cardiovascular diseases, among others [7-9].

Missing genes may be added into cells using various techniques in order to combat illnesses [10-13]. Genome-editing technologies may be able to edit or replace defective genes and eliminate genetic diseases all together [1]. Genome editing is the key to advancing treatment of inheritable diseases and human medicine. In theory, these techniques sound simple. In reality, the development of genome editing is sophisticated and has experienced numerous setbacks. One of the most notable setbacks being the death of Jesse Gelsinger in 1999, the first death associated with gene therapy [14]. Gelsinger took part in an experimental gene therapy trial to treat a rare metabolic disorder known as ornithine transcarbamylase (OTC) deficiency. His body overreacted to the viral vector used and he died after multiple of his organ systems failed. His death shocked the research community and no gene therapy clinical trials relating to OTC were proposed until 2016 [15]. This clinical case is a manifestation that efficacy and safety are equally important in developing gene therapies.

In vitro and in vivo DNA deliveries are key to numerous aspects of life science research which include, but are not limited to, discovery of fundamental principles in biology (e.g., gene structure, regulation, and function), understanding the nature of human diseases (e.g., genetic defect and correction), and biomedical applications (e.g.,

gene therapy, drug delivery, and DNA vaccination). One of the major obstacles in DNA delivery is the mammalian cell membrane due to its non-polar and hydrophobic nature. Over the course of evolution, cells have survived by making their membranes selective. On one hand, selectivity allows for the efficient passage of nutrients, minerals, and other essential materials into cells for growth and removal of cellular wastes [16]. On the other hand, selectivity helps fend off harmful materials from entering into cells. Polyanions, such as nucleic acids, are poorly internalized but can be delivered into cells using various carriers and methods. Before the benefits of DNA therapy can be relished, inefficiency in delivery must be addressed.

Delivery of nucleic acids into mammalian cells can be generally divided into two main strategies: viral and nonviral delivery. Nonviral delivery tools can be based on physical methods or various classes of chemicals, such as cationic lipids, polymers, peptides, or carbohydrate analogs [17]. Physical nonviral methods discussed in this review encompass microinjection, bioballistics, hydrodynamic force, ultrasonic nebulization, and electroporation. Chemical and biochemical nonviral methods include calcium phosphate co-precipitation and membrane infiltration mediated by artificial lipids and peptides. Importantly, small delivery peptides, termed cell-penetrating peptides (CPPs), have gained great interest among these nonviral tools. Viral delivery of genetic material takes advantage of the natural life cycle of viruses, using viruses with modified or synthetic genomes to inject therapeutic genes into cells. Depending on the virus used, delivered genes may exist as a plasmid inside cells or be integrated into the host genome. Viral vectors discussed here include adenovirus, adeno-associated virus, gamma-retrovirus, and lentivirus.

Each delivery method has its benefits. Viral methods are efficient, but may cause adverse immune responses. Nonviral gene transfer is likely to be nonimmunogenic, but often suffers from lower transfection rates and toxic carriers. Nonviral methods of delivery also are often limited by transient transfection [5], with expression of delivered genetic material often only lasting for a short period due to low integration rates [18]. This is due to the low chance that plasmid DNA can enter the nucleus, with the only time period to enter being when nuclear membrane is destabilized (e.g., during replication) [19]. Integrating viral vectors have higher rates of transient transection than nonviral vectors; however, it should be noted that integration at random locations in the genome can result in mutagenesis and oncogenesis [1]. Nevertheless, the importance of viral vectors as a DNA delivery tool cannot be overlooked, as they have been a pivotal partner in revolutionary genetics, cell biology, molecular biology, and medical discoveries.

Genome editing, also known as gene editing, is defined as a group of technologies used to change an organism's genome according to the US National Institutes of Health (NIH) [20]. These technologies allow genetic material to be artificially added, removed, or altered at particular locations in the genome. Many strategies are currently available for programmable and targeted genome editing, including zinc finger nucleases (ZFNs) and transcription activator-like effector nucleases (TALENs). The clustered regularly interspaced short palindromic repeats (CRISPR)-CRISPR-associated protein (Cas) system is a next-generation genome editing technology, which is originally based on a system used by bacteria and archaea to combat recurrent viral infections.

The number of clinical trials involving gene therapy has steadily increased over the years, with approximately 2,600 trials up until 2017 [21]. The majority of clinical

trials use viral vectors, including adenovirus (20.5%), retrovirus (17.9%), adeno-associated virus (7.6%), lentivirus (7.3%), vaccinia virus (6.6%), poxvirus (4%), and herpes simplex virus (3.5%). Naked DNA (16.6%), often in combination with electroporation, and lipofection (4.4%) are the most common nonviral methods used in clinical trials [21]. It should be kept in mind that certain types of delivery methods will become more or less popular as techniques are refined, efficiency is fine-tuned, or new technologies are developed.

Here, historically important discoveries for gene transfection and gene editing methods are discussed, as well as method advantages and disadvantages. A timeline of significant milestones in gene delivery and gene therapy is provided in Figure 1.

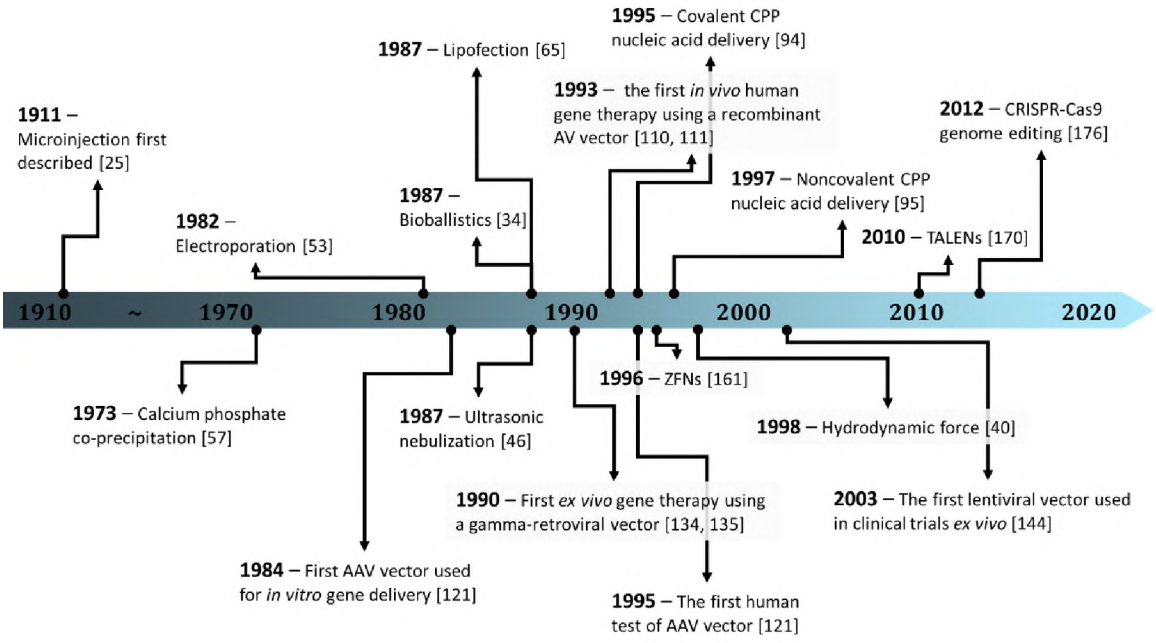

Figure 1. Significant milestones in gene delivery and gene therapy. Adeno-associated virus (AAV), adenovirus (AV), cell-penetrating peptide (CPP), zinc finger nuclease (ZFN), transcription activator-like effector nuclease (TALEN), clustered regularly interspaced short palindromic repeats (CRISPR), CRISPR-associated protein 9 (Cas9).

2. PHYSICAL METHODS

Physical methods of gene delivery act by directly penetrating or compromising the cell membrane in order for nucleic acids to pass into cells. They are some of the earliest methods of gene delivery, though cell viability and transfection efficiency for many of the techniques is lacking. Physical methods are diagramed in Figure 2.

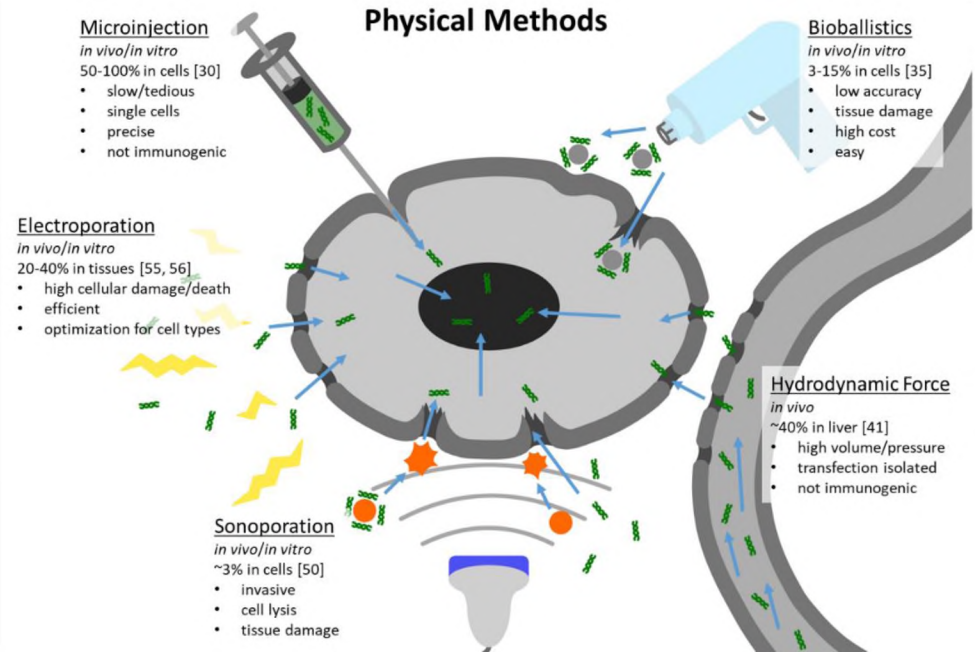

Figure 2. Physical methods of gene delivery. The cell membrane is compromised by different means in order to facilitate nucleic acid internalization. Microinjection, bioballistics, hydrodynamic force, ultrasonic nebulization (a.k.a. sonoporation), and electroporation are common physical delivery techniques.

2.1. MICROINJECTION

Microinjection, or the direct injection of genetic material into cells [22], was one of the first methods used to transform cells. It is a simple method, but delicate and

therefore difficult to carry out [23]. It does not rely on a carrier for DNA, making it not immunogenic or toxic [24]. Nucleic acids are injected into a single cell using a needle. DNA can then be localized to the nucleus after injection into the cytoplasm or be directly injected into the nucleus to transform a cell. Microinjection is perfect for cloning and single cell manipulation. The first cases of microinjection date back to 1911, when Marshall Barber used the technique to clone bacteria [25]. The first animal clones were created by transferring the whole nucleus of one embryonic frog cell to the oocyte of another in 1952 [26]. However, the older the transplanted nuclei, the less likely a normal tadpole was to develop. In 1974, microinjection was used to create the first transgenic animal by injecting viral DNA into a mouse blastocyst [27]. In the 1990s, regional transfection of tissue by DNA injection was demonstrated [18]. However, it was not until 1997 that adult cells were able to be used to create viable clones, resulting in the famous Dolly the sheep [26, 28]. Using small amounts of DNA, the technique is cost effective [29]. While efficiency is high when DNA is injected directly into the nucleus, transformation can be low if DNA is degraded by cytoplasmic nucleases [23]. A mouse cell line showed expression in 50 to 100% of cells given genes by direct nuclear injection [30]. The process can be slow and tedious when many cells are to be transformed [22]. On the other hand, the method is not dependent on cell type, so it can be used with cells that are difficult to transform [24]. Attentional benefits to this technique are the precise control of the amount of genetic material passed to cells and the surety that most cells treated will receive genetic material [31], with the nucleus receiving around 90% of fluid directly injected [30]. More recent advances in microinjection techniques have led to the development of devices used to inject multiple cells at once [32].

2.2. BIOBALLISTICS

One forceful method of genetic transduction is bioballistics. In this technique, a "gun" is used to accelerate metal particles covered in genetic material through cells [18]. Any particles that travel through the cells have a chance to leave behind the nucleic acids that were on the surface of the metal. Tungsten, silver, and gold particles are most commonly used as the carrier and are accelerated using pressurized inert gases or electric charges [18, 33]. The size and speed of the particles play a major role in the gene transfer efficiency [33]. Klein et al. first applied this method using plant cells in 1987 [18, 34]. The group used tungsten particles coated in nucleic acid and accelerated them using a gunpowder blast [34]. A downside to bioballistics is that if a cell is hit with a large number of particles, viability is reduced [34]. Low accuracy, tissue damage, and low efficiency [35], in part due to high DNA degradation [36], are also issues. Only around 3 to 15% of cells targeted with bioballistic gene transfer show high expression [35]. The cost of materials is also high [23], which can be a detriment to researchers if a large number of transformations must be performed. However, the method is relatively easy to carry out and stability of the carrier is not a concern [35]. The size and properties of the metal particles also enable them to deliver multiple or large DNA molecules that other methods may not [35]. A large concern from a toxicological perspective is that the ultimate fate of the particles is often not known [37]. Metal particles may oxidize in biological systems and result in unintended toxicity if they are not removed. Bioballistics can be applied to both organisms and cells [23]. Advances in this method resulted in the development of a hand-held gun, the Helios Gene Gun, which allowed in situ

transformation more easily [36]. Xia et al. used the Helios Gene Gun to transfect the skin and livers of mice with bioluminescent reporter genes [38].

2.3. HYDRODYNAMIC FORCE

Hydrodynamic force uses pressure in the circulatory system to increase the permeability of cells [18]. The first successful application of hydrodynamic force for gene delivery is attributed to Budker et al. in 1998 [39, 40]. This method was designed for use in vivo, originally in rodents, but has been used in various animals including rabbits, dogs, fish, pigs, monkeys, and humans [39]. Immunogenicity and toxicity of carriers are not a concern as naked DNA is used in solution [41]. A solution around 8 to 12% of the subject's body weight is injected quickly, in 5 to 7 seconds, to achieve the systemic pressure needed to facilitate nucleic acid uptake [39, 41]. Transfection rate is highly dependent on injection volume, injection time, and DNA concentration [41]. However, large injection volumes have been deemed unsafe for people [18] as too much fluid in the circulatory system can lead to cardiac arrest [39]. Along with this, large volumes of DNA may be difficult to cultivate for each individual injection. Due to the need for a pressurized system, this method is not applicable to individual cells [39]. Transfection also often accumulates in specific organs, especially the liver [41, 42]. Lui et al. showed that 40% of the hepatocytes of mice injected with plasmid DNA via the tail vein expressed a reporter gene, while the lung, kidney, spleen, and heart all had expression levels less than 1000-fold of the liver expression [41]. This makes the technique particularly useful for gene expression in specific organs, but not useful if expression is desired elsewhere. This method has been used to develop a mouse model of

hepatitis B infection, which normally is unable to infect rodents, by forcing viral genomes into mice hepatocytes [39, 42, 43]. One technique used to decrease injection volumes in animals larger than rodents is to use a balloon catheter to isolate a particular organ so pressure can be increased locally [44]. When balloon catheters where used to isolate the liver of pigs, injection volumes could be reduced from 10% to 1.25% of the individual's body weight [44]. This also allows organs and tissues with lower affinity for transfection in whole body injections to be targeted.

2.4. ULTRASONIC NEBULIZATION

Fecheimer et al. were the first to demonstrate cells transfection using ultrasonic nebulization, also known as sonoporation, in 1987 [45, 46]. This method relies on the formation of pores in cell membranes by ultrasonic waves [33]. The intensity and frequency of the ultrasonic waves used, as well as tissue type, determine the biological effects [18]. Typically, ultrasound in the 2 to 20 MHz range, with maximum intensities limited to 720 mW/cm2 by the US Food and Drug Administration (FDA) [47], is used for medical imagining [48]. However, only 1 to 3 MHz, with higher intensities ranging from 0.5 to 2.5 W/cm2, are used for gene delivery [18]. Initial studies demonstrated sonoporation using 20 kHz [48]. Ultrasound can result in heating and cavitation within tissues, depending on the intensity of the waves [48]. Cavitation can concentrate ultrasonic energy and occurs when ultrasound waves produce and interact with microbubbles in solution, resulting in wave deflection, resonance frequency vibration of bubbles, and bubble imploding [45, 48]. Cavitation of microbubbles causes mechanical damage in cells and tissues, which can be observed as pore formation or cell lysis [48].

The utilization of ultrasound in gene delivery was dramatically improved by combining ultrasound wave application with injected microbubbles in the mid-1990s [18, 45]. The addition of microbubbles "lowers the threshold for cavitation," [45], as bubbles do not need to be generated. Injected microbubbles are gas-filled vesicles with a shell that can be composed of various substances, including phospholipids, proteins, and polymers [18], and can vary between 1 to 10 μm in diameter [45]. Clinically, microbubbles are routinely used as contrast agents for ultrasonic imaging [45]. During gene transfection, DNA can be injected as a solution or integrated into microbubbles [33]. Ultrasound is applied to a target location, limiting where cavitation occurs. Sonoporation has potential for in vivo applications as it is noninvasive [45]. Ultrasound and site-injected phospholipid microbubbles were able to successfully transfer a luciferase reporter gene into mouse muscle tissue [49]. However, despite the potential applications, ultrasound has not been applied for clinical gene therapy, due to low efficiency and high cell death [45]. Primary rat cells treated with ultrasound only showed a 2.4% transient transfection rate and a 0.3% stable transfection rate, with only 50% of cells surviving the process [50].

2.5. ELECTROPORATION

It has been known that electricity alters membrane permeability since the 1960s [18]. Electric fields can result in the formation of membrane pores, cell fusion, and cell movement [51]. When electric pulses are applied to cells, the pores formed allow nucleic acids to move across the plasma membrane [51]. The electric field causes the cell membrane to polarize and breakdown temporarily [33]. Timing and intensity of the electric pulses, as well as buffers, affect the delivery of nucleic acids [51].

Electroporation parameters must be optimized for individual cell types because if the intensity used is too high, cell membranes may not be able to close [51, 52]. Applying electric pulses to cells can result in death, in part due to membranes no being able to seal [22]. Different cell types are more effectively transformed with specific pulse length and strength [33]. It can be time consuming to determine the best buffers and electric intensity to use for various cell types [52]. However, the technique is useful for cells that are hard to transform, such as T cells, hMSC, and HUVECs, and is efficient when low cell viability is not a concern [51]. Electricity was first applied for genetic transformation in 1982 in mouse lyoma cells by Neumann et al. [53], who coined term for electroporation [51]. In 1991, the first in vivo transformation using electroporation was demonstrated with mouse skin cells [18, 54]. In this process, a target location in the body is injected with DNA. Electrodes are then used to apply pulses of electricity to induce cell membrane permeability [18]. The efficiency is dependent on the distribution of the electric field, which may be altered by electrode type and placement [51]. This method has been demonstrated locally in the testis and eyes of mice and the forebrain of zebrafish [51]. When DNA was directly injected into rat livers and treated with electric pulses, 30 to 40% of hepatocytes expressed a reporter gene [55]. Additionally, Heller et al. reported that 20 to 30% of skin cells expressed a luciferase gene after transfection using electroporation [56]. However, ability to access different organs noninvasively with electrodes in vivo limits its applications [18].

3. CHEMICAL AND BIOCHEMICAL METHODS

Chemical and biochemical methods of gene transfection involve complexing nucleic acids with organic or inorganic compounds to facilitate cellular uptake. Complexes interact with the cell surface and cell membrane molecules to induce endocytosis or internalization. Chemical methods are diagramed in Figure 3.

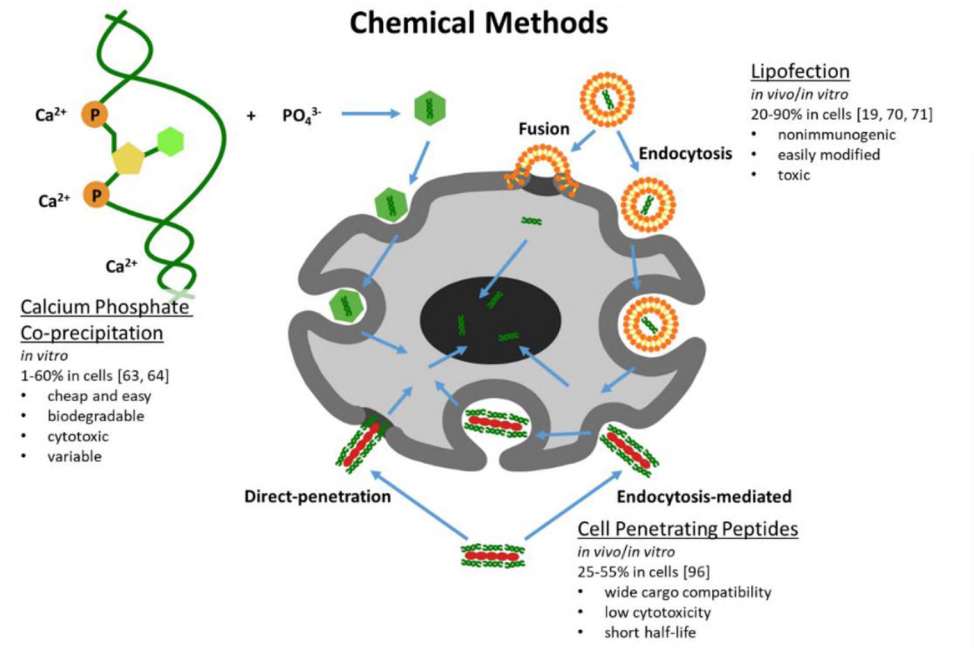

Figure 3. Chemical methods of gene delivery. Chemical methods complex with nucleic acids and mediate uptake by interacting with the cell membrane. Calcium phosphate co-precipitation, as well as peptide and lipid carriers, are commonly used chemical transfection methods.

3.1. CALCIUM PHOSPHATE CO-PRECIPITATION

Calcium phosphate co-precipitation was first described by Frank Graham and A.J. van der Eb in 1973 [22, 57]. This method utilizes the phosphates lining the backbone of

nucleic acids. A stable ionic complex is formed between the backbone phosphates and divalent metal cations, originally Ca2+ but Mg2+, Ba2+, and Mn2+ have also been used in similar co-precipitations [58]. The ion-DNA phosphate complex can be endocytosed by cells after coming in contact with the cell surface [22]. To form and precipitate complexes, phosphate buffered saline is added to a mixture of DNA and calcium chloride in solution [59]. Precipitates used for gene delivery usually range in size from 10 to 100 nm [59]. The method is relatively cheap, easy to carry out [24], and benefits from the biodegradability of calcium phosphate [59]. It can be used with many cell types and is often used when transfecting large numbers of cells [24]. However, cytotoxicity is a concern as intracellular calcium levels are generally low [22, 59]. Increased intracellular calcium levels could be a particular issue for muscle cell transfection, as calcium ions regulate muscle contraction [60]. Ca2+ membrane pumps may be able to mitigate calcium toxicity by pushing excess Ca2+ outside of cells [61]. Results from calcium phosphate co-precipitation can be highly variable due to differences in complex size [22]. Transfection efficiency is controlled by the cell type and the precipitation conditions, including calcium chloride and DNA concentration, pH, temperature, and crystal growth time [59]. Smaller precipitates show higher transfection rates than larger particles [62]. As such, precipitates are not able to transfect cells if they are stored for long periods due to nanocrystals growing into microcrystals [33, 59]. Jordan et al. demonstrated transfection efficiencies of approximately 60% in CHO cells and approximately 40% in HEK-293 cells using small particles, but efficiencies dropped to 3 to 5% when large particles were used [63]. The variation in transfection efficiency between cell types is also apparent, as transfection efficiency in neuronal cells is generally low, ranging from 1

to 5% [64]. Efficiency variation and low reproducibility may be due to rapid nucleation and growth of the particles [61]. This method is difficult to apply in vivo [22, 58], in part due to "poor colloidal stability and uncontrolled growth" [61]. However, calcium phosphate precipitates modified with polymer and lipid coatings have shown promise for in vivo delivery [61]. Roy et al. modified calcium phosphate precipitates with a polymer and a targeting ligand to increase gene delivery to liver cells in mice by 400 to 500% compared to unmodified particles [58].

3.2. LIPOFECTION

Gene transfection using lipids, also called lipofection, is one of the most used nonviral methods for genetic transfer [18]. Lipofection was developed and first demonstrated by Felgner et al. in 1987 [52, 65]. A variety of lipids are used in lipofection but most are cationic and amphiphilic, generally being composed of a hydrophilic amine head, linker, and hydrophobic hydrocarbon tail [66]. These lipids form micelles and liposomes when placed in aqueous solutions, with hydrophobic tails associating together and hydrophilic heads interacting with the environment [66]. Negatively charged DNA can be electrostatically complexed to the positively charged anime head of the lipids; the complexes are often referred to as lipoplexes [66]. DNA is protected from nucleases in the lipoplex as the nucleic acid becomes surrounded in lipids [18]. Additionally, positively charged heads are able to interact with the negatively charged cell membrane molecules, such as proteoglycans and glycoproteins, mediating internalization [18]. Lipoplexes can be endocytosed or can merge into the cell membrane, depending on the properties of the lipids and cells used [67]. Since lipids are basic components of cell

membranes, lipofection is nonimmunogenic [66]. The lipids are easily modified to improve efficiency [66]. "Helper" lipids, such as dioleoylphosphatidylethanolamine (DOPE) or cholesterol, can be included in the lipoplex mixture to improve gene delivery [66]. Lipid composition and the ratios of helper lipids can be optimized to improve efficiency for specific cell lines [19]. Functional groups, such as polyethylene glycol (PEG), may also be added [66]. Transfection efficiency is influenced greatly by the size of the lipoplex [68]. Larger lipoplexes are more efficient at delivering DNA in vitro [69]. However, larger lipoplexes are cleared from the blood faster than smaller ones in vivo [68]. The type of lipids used, lipid and DNA concentration, and transfection media also affect delivery efficiency [69]. One of the most commonly used and commercially available lipids for transfection is lipofectamine [19, 70, 71]. Using Lipofectamine® 2000, Dalby et al. showed transfection in 20 to 30% of primary rat neurons [70]. However, lipofectamine and other lipoplexes can be toxic. For example, lipofectamine and several lipoplexes containing helper lipids reduced the viability of A549 and H1299 cells by around 20% [71]. Kulkarni et al. treated primary chicken embryonic cells with lipofectamine and saw only 33% cell survival, with around a 50% transfection rate [19]. The group was able to increase survival to 85% and transfection to 90% in the same cells by modifying the ratios and composition of the lipids used.

3.3. CELL-PENETRATING PEPTIDES (CPPs)

3.3.1. Introduction to CPPs. CPPs, also known as protein transduction domains (PTDs), Trojan peptides, or membrane transduction peptides, are short peptides generally containing 5 to 30 amino acids [17, 72-75]. They are characterized by their remarkable

ability to translocate through plasma membranes and enter into cells, tissues, and even organisms [76, 77]. CPPs possess the ability to traverse biological membranes efficiently in a process termed protein transduction [78]. Importantly, CPPs are capable of transporting numerous cargo molecules, such as DNA, RNA, oligonucleotides, liposomes, proteins, and nanoparticles, both in vitro and in vivo [73, 76, 77].

CPPs have very different origins and are ambiguous in many ways [17]. CPPs may originate from naturally occurring peptides in living organisms, chimeric peptides from naturally modified proteins, and synthetic peptides from design [73]. Many early CPPs were identified from naturally occurring protein sequences that were found to possess membrane-translocating properties. The first protein discovered to translocate into the nucleus was the HIV-1 transcription-transactivating (Tat) protein, demonstrated by Frankel and Pabo in 1988, with the minimal sequence being isolated in 1997 [79]. Penetratin, a 16-residue CPP isolated from the Drosophila Antennapedia (ANTP) homeodomain, was discovered in 1994 [79]. Protein/peptide engineering has developed a combination of domains with different properties to generate chimeric CPPs. Subsequently, growing knowledge based on the identified properties of CPPs has led to the development of novel CPPs with completely designed sequences. Based on their physicochemical properties, CPPs may be classified as cationic peptides with positively charged surfaces, hydrophobic peptides with high hydrophobic amino acid content, or amphipathic peptides with both hydrophobic and hydrophilic fragments [73]. As summarized in Table 1, independent of CPP origin or classification, several algorithms have recently been built to allow for prediction of amino acid sequences that potentially have translocating properties [80-91].

Intracellular delivery of various cargos is mediated by binding to CPPs either covalently or noncovalently [17, 72, 76]. CPPs can be directly attached to their cargo molecules through covalent linkage, termed covalent protein transduction (CPT). However, CPT involves relatively expensive and labor-intensive synthesis, and may not be suitable for the delivery of nucleic acids and nanoparticles. Noncovalent protein transduction (NPT) utilizes noncovalent association, such as electrostatic interactions and hydrophobic effects, between CPPs and cargo molecules. The major advantages of NPT over CPT are simplicity of preparation, cargo versatility, and low working concentrations, which possibly contribute to reduced toxicity. However, NPT may suffer from premature dissociation of cargos from CPPs and off-target effects within cells due to the relatively weak interacting forces between CPPs and cargos.

Table 1. Predictors of cell-penetrating peptides.

Name	Website	Reference
CPPsite 2.0	http://crdd.osdd.net/raghava/cppsite/	[80]
CPPpred	http://bioware.ucd.ie/~compass/biowareweb/Server_pages/cpppred.php	[81]
KELM-CPPpred	http://sairam.people.iitgn.ac.in/KELM-CPPpred.html	[82]
CellPPD	http://crdd.osdd.net/raghava/cellppd/submission.php	[83]
C2Pred	http://lin-group.cn/server/C2Pred	[84]
CPPred-RF	http://server.malab.cn/CPPred-RF/	[85]
SkipCPP-Pred	http://server.malab.cn/SkipCPP-Pred/Index.html	[86]
MLCPP	http://www.thegleelab.org/MLCPPExample.html	[87]
CPPred-FL	http://server.malab.cn/CPPred-FL/	[88]
G-DipC	N/A	[89]
StackCPPred	https://github.com/Excelsior511/StackCPPred	[90]
TargetCPP	N/A	[91]

N/A: not available

3.3.2. Mechanisms of CPP Action. Due to their inherent ability to cross plasma membranes, CPPs have been employed extensively to facilitate the transport of cargo molecules into cells. However, the detailed cellular uptake mechanism of CPPs is not

well understood. Generally, it is accepted now that CPPs and CPP-cargo complexes are predominantly internalized into cells by two main pathways: endocytosis and direct translocation [17, 76, 77, 92]. However, the exact cellular uptake mechanism of CPPs and CPP-cargo complexes is determined by numerous factors, such as the amino acid sequences of CPPs (hydrophobicity and net charge), extracellular concentration of CPPs, cargo properties, cell type, and the assay temperature [92]. No matter what mechanism, the electrostatic interactions between the positively charged residues of CPPs and negatively charged glycosaminoglycans, especially heparan sulfate proteoglycans, of the membrane are the first crucial step for cellular uptake of CPPs and CPP-cargo complexes [92].

Endocytosis is a natural and energy-dependent process, occurring in almost all cells by direct interaction with the plasma membrane or by electrostatic interactions with cell surface proteoglycans [76, 92]. Endocytosis can be classified as phagocytosis (cell eating) or pinocytosis (cell drinking) [76]. Different types of pinocytosis include macropinocytosis, clathrin-mediated endocytosis, caveolae-mediated endocytosis, and clathrin- and caveolae-independent endocytosis [93]. The internalization mechanism for CPP-cargo complexes may involve a combination of specific pathways [76]. Moreover, several endocytic pathways can be used in parallel, or alternative pathways can compensate for the inhibition of specific pathways [17].

Direct translocation, also known as direct membrane penetration, is an energy-independent process where CPPs and CPP-cargo complexes directly penetrate through cellular membranes [76]. This direct translocation model involves a passive membrane diffusive or destabilization process that does not require binding to proteinaceous cell

surface receptors. Direct physical interaction between the cationic residues of CPPs and the anionic phospholipids of the plasma membrane leads to direct membrane penetration [17]. Direct translocation usually completes in a short timescale, as little as 5 minutes. Energy-independent internalization of CPP-cargo complexes can be observed by incubating cells at low temperatures (4°C), since low temperature treatment seizes all energy-dependent movement across the cell membrane. CPP-cargo complexes that directly penetrate the membrane have similar uptake at 4 or 37°C [17]. So far, the mechanism of direct translocation can be explained by three main models: the inverted cell model, the pore formation model, and the carpet model [92].

3.3.3. Applications of CPPs in Clinical and Gene Therapies. Today, there is an urgent need to develop new therapeutic agents. Many conventional treatments are outdated and less desirable due to drug resistance, low selectivity, and poor solubility [74]. Therapeutic peptides are a promising and novel approach to treat many diseases, including cancer and genetic disorders. Therapeutic peptides have several advantages over proteins or antibodies, as they are easy to synthesize, have high target specificity as well as selectivity, and have low toxicity. Nevertheless, therapeutic peptides do have significant drawbacks related to their stability and short half-life [74].

In 1995, one of the earliest examples of a CPP used in gene therapy was demonstrated. The ANTP CPP was covalently linked to an antisense DNA of amyloid precursor protein (APP), which gave the antisense treatment direct access to the cell cytosol and nucleus [78, 94]. Internalized antisense oligonucleotides mediated by ANTP decreased APP protein expression, resulting in the inhibition of neurite outgrowth [94]. Later, in 1997 the first noncovalent delivery of oligonucleotides was demonstrated using

MPG, a 27-residue chimeric CPP [79, 95]. Kardani et al. demonstrated reporter gene expression in 25 to 55% of mammalian cells transfected with CPPs [96]. Accordingly, numerous CPPs have been reported to assemble antisense oligonucleotides, small interfering RNA (siRNA), or plasmid DNA into CPP-cargo nanoparticles, possessing positive charges that allow them to interact with cellular membranes and to internalize into cells [73, 97, 98].

In vivo delivery of nucleic acids is a challenge that has to be solved before gene therapeutic applications can be translated into the clinics [99]. Preferably, the delivery should be applicable for systemic administration, because this has the potential to reach all corners of the body. Despite intensive research over the last 20 years, only a few gene therapeutic vectors have been approved for the use in clinics [100]. Many clinic studies have revealed safety issues along with inefficiency problems. In 2012, the first statistically significant clinical trial opened the door for clinical delivery of macromolecular therapeutics [101]. Subsequently, there were over 25 clinical trials performed predominantly using CPPs in 2015 [102], and many pre-clinical and clinical trials with CPP-derived therapeutics were conducted in 2017 [103].

In addition to positive or negative regulation of gene products, CPPs may be used for the delivery of genome editing tools [73, 98, 104, 105]. In fact, an innovative application of CPP-mediated delivery of the CRISPR-Cas9 system in genome editing was reported in 2014 [106]. Both covalent conjugation of Cas9-CPP by a thioether bond and noncovalent CPP/single-guide RNA (sgRNA) complexing led to efficient gene disruptions in several human cell types with low off-target incision effects. This study demonstrated CPP-enabled direct delivery of both recombinant Cas9 protein and sgRNA

into cultured mammalian cells [98, 105]. However, the genome editing frequency of this Cas9-CPP and CPP/sgRNA treatment tended to be low (less than 15% after three rounds of treatment) [107].

Collectively, CPPs have long been regarded as promising therapeutic delivery vehicles, not only because of their high internalization ability but also their potential for modification [92]. As promising carriers, CPPs generally have several advantages, such as low cytotoxicity, ease of preparation, and a wide variety of cargo type compatibility [74, 92, 108]. However, there are still shortcomings for drug delivery in vivo, such as cell-free specificity, short duration of action, and lack of oral bioavailability [74, 92, 108].

4. VIRAL METHODS

The goal of any virus is to infect and exploit host cells by injecting nucleic acids into their cytoplasm and taking over the host's cellular machinery. The life-cycle of a virus makes them a particularly promising carrier for gene therapeutics. However, for safety reasons, viral and retroviral vectors have to be modified to reduce their immunogenicity and cytotoxicity. Modification usually involves deletion or truncation of viral genes necessary for viral replication. Currently, viruses used as vectors for nucleic acid delivery have recombinant, replication-defective genomes that have had therapeutic genes added into them. Often, helper vectors or viruses are used to package the replication-defective viruses that carry therapeutic genes, which reduces the chance for viruses to gain competency. In the below sections, applications, advantages, and

disadvantages of viral and retroviral vectors as carrier platforms are discussed. Viral delivery methods are diagramed in Figure 4.

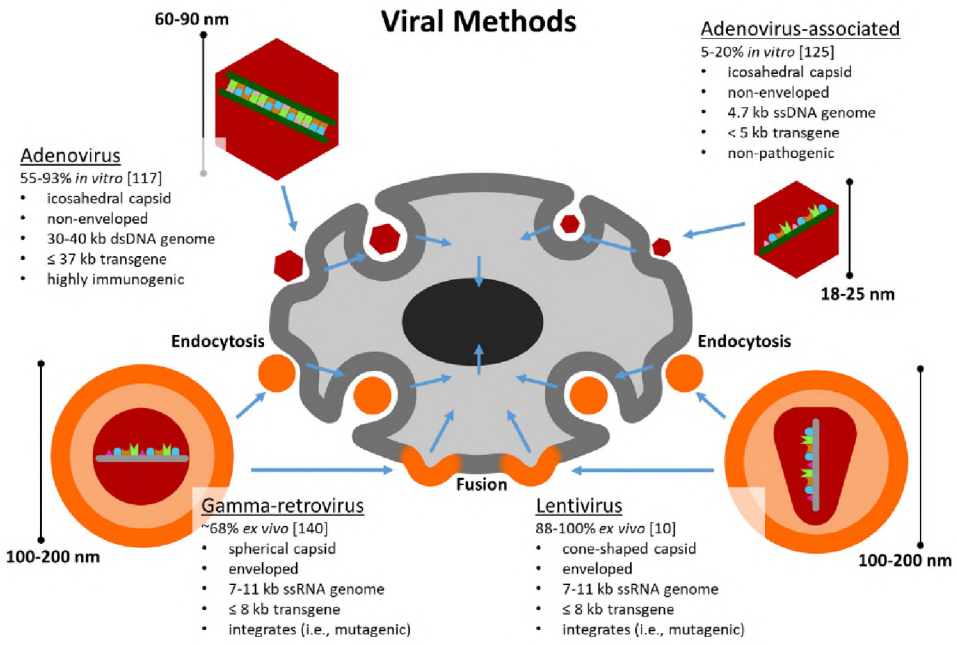

Figure 4. Viral methods of gene delivery. Viral vectors vary in particle size, genome size and type, transgene capacity, capsid geometry, and whether they have an envelope or not. Vectors enter either by endocytosis or through membrane fusion. Integration of delivered nucleic acids into the host genome is dependent on the virus type.

4.1. ADENOVIRUS (AV) VECTORS

Adenoviruses (AVs) were first isolated from human adenoid tissue in 1953 [109]. These viruses were the first viruses used for gene therapy in the 1990s and later they began to be tested in clinical trials [109]. In 1993, the first in vivo human gene therapy was performed in a cystic fibrosis patient using a recombinant AV vector [110, 111]. However, sufficient precautions were not taken with this early vector and later trials led to the death of Jesse Gelsinger in 1999 [14].

Adenoviruses are non-enveloped viruses with icosahedral capsids ranging from 60 to 90 nm in size. They contain a linear, double-stranded DNA genome of 30 to 40 kb and enter host cells by clathrin-mediated endocytosis [112]. The genome of adenoviruses includes various transcriptional units, which can be categorized based on when they are transcribed [6]. The units are early genes (E1A, E1B, E2, E3, and E4), delayed early (IX and Iva2), major late (ML), and late genes used in post-translational processing (L1, L2, L3, L4, and L5) [6]. The E1 region and a portion of E3 region in the AV genome were eliminated in the first-generation of recombinant AVs in order to accommodate a transgene. In addition to the potential of gaining replication competency in packaging cell lines, recombinant AVs tend to elicit a powerful immune response and cytotoxicity. To alleviate these undesired outcomes, vectors were further modified in a second generation where the E2 and E4 regions, which are responsible for immune reactions, were deleted [113, 114]. This also allowed the transgene packaging capacity of the vectors to increase from 5 kb to 14 kb. Further manipulations to produce a third generation of AV vectors nearly depleted the entire AV genome while allowing it to accommodate up to 37 kb target genes for delivery [115]. Genome components crucial for viral DNA replication and packaging were retained [6]. The onset of expression can occur as early as 16 to 24 hours after infection.

Adenoviral DNA cannot integrate into the genome and is unable to replicate during cell division, which imposes limitations for broader gene therapy; on the other hand, this eliminates the possibility of chromosomal rearrangements that could lead to potential tumor formation [116]. One group showed gene transduction efficiencies of 55 to 93% after using 4 different adenoviral vectors to infect CD34+ cord blood cells in vitro

[117]. Their highly efficient transduction of most tissue, high levels of protein expression, and transient gene expression make them attractive in gene transfer and therapy [118]. Including trials up to 2017, 20.5% of gene therapy trials used adenoviral vectors [21].

4.2. ADENO-ASSOCIATED VIRUS (AAV) VECTORS

Adeno-associated virus (AAV) was discovered in the mid-1960s when scientists were studying adenovirus and later identified AAVs in human tissues [119, 120]. A journey of 20 years to understand AAV biology eventually yielded the first AAV vector used for in vitro gene delivery in 1984. The first human test of AAV vectors was to treat a patient with cystic fibrosis in 1995 [121]. In 2012, the European Medicine Agency approved the first AAV vector-based gene therapy drug to treat lipoprotein lipase deficiency.

Adeno-associated viruses are non-enveloped, single-stranded DNA viruses with 4.7 kb genomes that are encapsulated in icosahedral capsids 18 to 25 nm in diameter. Wild-type AAVs require a helper virus to complete their life cycle. The non-pathogenic nature and the ability to package various transgenes make AAVs an ideal vehicle for gene therapy [121, 122]. AAVs are internalized by endocytosis mediated by clathrin [6]. The genome of the most commonly used serotype, AAV2, contains genes that encode regulatory Rep proteins and structural Cap proteins. The former carry out genome excision from the host chromosome, replication, packaging, and integration whereas the latter produce capsid proteins. Inverted terminal repeats flanking the genome possess regulatory cis-acting sequences needed for the virus to complete its life cycle and for

integration into the host genome. In making AAV vectors, Rep and Cap were removed from AAV DNA to make room for therapeutic genes. Required proteins are provided to the virus by helper vectors during vector production [123]. An example of vector production in HEK293 cells would involve the functions of Rep and Cap being supplied in a separate helper vector, with an additional helper vector containing the E4, E2a, and VA regions required for replication [123].

The primary disadvantages of AAV vectors are that delivery is limited to smaller sized genes of interest (less than 5.0 kb of DNA), a slower onset of expression (2 to 7 days for in vitro and 3 to 21 days for in vivo), and relatively low levels of protein expression that leads to a necessity to re-administration AAV vectors. Another significant drawback of AAVs is that they often trigger immune responses. For instance, neutralizing antibodies lead to rapid clearance of AAVs from the circulatory system by opsonizing viral particles and thus facilitate uptake by phagocytic cells. To overcome this issue, certain strategies have been employed that include re-engineering AAV vectors, use of capsid decoys, changing the route of administration, plasmapheresis, disruption of B cell activation and reduction of the number of activated B cells, and targeting T cell activation. Each method has disease-dependent pros and cons [124].

Currently more than nine different serotypes of AAV vectors have been used in clinical trials. The infectivity of AAVs in different cell types can be increased by utilizing different serotypes. Liver, eye, heart, muscle, brain, and bone have been targeted for therapy. Most of these trials are in phase I and/or II, while only a few have entered phase III. Around 7.9% of gene therapy clinical trials used AAV vectors up until 2017 [21]. The transduction of AAV vectors is rate-limited by the necessity for AAV single-stranded

DNA to be converted to double-stranded DNA before transcription [121]. It was demonstrated that an AAV alone was only able to transduce approximately 5 to 20% of HEK293T or HepG2 cells [125]. However, this has been improved by using methods, such as self-complementary vectors, to overcome the rate-limiting step [126].

4.3. RETROVIRAL VECTORS

Retroviruses are enveloped viruses with two identical copies of single-stranded RNA that range in length from 7 to 10 kb [127-130]. The entire viral particle is about 100 to 200 nm. Retroviruses are classified as simple retroviruses or complex retroviruses according to their genomic organization and biological features. Gamma-retroviruses and lentiviruses are representative simple retroviruses and complex retroviruses, respectively. All retroviruses enter into cells either by receptor-mediated endocytosis or membrane fusion [131, 132]. The unique features of retroviruses lie in their capability to reverse transcribe their RNA into complementary DNA (cDNA) via reverse transcriptase activity and to integrate the cDNA into the host genome via integrase activity. The integration allows for hijacking the host's replication machinery for viral reproduction for further infection. In the below sections, two major types of retroviral vectors for gene therapy are discussed.

4.3.1. Gamma-Retroviral Vectors. Gamma-retrovirus possesses a simple genome structure. The gag gene encodes structural proteins and proteins pertaining to the budding process. The pol gene codes for a protease, a reverse transcriptase, and an integrase. The protease cleaves the gag polyprotein. The reverse transcriptase is needed for the generation of viral cDNA from viral RNA and the integrase aids integration of

viral cDNA into the host cell genome. All regulatory elements involved in viral RNA processing lie in the long terminal repeat (LTR) regions of viral genome.

The most commonly used retroviral vector for gene therapy was derived from murine leukemia virus (MLV), which is a simple gamma-retrovirus [132] with a nearly spherical capsid [133]. The first ex vivo gene therapy trial was approved in 1990 by the FDA. This trial treated the white blood cells of two young adenosine deaminase deficiency patients with a modified MLV vector carrying a normal gene [134, 135]. The efficiency of the therapy was debated [134]. Throughout decades, safety considerations have directed the evolution and development of the MLV vector system. The goal of manipulating vector arrangement was to remove its replication competence. The most advanced third generational gamma-retroviral vectors utilize a split-genome approach comprised of three plasmids. The main retroviral vector contains the LTR, a primer binding site for reverse transcription, and the packaging signal, as well as the transgene which can be up to 8 kb long. The structural and enzymatic retroviral genes are located in two helper plasmids. The gag, pol, and env genes in the helper plasmids do not contain retroviral elements pertaining to packaging, thereby reducing the probability of recombination [132]. To further improve safety, self-inactivating (SIN) vectors were developed by making the 3'-LTR nonfunctional. Even with so many modifications, once genes are delivered to cells, insertional mutagenesis, enhancer interaction, or premature termination may occur, which can lead to severe side effects.

Gamma-retroviral vectors have been used to transfer genes to hematopoietic stem cells to correct blood-related genetic disorders and skin diseases, such as Wiskott-Aldrich Syndrome, SCID-X1, SCID-ADA, epidermolysis bullosa, and melanoma [11, 136-143].

In an ex vivo trial using gamma-retroviruses to treat SCID-X1, Gaspar et al. demonstrated an approximate 68% transfection efficiency in CD34+ bone-marrow stem cells [140]. Currently, approximately 17.9% of gene therapy clinical trials use retroviral vectors [21]. However, treating patients with integrating viruses is risky as integration has been associated with mutagenesis and oncogenesis when normal genes are disrupted or onco-genes are activated. For instance, in one trial of nine SCID-X1 patients, four patients treated with gamma-retroviral vectors developed T cell leukemia after gene therapy [136, 139].

4.3.2. Lentiviral (LV) Vectors. Lentivirus (LV) vectors are derived from HIV-1. They were first used in clinical trials in 2003 to deliver an antisense sequence for the HIV-1 envelope gene to CD4+ cells ex vivo [144]. In addition to gag, pol, and env found in gamma-retroviruses, the HIV-1 virus contains two regulatory genes, tat and rev, that are essential for replication. Tat and rev regulate trans-activation of gene expression and nuclear export of mRNAs. Importantly, HIV-1 contains four accessory genes that encode critical virulence factors for virus transmission enhancement. The lentiviral capsid is cone-shaped, rather than spherical [133]. In order for HIV-1 to be used safely in gene therapy, significant modifications to its genome were carried out [145].

The first generation of lentiviral vectors consisted of a major portion of the HIV genome, including retention of the gag and pol genes. The envelope protein (env) was supplied by another virus called VSV-G, which broadened the range of mammalian cells that could be transduced. The second generation took out accessory virulence genes, such as vif, vpr, vpu, and nef, without compromising transduction efficiency. The third generation of lentiviral vector systems underwent significant genome rearrangement and

contained four plasmids: a vector plasmid, two packaging plasmids (containing gag, pol, and rev separately), and one envelope plasmid (containing env from VSV-G). The split-genome approach was intended to maximize the segregation of cis- and trans-acting functions and to minimize the possibility of homologous recombination events in order to reduce the generation of replication-competent lentiviruses. The removal of all accessory genes in the vector plasmid achieved a higher safety level. The gene tat was replaced by a modified LTR with a constitutively active promoter sequence [146]. The LTR sequence was further modified to become self-inactivating (i.e., SIN 5' and 3' LTR) [131]. To enhance viral titers and transgene expression, central polypurine tract/central termination sequence (cPPT/CTS), an enhanced promoter, and a woodchuck hepatitis virus posttranscriptional regulatory element were included [123]. Similar to gamma-retroviral vectors, lentiviral vectors can deliver transgenes up to 8 kb in length [67].

The most distinctive advantage of LVs over other retroviral vectors is their ability to penetrate the nuclear envelope of non-dividing cells. This extraordinary characteristic allows lentiviral vectors to be used in neurons and other non-dividing cells in adult organisms [147]. In addition, lentiviral gene therapies have been used in vascular transplantation, chronic granulomatous diseases, prostate cancer, heamophillia A, rheumatoid arthritis, and diabetes mellitus [148-151]. In the past decade, the clinical use of LVs has gained significant traction in gene transfer into CD34+ hematopoietic stem cells (HSC) to treat a variety of genetic disorders, such as β-thalassemia, X-linked adrenoleukodystrophy, metachromatic leukodystrophy, and Wiskott-Aldrich Syndrome [10, 12, 13, 152, 153]. Ex vivo transduction of HSCs with a lentiviral vector to treat Wiskott-Aldrich Syndrome resulted in 88 to 100% gene transfer efficiencies in CD34+

bone-marrow stem cells [10]. Approximately 7.3% of gene therapy clinical trials utilized lentiviral vectors up until 2017 [21].

5. GENOME EDITING

Zinc finger nucleases (ZFNs), transcription activator-like effector nucleases (TALENs), and CRISPR systems recognize and cut DNA sequences and have been utilized for genome editing [1]. ZFNs, TALENs, and CRISPR systems function through a DNA-targeting domain and a non-specific nuclease domain, resulting in a double strand break (DSB) in the DNA at the target site. The DNA-targeting domain is unique to each system, but the cleavage and cellular repair of a break are similar.

After a double-stranded DNA break in a eukaryotic cell, the conserved homology-directed repair (HDR) or non-homologous end joining (NHEJ) pathways are used to repair the gap [154]. NHEJ repairs the DNA break by quickly ligating the strands; however, it is not accurate and frequently results in short insertions and/or deletions that generate loss-of-function mutations [154, 155]. This may be desirable if gene inactivation is the goal. NHEJ-mediated repair is dominant in cells in the G0 and G1 phases of the cell cycle [156]. In HDR, a strand of template DNA similar to the breakage site is used to repair the gene [154, 155]. Homologous DNA with corrected bases can be delivered with gene editing tools and used as a template to fix the gene or add in a new gene [154]. However, HDR is restricted to cells in the S and G2 phases of the cell cycle [156].

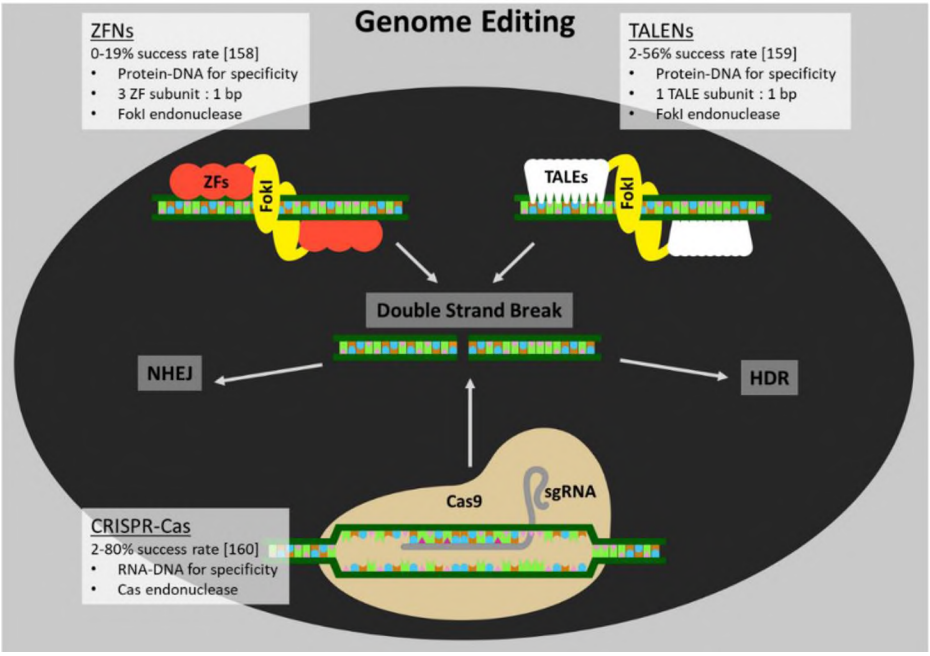

Figure 5. Genome editing techniques. All methods function by causing double strand breaks in DNA at targeted sequences. Cells repair the damage through non-homologous end joining (NHEJ) or homology-directed repair (HDR). ZFNs and TALENs share the same endonuclease (FokI) to induce breaks but target sequences using either zinc finger (ZF) or transcription activator-like effector (TALE) protein subunits. CRISPR uses a Cas endonuclease and targets DNA with a single-guide RNA (sgRNA).

ZFNs and TALENs rely on proteins to specifically interact with DNA sequences and CRISPR systems use a RNA guide sequence [1, 157]. The use of RNA for targeting makes CRISPR-Cas9 systems easier to manipulate than ZFNs and TALENs as proteins must be engineered to bind new DNA sequences [157]. The rate of mutations induced by these systems varies, with ZFNs having low success rates ranging from 0 to 19% [158], TALENs ranging from about 2 to 56% [159], and CRISPR ranging from approximately 2 to 80% [160]. CRISPR systems have emerged as the front-runner for genome editing due to higher success rates and simpler target alteration. However, in order to function, editing tools need to be delivered into cells [1]. Some of the above methods may be used,

but the safety and efficiency of these delivery systems still need to be considered. Genome editing techniques are diagramed in Figure 5.

5.1. ZINC FINGER NUCLEASES (ZFNs)

Zinc finger nucleases (ZFNs) are site-specific endonucleases that induce double-strand breaks in DNA [154]. They can be designed to target specific DNA sequences. ZFNs are zinc finger proteins, a type of eukaryotic transcription factor, linked to a FokI restriction enzyme nuclease domain, which is of bacterial origin [154, 161]. The zinc finger proteins provide specificity and the restriction enzyme enables the DNA to be cut [154]. Both segments can be modified individually for optimization and then joined. The combination of modular DNA sequence-specific proteins and the non-specific FokI nuclease domain was first developed in 1996 [157, 161], with initial applications demonstrated in mammalian cells and Drosophila [157]. ZFNs have been used to target gene sequences in CHO cells, human cells, Drosophila, zebrafish, tobacco plants, and nematodes [155].

Zinc fingers proteins are very diverse in nature and very few residues are conserved between them [162]. They often contain cysteine and histidine amino acids that provide essential interactions with a zinc ion, which stabilizes the folding of the protein [162, 163]. Zinc fingers containing two cysteines and two histidines (Cys2-His2) play roles in protein interactions with DNA, RNA, and other proteins [162] and many are transcription factors [163]. Zinc fingers used in ZFNs are of this type [154]. Cys2-His2 zinc fingers often fold into a two-stranded antiparallel β-sheet and an α-helix, which bind around the zinc ion [162]. Generally, the cys residues are located at one end of one β-

sheet and the his residues are in the α-helix C-terminal area, with variable spacing. Loss of function results from alteration of the either the cys or his residues, indicating their essential role. The fingers in a protein are linked with a spacer sequence that influences "the spacing of the fingers along the DNA site" and is important for DNA binding affinity [162]. When binding DNA, the protein wraps around the helix, with each α-helix of individual fingers interacting with the major groove. The residues along the surface of the finger's α-helix seem to be responsible for base-specific interactions [162, 163]. Finger proteins also interact with the phosphate backbone of the same DNA strand base interactions are made with, further securing the protein [162].

The FokI domain is only functional as a dimer, formed by two separate ZFNs binding DNA and orienting their nuclease monomers into the proper orientation [154]. Each finger binds specifically to about 3 DNA base pairs, with early studies incorporating 3 fingers and more recent ones using up to 6 per monomer, allowing 18 to 36 base pairs to be recognized with the dimer [154]. Libraries of zinc fingers have been assembled that specifically bind combinations of the three base pair sequence, allowing zinc fingers to be selected and bound sequentially in order to target the desired DNA sequence [164]. Using different combinations of fingers in the set of dimers allows for longer sequences to be targeted [154]. However, designing ZFNs with sequence-specificity can be difficult because combining natural and synthetic fingers modularly can result in unforeseen interactions between other fingers and DNA bases [154]. Engineering new synthetic fingers can be complex [1].

Off-targeting is a major concern with ZFNs. Fingers may bind to and cut similar sequences in the genome, other than the one intended [154]. If two different ZFNs are

paired together to target a sequence, off-targeting may also occur because homodimers can form. However, this particular issue has been resolved by developing ZFNs that only function as heterodimers [154, 165]. ZFNs can also be toxic, likely due to off-targeting, with only 20 to 60% of 293T cells surviving transfection with ZFN plasmids [166]. ZFNs may not efficiently break a sequence if chromatin structure is too dense, due to the necessity of the protein fingers wrapping around the DNA helix [154]. ZFNs have not been used extensively since their development because of the complexity in designing fingers to target new sequences and the difficulty in validating binding [157].

5.2. TRANSCRIPTION ACTIVACTOR-LIKE EFFECTOR NUCLEASES (TALENS)

Similar to ZFNs, transcription activator-like effector nucleases (TALENs) cause double strand breaks in DNA using a FokI nuclease domain joined with a DNA-targeting domain [167, 168]. TALENs were created in 2010 [169, 170], originally with FokI because the targeting domain was inserted into the same plasmid used to create ZFNs [171].

The DNA targeting domain of TALENs, transcription activator-like effectors (TALEs), were discovered in Xanthomonas, a genus of bacterial plant pathogens [171]. TALEs mimic eukaryotic transcription factors and are secreted by the bacteria to weaken plant cells, making them more vulnerable to attack after their gene transcription is altered. TALEs can be engineered for DNA binding specificity [168]. Since their discovery, TALENs have been applied in a variety of cells and organisms, including yeast, Drosophila, human cell lines, zebrafish, frogs, rice, and roundworms [168].

The potential of TALEs for DNA targeting is greater than zinc fingers. Individual TALE subunits can be modularly combined in order to produce a sequence-specific binding protein [164]. TALE subunits are composed of a highly conserved amino acid sequence ranging from 33 to 35 residues long and were discovered because of their repeating sequence [168]. TALE repeats in the natural protein are flanked by amino- and carboxy-domains, which are also incorporated into TALENs. Each subunit in a TALE array binds one nucleotide. Hypervariable residues at positions 12 and 13 are responsible for base-specificity [171]. Multiple of these diresidues can bind the same base with varying efficiency. The most common diresidues used in research to bind the DNA bases A, T, G, and C are the amino acid pairs NI, NG, NN, and HD, respectively; however, NN has also been shown to bind A so NH and NK have been implemented to decrease off-targeting [171]. The conserved amino acids in each monomer fold into α-helices on either side of the hypervariable residues, forming a v-shape [168]. These v-shaped subunits fit into the DNA major-groove so that their diresidues make contact with the bases and together wrap around the DNA to form a superhelix [168].

Due to the use of FokI, TALENs also function in pairs [171]. Targeting domains are designed to bind to opposite DNA strands with 12 to 25 base pair spacing between the binding points. TALENs are often created to target 18 or more base pair sequences, though specificity may decrease with longer chains [167]. TALENs have lower toxicity and higher specificity than ZFNs [165]. Production and validation of TALENs is also easier [157]. However, off-targeting may still be a concern and they are much larger than ZFNs, making them more difficult to deliver to cells as many delivery methods have limits to cargo size [165]. Although, off-targeting seems to be less when TALENs are

used to target the same genes as ZFNs [167]. Each pair of TALENs still must be engineered when a new DNA sequence is to be targeted [169], which may have contributed to their limited application [157]. Regular use of TALENs may have also been hampered by the discovery of CRISPR-Cas9 shortly after they were developed.

5.3. CRISPR-CAS SYSTEMS

5.3.1. Development History. The CRISPR-Cas system was derived from an adaptive immune system of bacterial defense against foreign invaders, such as viruses, phages, and certain plasmids. In 1987, clusters of short palindromic DNA repeats separated by hypervariable spacer sequences were discovered in Escherichia coli [172]. It was revealed that the bacteria captured DNA segments from invading viruses or foreign DNA, and used them to create DNA repeats, termed clustered regularly interspaced short palindromic repeats (CRISPR) in 2002 [173]. These CRISPR allow the bacteria to retain a history of previous viral infections or transformed DNA in the bacterial genome. When the viruses or closely related ones attack again, the bacteria produce RNA segments transcribed from these CRISPR to target the invasive genetic material, similar to current uses of iRNA. CRISPR-associated (Cas) genes are usually located adjacent to each CRISPR locus and code for a variety of polymerases, nucleases (both DNA and RNA), helicases, and RNA-binding proteins. The bacteria use Cas9 or a similar enzyme to cut foreign DNA apart, which disables the viruses or destroys other harmful DNA.

In 2012, two research teams first developed the CRISPR-Cas9 system for genome editing based on the bacterial defense system [174-177]. As summarized in Table 2, the original developers have launched their own biotechnology companies. They shared the

2016 Tang Prize in Biopharmaceutical Science for their work in "the development of CRISPR/Cas9 as a breakthrough genome editing platform that promises to revolutionize biomedical research and disease treatment" [178]. They were also winners of the Canada Gairdner International Award in 2016. This genome editing approach has inarguably revolutionized the field of molecular biology and medical research, and has had a profound and rapid impact on the development of more effective strategies to conquer human genetic diseases and cancers. In terms of experimental practice, the CRISPR-Cas system is characterized by its simplicity to use, high success rate, and easiness in design, construction, as well as delivery [156]. Additionally, targeted mutations in multiple genes (also known as multiplex genome engineering) are possible with the CRISPR-Cas system. Thus, these features make the innovative CRISPR-Cas system an extremely valuable tool for the evaluation of investigational gene therapies. Ultimately, Emmanuelle Charpentier and Jennifer Doudna won the 2020 Nobel Prize in Chemistry "for the development of a method for genome editing".

Table 2. Three original developers of the CRISPR-Cas9 system.

Principal investigator	**Jennifer A. Doudna**	**Emmanuelle Charpentier**	**Feng Zhang**
Institute	University of California, Berkeley, USA	Umea University, Sweden	Massachusetts Institute of Technology, USA
Discovery	The use of CRISPR-Cas9 system to edit DNA	The use of CRISPR-Cas9 system to edit DNA	The application of CRISPR-Cas9 in mammalian cells
Company founder	Caribou Biosciences, Inc. and Editas Medicine, Inc.	CRISPR Therapeutics Co.	Editas Medicine, Inc.
Reference	[176]	[176]	[177]

5.3.2. Mechanism of CRISPR-Cas Action. The CRISPR/Cas system is a ribonucleoprotein complex and comprises two key components: a chimeric single-guide RNA (sgRNA) and a DNA endonuclease Cas protein for genome editing [105, 179]. Together, an appropriate sgRNA carries a Cas nuclease to target a specific genomic sequence. The detailed mechanism of CRISPR-Cas system comprises three phases, which are adaptation of spacer sequences, expression and mutation, and interference [180]. As of 2018, CRISPR-Cas systems are classified into three main types of Cas variants (and a dozen subtypes) have been developed and differ in their mechanisms of action [175, 179].

The first Cas system is the wild-type Cas9 protein from the type II CRISPR system of Streptococcus pyogenes, and is commonly used as a genome editing tool [176]. The original activity of this Cas9 protein cleaves DNA at specific sites, resulting in the creation of double strand breaks (DSBs). DSBs are then subjected to the error-prone repair by NHEJ or HDR [156]. The efficiency of CRISPR-induced HDR may be very low in vivo due to HDR being limited to S and G2 phase cells. The second Cas9 variant is Cas9D10A (a.k.a., nickase) [181], a mutant form of the Cas9 protein which cleaves only one DNA strand or modifies only one specific nucleotide [175, 179]. This activates the high-fidelity HDR pathway and downregulates NHEJ-mediated repair. The third Cas9 version is dCas9 (dead Cas9, nuclease-deficient Cas9, or CRISPR interference; i.e., CRISPRi) [182], in which certain mutations were introduced to inactivate the protein's cleavage activity but retain the DNA-binding activity. This dCas9 is a DNA complexing protein that can specifically interfere with transcription and modulate gene expression. It shall be remarked that the number and diversity of CRISPR-Cas systems are continuously

expanding. Recently, a new evolutionary classification has been introduced to include 2 classes, 6 types, and 33 subtypes [183]. The class 1 systems include multiple Cas proteins that form a CRISPR RNA-binding complex. By contrast, class 2 systems have a single, multidomain CRISPR RNA-binding protein, such as Cas9 in type II systems.

Several methods have also been developed related to CRISPR-Cas systems. Prime editing is a genome editing technique that produced higher precision and a wider selection of applications, potentially enabling researchers to correct up to 89% of known genetic variants [184]. This versatile and precise genome editing method uses a catalytically impaired Cas9 fused to an engineered reverse transcriptase and a prime editing guide RNA (pegRNA) that both specify the target site and encode the desired edit. Anti-CRISPRs (Acrs) are small proteins that have been identified to inhibit the RNA-guided DNA targeting activity of CRISPR-Cas proteins [185]. Three inhibitors, AcrIIA13, AcrIIA14, and AcrIIA15, were found to block CRISPR-Cas-mediated genome editing in human embryonic kidney cells. These inhibitors share a conserved N-terminal sequence that is required in DNA cleavage inhibition. Notably, a new base editor (BE) was developed by fusing dCas9 and cytidine deaminase that enabled the direct, irreversible conversion of one target DNA base into another in a programmable manner, without DSBs [186]. Instead of possible disruption of the entire genome, this BE creates point mutations at a targeted genomic locus with an efficiency of up to 75% using a CRISPR framework. This tool is like using an eraser and pencil to fix just a single letter. Another new CasRx ribonuclease effector was recently identified to exhibit favorable efficiency and specificity relative to RNA interference (RNAi) across diverse endogenous transcripts [187]. CasRx can be flexibly packaged into adeno-associated viruses to

manipulate alternative splicing, reducing pathological tau isoforms in a neuronal model of frontotemporal dementia.

5.3.3. Applications of CRISPR-Cas in Gene Therapy. In the post-CRISPR-Cas era, we have observed incredible increases in laboratory research from academic institutes and clinical applications from pharmaceutical companies. It was estimated that the genome editing market will be worth more than US$5 billion by 2021 [188]. Although the driving force of this rapid development was certainly CRISPR-Cas, both ZFNs and TALENs platforms reached the clinical stage before CRISPR-Cas. Many teams and companies have been working to translate CRISPR-Cas technologies into safe and effective human therapeutics [1, 188-192]. For instance, the Genome Project-write (GP-write) is an open, international research project, which focuses on whole genome engineering of human cell lines and other organisms of agricultural and public health significance [193]. In any case, genome editing must be accurate, efficient, and deliverable to the desired cells or tissues for safe and effective clinical use ex vivo and in vivo [194]. Currently, there are 10 clinical CRISPR studies under either recruiting or not yet recruiting status according to ClinicalTrials.gov [195]. In 2020, there were 19 ongoing clinical trials using CRISPR-based gene editing [196]. However, none of these proposed clinical trials has been officially approved as new drugs by the US FDA. [190].

Since the discovery of the CRISPR-Cas system in 2012, the progress toward human trials has been slow [197]. For example, US FDA halted the proposed trial of CTX001 to use the CRISPR-Cas system for a single genetic change in patients with sickle cell disease. The status of the European trial using the same treatment in patients with beta-thalassemia was unaffected by this US FDA decision, and was still planned to

be initiated later in 2018. In 2015, it was reported that the first CRISPR-Cas human clinical trial took place in China [190, 198]. There were 86 patients with various cancers that participated in these clinical CRISPR-Cas trials from 2015 to 2017. At least 15 patients died during the trials, although the directors of clinical research claimed they died from their own cancers. One of the clinical trial directors from Hangzhou Cancer Hospital revealed that the cure rate of an ex vivo clinical CRISPR-Cas trial after 11 months was approximately 40% from 21 patients with esophageal cancer [199]. However, no official or complete results from Chinese CRISPR-Cas human clinical trials have been reported to date. In November 2018, a Chinese biophysics researcher, He Jiankui, sent shockwaves across the world by claiming that he had utilized CRISPR technology to edit the genomes of two twin babies, Lulu and Nana [200]. His team attempted to introduce a mutation into their CCR5 genes, a gene encoding the T cell receptor that HIV viruses bind to, in order to prevent HIV infection. However, the ethically controversial announcement lead to his dismissal from the Southern University of Science and Technology in Shenzhen, China. He was also fined three million yuan and imprisoned for three years by the Chinese People's Court in 2019.

The ongoing global pandemic of coronavirus disease 2019 (COVID-19), caused by severe acute respiratory syndrome coronavirus 2 (SARS-CoV-2), is one of the most devastating viral outbreaks in the past 100 years [201]. A rapid (less than 40 minute), easy-to-implement, and accurate CRISPR-Cas12-based diagnostic assay was developed for detecting SARS-CoV-2 from RNA extracts of respiratory swabs [202]. This DNA endonuclease-targeted CRISPR trans reporter (DETECTR) assay provides a visual and faster alternative to general assays. Additionally, a CRISPR-Cas13-based antiviral

strategy was recently developed to target conserved sequences of coronaviruses and influenza A virus [203]. This strategy was named prophylactic antiviral CRISPR in human cells (PAC-MAN) and effectively degrades RNA from SARS-CoV-2 and influenza A virus in human lung epithelial cells. Bioinformatic analysis showed that a group of only six CRISPR RNAs can target more than 90% of all coronaviruses.

5.3.4. Concerns of CRISPR-Cas in Gene Therapy. Serious safety concerns about the use of CRISPR-Cas have been raised after the development of therapeutic genome editing applications [204]. CRISPR-Cas technology has enabled efficient genome editing and modifications in several model organisms, and has successfully been applied in biomedicine and biomedical engineering [205]. Much attention has also focused on the development of potential CRISPR-Cas therapies to cure complex heritable diseases in humans [206]. However, major challenges related to the effectiveness, specificity, and safety of the CRISPR-Cas system remain. Notably, safety guidelines for preclinical trial studies and ethical issues concerning genome editing and genomic analysis at the population level remain unsettled.

6. CONCLUSIONS

Gene therapy has evolved and improved over the past five decades. Methods started from non-specific and non-targeting and have become specific and precise with the ability to target genes that need to be corrected to eliminate disease. Correction can be an addition or a simple edit to a small stretch of a gene. Genetic delivery has been achieved at the cellular level and organismal level. CRISPR systems have gathered the

main attention of gene therapy research due the system being viewed as an accurate and efficient technique with the potential to challenge all diseases. Gene delivery and genome editing will continue to develop in the twenty-first century, with advances in delivery efficiency and targeting specificity, though progress may be gradual due to necessary safety precautions. We have learned from past mistakes, where safety was not fully considered, and have faced morbidity and mortality among patients. Certain methods are likely to become more effective and safer for disease management, but other methods will still remain competitive due to ease of preparation and use, low cost, simplicity, and will still contribution to fundamental scientific endeavors in cell and molecular biology. As these techniques continue to develop, more applications will arise, treatments will be further tailored to individuals, and diseases with more complex genotypes will be able to be treated. As genome therapy becomes safer and highly efficient, we will be faced with more cases of edited humans and must question the line between disease treatment and playing god with our genetic code.

REFERENCES

[1] Yin H, Kauffman KJ, Anderson DG. Delivery technologies for genome editing. Nat Rev Drug Discov 2017; 16(6): 387-99.

[2] Burney TJ, Davies JC. Gene therapy for the treatment of cystic fibrosis. Appl Clin Genet 2012; 5: 29-36.

[3] Hoban MD, Orkin SH, Bauer DE. Genetic treatment of a molecular disorder: gene therapy approaches to sickle cell disease. Blood 2016; 127(7): 839-48.

[4] Dickey AS, La Spada AR. Therapy development in Huntington disease: From current strategies to emerging opportunities. Am J Med Genet A 2018; 176(4): 842-61.

[5] van Gaal EV, Hennink WE, Crommelin DJ, Mastrobattista E. Plasmid engineering for controlled and sustained gene expression for nonviral gene therapy. Pharm Res 2006; 23(6): 1053-74.

[6] Giacca M, Zacchigna S. Virus-mediated gene delivery for human gene therapy. J Control Release 2012; 161(2): 377-88.

[7] Laham-Karam N, Pinto GP, Poso A, Kokkonen P. Transcription and Translation Inhibitors in Cancer Treatment. Front Chem 2020; 8: 276.

[8] Bennett CF, Krainer AR, Cleveland DW. Antisense Oligonucleotide Therapies for Neurodegenerative Diseases. Annu Rev Neurosci 2019; 42: 385-406.

[9] Laina A, Gatsiou A, Georgiopoulos G, Stamatelopoulos K, Stellos K. RNA Therapeutics in Cardiovascular Precision Medicine. Front Physiol 2018; 9: 953.

[10] Aiuti A, Biasco L, Scaramuzza S, et al. Lentiviral hematopoietic stem cell gene therapy in patients with Wiskott-Aldrich syndrome. Science 2013; 341(6148): 1233151.

[11] Aiuti A, Cassani B, Andolfi G, et al. Multilineage hematopoietic reconstitution without clonal selection in ADA-SCID patients treated with stem cell gene therapy. J Clin Invest 2007; 117(8): 2233-40.

[12] Cartier N, Hacein-Bey-Abina S, Bartholomae CC, et al. Hematopoietic stem cell gene therapy with a lentiviral vector in X-linked adrenoleukodystrophy. Science 2009; 326(5954): 818-23.

[13] Cavazzana-Calvo M, Payen E, Negre O, et al. Transfusion independence and HMGA2 activation after gene therapy of human beta-thalassaemia. Nature 2010; 467(7313): 318-22.

[14] Stolberg SG. The biotech death of Jesse Gelsinger. In: Cohen J, Ed. The Best of the Best American Science Writing. HarperCollins Publishers: New York, NY 2010; pp. 30-44.

[15] Gene-therapy trials must proceed with caution. Nature 2016; 534(7609): 590.

[16] Lodish H, Berk A, Matsudaira P, et al. Transport of ions and small molecules across cell membranes. In: Molecular cell biology. 5th ed. W. H. Freeman and Company: New York, NY 2003; pp. 245-300.

[17] Lehto T, Ezzat K, Wood MJA, El Andaloussi S. Peptides for nucleic acid delivery. Adv Drug Deliv Rev 2016; 106(Pt A): 172-82.

[18] Al-Dosari MS, Gao X. Nonviral gene delivery: principle, limitations, and recent progress. AAPS J 2009; 11(4): 671-81.

[19] Kulkarni JA, Myhre JL, Chen S, et al. Design of lipid nanoparticles for in vitro and in vivo delivery of plasmid DNA. Nanomedicine 2017; 13(4): 1377-87.

[20] Genetics Home Reference. What are genome editing and CRISPR-Cas9? [Online] 2020 [cited 2020]. Available at: https://ghr.nlm.nih.gov/primer/genomicresearch/genomeediting

[21] Ginn SL, Amaya AK, Alexander IE, Edelstein M, Abedi MR. Gene therapy clinical trials worldwide to 2017: An update. J Gene Med 2018; 20(5): e3015.

[22] Luo D, Saltzman WM. Synthetic DNA delivery systems. Nat Biotechnol 2000; 18(1): 33-7.

[23] Jinturkar KA, Rathi MN, Misra A. Gene delivery using physical methods. In: Misra A, Ed. Challenges in delivery of therapeutic genomics and proteomics. 1st ed. Elsevier Inc. 2011; pp. 83-126.

[24] Kaestner L, Scholz A, Lipp P. Conceptual and technical aspects of transfection and gene delivery. Bioorg Med Chem Lett 2015; 25(6): 1171-6.

[25] Korzh V, Strahle U. Marshall Barber and the century of microinjection: from cloning of bacteria to cloning of everything. Differentiation 2002; 70(6): 221-6.

[26] Di Berardino MA, McKinnell RG, Wolf DP. The golden anniversary of cloning: a celebratory essay. Differentiation 2003; 71(7): 398-401.

[27] Tonelli FMP, Lacerda S, Tonelli FCP, et al. Progress and biotechnological prospects in fish transgenesis. Biotechnol Adv 2017; 35(6): 832-44.

[28] Wilmut I, Schnieke AE, McWhir J, Kind AJ, Campbell KH. Viable offspring derived from fetal and adult mammalian cells. Nature 1997; 385(6619): 810-3.

[29] Chow YT, Chen S, Wang R, et al. Single Cell Transfection through Precise Microinjection with Quantitatively Controlled Injection Volumes. Sci Rep 2016; 6: 24127.

[30] Capecchi MR. High efficiency transformation by direct microinjection of DNA into cultured mammalian cells. Cell 1980; 22(2 Pt 2): 479-88.

[31] Dean DA. Microinjection. In: Maloy S, Hughes K, Eds. Brenner's encyclopedia of genetics. 2nd ed. Academic Press: Cambridge, MA 2013; pp. 409-10.

[32] Donnelly RF, Raj Singh TR, Woolfson AD. Microneedle-based drug delivery systems: microfabrication, drug delivery, and safety. Drug Deliv 2010; 17(4): 187-207.

[33] Ramamoorth M, Narvekar A. Non viral vectors in gene therapy- an overview. J Clin Diagn Res 2015; 9(1): GE01-6.

[34] Klein TM, Wolf ED, Wu R, Sanford JC. High-velocity microprojectiles for delivering nucleic acids into living cells. Nature 1987; 327: 70–3.

[35] Davidson JM, Krieg T, Eming SA. Particle-mediated gene therapy of wounds. Wound Repair Regen 2000; 8(6): 452-9.

[36] Finer JJ, Finer KR, Ponappa T. Particle bombardment mediated transformation. Curr Top Microbiol Immunol 1999; 240: 59-80.

[37] Wagner DE, Bhaduri SB. Progress and outlook of inorganic nanoparticles for delivery of nucleic acid sequences related to orthopedic pathologies: a review. Tissue Eng Part B Rev 2012; 18(1): 1-14.

[38] Xia J, Martinez A, Daniell H, Ebert SN. Evaluation of biolistic gene transfer methods in vivo using non-invasive bioluminescent imaging techniques. BMC Biotechnol 2011; 11: 62.

[39] Suda T, Liu D. Hydrodynamic gene delivery: its principles and applications. Mol Ther 2007; 15(12): 2063-9.

[40] Budker V, Zhang G, Danko I, Williams P, Wolff J. The efficient expression of intravascularly delivered DNA in rat muscle. Gene Ther 1998; 5(2): 272-6.

[41] Liu F, Song Y, Liu D. Hydrodynamics-based transfection in animals by systemic administration of plasmid DNA. Gene Ther 1999; 6(7): 1258-66.

[42] Bonamassa B, Hai L, Liu D. Hydrodynamic gene delivery and its applications in pharmaceutical research. Pharm Res 2011; 28(4): 694-701.

[43] Yang PL, Althage A, Chung J, Chisari FV. Hydrodynamic injection of viral DNA: a mouse model of acute hepatitis B virus infection. Proc Natl Acad Sci U S A 2002; 99(21): 13825-30.

[44] Kamimura K, Yokoo T, Abe H, et al. Image-Guided Hydrodynamic Gene Delivery: Current Status and Future Directions. Pharmaceutics 2015; 7(3): 213-23.

[45] Tomizawa M, Shinozaki F, Motoyoshi Y, et al. Sonoporation: Gene transfer using ultrasound. World J Methodol 2013; 3(4): 39-44.

[46] Fechheimer M, Boylan JF, Parker S, et al. Transfection of mammalian cells with plasmid DNA by scrape loading and sonication loading. Proc Natl Acad Sci U S A 1987; 84(23): 8463-7.

[47] Nelson TR, Fowlkes JB, Abramowicz JS, Church CC. Ultrasound biosafety considerations for the practicing sonographer and sonologist. J Ultrasound Med 2009; 28(2): 139-50.

[48] Miller DL, Pislaru SV, Greenleaf JE. Sonoporation: mechanical DNA delivery by ultrasonic cavitation. Somat Cell Mol Genet 2002; 27(1-6): 115-34.

[49] Shapiro G, Wong AW, Bez M, et al. Multiparameter evaluation of in vivo gene delivery using ultrasound-guided, microbubble-enhanced sonoporation. J Control Release 2016; 223: 157-64.

[50] Kim HJ, Greenleaf JF, Kinnick RR, Bronk JT, Bolander ME. Ultrasound-mediated transfection of mammalian cells. Hum Gene Ther 1996; 7(11): 1339-46.

[51] Luft C, Ketteler R. Electroporation Knows No Boundaries: The Use of Electrostimulation for siRNA Delivery in Cells and Tissues. J Biomol Screen 2015; 20(8): 932-42.

[52] Dean DA, Gasiorowski JZ. Nonviral gene delivery. Cold Spring Harb Protoc 2011; 2011(3): top101.

[53] Neumann E, Schaefer-Ridder M, Wang Y, Hofschneider PH. Gene transfer into mouse lyoma cells by electroporation in high electric fields. EMBO J 1982; 1(7): 841-5.

[54] Titomirov AV, Sukharev S, Kistanova E. In vivo electroporation and stable transformation of skin cells of newborn mice by plasmid DNA. Biochim Biophys Acta 1991; 1088(1): 131-4.

[55] Heller R, Jaroszeski M, Atkin A, et al. In vivo gene electroinjection and expression in rat liver. FEBS Lett 1996; 389(3): 225-8.

[56] Heller LC, Jaroszeski MJ, Coppola D, et al. Optimization of cutaneous electrically mediated plasmid DNA delivery using novel electrode. Gene Ther 2007; 14(3): 275-80.

[57] Graham FL, van der Eb AJ. A new technique for the assay of infectivity of human adenovirus 5 DNA. Virology 1973; 52(2): 456-67.

[58] Roy I, Mitra S, Maitra A, Mozumdar S. Calcium phosphate nanoparticles as novel non-viral vectors for targeted gene delivery. Int J Pharm 2003; 250(1): 25-33.

[59] Sokolova V, Epple M. Inorganic nanoparticles as carriers of nucleic acids into cells. Angew Chem Int Ed Engl 2008; 47(8): 1382-95.

[60] Kuo IY, Ehrlich BE. Signaling in muscle contraction. Cold Spring Harb Perspect Biol 2015; 7(2): a006023.

[61] Xie Y, Chen Y, Sun M, Ping Q. A mini review of biodegradable calcium phosphate nanoparticles for gene delivery. Curr Pharm Biotechnol 2013; 14(10): 918-25.

[62] Chowdhury EH, Sasagawa T, Nagaoka M, Kundu AK, Akaike T. Transfecting mammalian cells by DNA/calcium phosphate precipitates: effect of temperature and pH on precipitation. Anal Biochem 2003; 314(2): 316-8.

[63] Jordan M, Schallhorn A, Wurm FM. Transfecting mammalian cells: optimization of critical parameters affecting calcium-phosphate precipitate formation. Nucleic Acids Res 1996; 24(4): 596-601.

[64] Jiang M, Deng L, Chen G. High Ca(2+)-phosphate transfection efficiency enables single neuron gene analysis. Gene Ther 2004; 11(17): 1303-11.

[65] Felgner PL, Gadek TR, Holm M, et al. Lipofection: a highly efficient, lipid-mediated DNA-transfection procedure. Proc Natl Acad Sci U S A 1987; 84(21): 7413-7.

[66] Wasungu L, Hoekstra D. Cationic lipids, lipoplexes and intracellular delivery of genes. J Control Release 2006; 116(2): 255-64.

[67] Carter M, Shieh J. Gene delivery strategies. In: Farra N, Ed. Guide to research techniques in neuroscience. 2nd ed. Academic Press: Cambridge, MA 2015; pp. 239-52.

[68] Zhao Y, Huang L. Lipid nanoparticles for gene delivery. Adv Genet 2014; 88: 13-36.

[69] Ross PC, Hui SW. Lipoplex size is a major determinant of in vitro lipofection efficiency. Gene Ther 1999; 6(4): 651-9.

[70] Dalby B, Cates S, Harris A, et al. Advanced transfection with Lipofectamine 2000 reagent: primary neurons, siRNA, and high-throughput applications. Methods 2004; 33(2): 95-103.

[71] Khatri N, Baradia D, Vhora I, Rathi M, Misra A. Development and characterization of siRNA lipoplexes: Effect of different lipids, in vitro evaluation in cancerous cell lines and in vivo toxicity study. AAPS PharmSciTech 2014; 15(6): 1630-43.

[72] McClorey G, Banerjee S. Cell-Penetrating Peptides to Enhance Delivery of Oligonucleotide-Based Therapeutics. Biomedicines 2018; 6(2).

[73] Gagat M, Zielinska W, Grzanka A. Cell-penetrating peptides and their utility in genome function modifications (Review). Int J Mol Med 2017; 40(6): 1615-23.

[74] Marqus S, Pirogova E, Piva TJ. Evaluation of the use of therapeutic peptides for cancer treatment. J Biomed Sci 2017; 24(1): 21.

[75] Liu BR, Huang YW, Aronstam RS, Lee HJ. Identification of a Short Cell-Penetrating Peptide from Bovine Lactoferricin for Intracellular Delivery of DNA in Human A549 Cells. PLoS One 2016; 11(3): e0150439.

[76] Chang M, Huang YW, Aronstam RS, Lee HJ. Cellular delivery of noncovalently-associated macromolecules by cell-penetrating peptides. Curr Pharm Biotechnol 2014; 15(3): 267-75.

[77] Huang YW, Lee HJ, Tolliver LM, Aronstam RS. Delivery of nucleic acids and nanomaterials by cell-penetrating peptides: opportunities and challenges. Biomed Res Int 2015; 2015: 834079.

[78] Schwarze SR, Dowdy SF. In vivo protein transduction: intracellular delivery of biologically active proteins, compounds and DNA. Trends Pharmacol Sci 2000; 21(2): 45-8.

[79] Heitz F, Morris MC, Divita G. Twenty years of cell-penetrating peptides: from molecular mechanisms to therapeutics. Br J Pharmacol 2009; 157(2): 195-206.

[80] Agrawal P, Bhalla S, Usmani SS, et al. CPPsite 2.0: a repository of experimentally validated cell-penetrating peptides. Nucleic Acids Res 2016; 44(D1): D1098-103.

[81] Holton TA, Pollastri G, Shields DC, Mooney C. CPPpred: prediction of cell penetrating peptides. Bioinformatics 2013; 29(23): 3094-6.

[82] Pandey P, Patel V, George NV, Mallajosyula SS. KELM-CPPpred: Kernel Extreme Learning Machine Based Prediction Model for Cell-Penetrating Peptides. J Proteome Res 2018; 17(9): 3214-22.

[83] Gautam A, Chaudhary K, Kumar R, et al. In silico approaches for designing highly effective cell penetrating peptides. J Transl Med 2013; 11: 74.

[84] Tang H, Su ZD, Wei HH, Chen W, Lin H. Prediction of cell-penetrating peptides with feature selection techniques. Biochem Biophys Res Commun 2016; 477(1): 150-4.

[85] Wei L, Xing P, Su R, et al. CPPred-RF: A Sequence-based Predictor for Identifying Cell-Penetrating Peptides and Their Uptake Efficiency. J Proteome Res 2017; 16(5): 2044-53.

[86] Wei L, Tang J, Zou Q. SkipCPP-Pred: an improved and promising sequence-based predictor for predicting cell-penetrating peptides. BMC Genomics 2017; 18(Suppl 7): 742.

[87] Manavalan B, Subramaniyam S, Shin TH, Kim MO, Lee G. Machine-Learning-Based Prediction of Cell-Penetrating Peptides and Their Uptake Efficiency with Improved Accuracy. J Proteome Res 2018; 17(8): 2715-26.

[88] Qiang X, Zhou C, Ye X, et al. CPPred-FL: a sequence-based predictor for large-scale identification of cell-penetrating peptides by feature representation learning. Brief Bioinform 2018.

[89] Wang S, Cao Z, Li M, Yue Y. G-DipC: An Improved Feature Representation Method for Short Sequences to Predict the Type of Cargo in Cell-Penetrating Peptides. IEEE/ACM Trans Comput Biol Bioinform 2020; 17(3): 739-47.

[90] Fu X, Cai L, Zeng X, Zou Q. StackCPPred: a stacking and pairwise energy content-based prediction of cell-penetrating peptides and their uptake efficiency. Bioinformatics 2020; 36(10): 3028-34.

[91] Arif M, Ahmad S, Ali F, et al. TargetCPP: accurate prediction of cell-penetrating peptides from optimized multi-scale features using gradient boost decision tree. J Comput Aided Mol Des 2020; 34(8): 841-56.

[92] Zhu P, Jin L. Cell Penetrating Peptides: A Promising Tool for the Cellular Uptake of Macromolecular Drugs. Curr Protein Pept Sci 2018; 19(2): 211-20.

[93] Conner SD, Schmid SL. Regulated portals of entry into the cell. Nature 2003; 422(6927): 37-44.

[94] Allinquant B, Hantraye P, Mailleux P, et al. Downregulation of amyloid precursor protein inhibits neurite outgrowth in vitro. J Cell Biol 1995; 128(5): 919-27.

[95] Morris MC, Vidal P, Chaloin L, Heitz F, Divita G. A new peptide vector for efficient delivery of oligonucleotides into mammalian cells. Nucleic Acids Res 1997; 25(14): 2730-6.

[96] Kardani K, Hashemi A, Bolhassani A. Comparison of HIV-1 Vif and Vpu accessory proteins for delivery of polyepitope constructs harboring Nef, Gp160 and P24 using various cell penetrating peptides. PLoS One 2019; 14(10): e0223844.

[97] Borrelli A, Tornesello AL, Tornesello ML, Buonaguro FM. Cell Penetrating Peptides as Molecular Carriers for Anti-Cancer Agents. Molecules 2018; 23(2).

[98] Radis-Baptista G, Campelo IS, Morlighem JRL, Melo LM, Freitas VJF. Cell-penetrating peptides (CPPs): From delivery of nucleic acids and antigens to transduction of engineered nucleases for application in transgenesis. J Biotechnol 2017; 252: 15-26.

[99] Park K. In vivo DNA delivery with NickFect peptide vectors. J Control Release 2016; 241: 242.

[100] Bender E. Gene therapy: Industrial strength. Nature 2016; 537(7619): S57-9.

[101] Glogau R, Blitzer A, Brandt F, et al. Results of a randomized, double-blind, placebo-controlled study to evaluate the efficacy and safety of a botulinum toxin type A topical gel for the treatment of moderate-to-severe lateral canthal lines. J Drugs Dermatol 2012; 11(1): 38-45.

[102] Lonn P, Dowdy SF. Cationic PTD/CPP-mediated macromolecular delivery: charging into the cell. Expert Opin Drug Deliv 2015; 12(10): 1627-36.

[103] Guidotti G, Brambilla L, Rossi D. Cell-Penetrating Peptides: From Basic Research to Clinics. Trends Pharmacol Sci 2017; 38(4): 406-24.

[104] Lostale-Seijo I, Louzao I, Juanes M, Montenegro J. Peptide/Cas9 nanostructures for ribonucleoprotein cell membrane transport and gene edition. Chem Sci 2017; 8(12): 7923-31.

[105] Huang YW, Lee HJ. Cell-penetrating peptides for medical theranostics and targeted gene delivery. In: Koutsopoulos S, Ed. Peptide applications in biomedicine, biotechnology and bioengineering. Woodhead Publishing: Oxford, UK 2017; pp. 359–70.

[106] Ramakrishna S, Kwaku Dad AB, Beloor J, et al. Gene disruption by cell-penetrating peptide-mediated delivery of Cas9 protein and guide RNA. Genome Res 2014; 24(6): 1020-7.

[107] Oude Blenke E, Evers MJ, Mastrobattista E, van der Oost J. CRISPR-Cas9 gene editing: Delivery aspects and therapeutic potential. J Control Release 2016; 244(Pt B): 139-48.

[108] He Y, Li F, Huang Y. Smart Cell-Penetrating Peptide-Based Techniques for Intracellular Delivery of Therapeutic Macromolecules. Adv Protein Chem Struct Biol 2018; 112: 183-220.

[109] Goswami R, Subramanian G, Silayeva L, et al. Gene Therapy Leaves a Vicious Cycle. Front Oncol 2019; 9: 297.

[110] Crystal RG. Adenovirus: the first effective in vivo gene delivery vector. Hum Gene Ther 2014; 25(1): 3-11.

[111] Zabner J, Couture LA, Gregory RJ, et al. Adenovirus-mediated gene transfer transiently corrects the chloride transport defect in nasal epithelia of patients with cystic fibrosis. Cell 1993; 75(2): 207-16.

[112] Goncalves MA, de Vries AA. Adenovirus: from foe to friend. Rev Med Virol 2006; 16(3): 167-86.

[113] Chirmule N, Propert K, Magosin S, et al. Immune responses to adenovirus and adeno-associated virus in humans. Gene Ther 1999; 6(9): 1574-83.

[114] Liu Q, Muruve DA. Molecular basis of the inflammatory response to adenovirus vectors. Gene Ther 2003; 10(11): 935-40.

[115] Alba R, Bosch A, Chillon M. Gutless adenovirus: last-generation adenovirus for gene therapy. Gene Ther 2005; 12 Suppl 1: S18-27.

[116] Yoon SO, Lois C, Alvirez M, et al. Adenovirus-mediated gene delivery into neuronal precursors of the adult mouse brain. Proc Natl Acad Sci U S A 1996; 93(21): 11974-9.

[117] Lv Y, Xiao FJ, Wang Y, et al. Efficient gene transfer into T lymphocytes by fiber-modified human adenovirus 5. BMC Biotechnol 2019; 19(1): 23.

[118] Ramos-Kuri M, Rapti K, Mehel H, et al. Dominant negative Ras attenuates pathological ventricular remodeling in pressure overload cardiac hypertrophy. Biochim Biophys Acta 2015; 1853(11 Pt A): 2870-84.

[119] Atchison RW, Casto BC, Hammon WM. Adenovirus-Associated Defective Virus Particles. Science 1965; 149(3685): 754-6.

[120] Blacklow NR, Hoggan MD, Rowe WP. Isolation of adenovirus-associated viruses from man. Proc Natl Acad Sci U S A 1967; 58(4): 1410-5.

[121] Wang D, Tai PWL, Gao G. Adeno-associated virus vector as a platform for gene therapy delivery. Nat Rev Drug Discov 2019; 18(5): 358-78.

[122] Berns KI, Linden RM. The cryptic life style of adeno-associated virus. Bioessays 1995; 17(3): 237-45.

[123] Merten OW, Gaillet B. Viral vectors for gene therapy and gene modification approaches. Biochem Eng J 2016; 108: 98-115.

[124] Tse LV, Moller-Tank S, Asokan A. Strategies to circumvent humoral immunity to adeno-associated viral vectors. Expert Opin Biol Ther 2015; 15(6): 845-55.

[125] Liu Y, Kim YJ, Ji M, et al. Enhancing gene delivery of adeno-associated viruses by cell-permeable peptides. Mol Ther Methods Clin Dev 2014; 1: 12.

[126] Wu Z, Asokan A, Samulski RJ. Adeno-associated virus serotypes: vector toolkit for human gene therapy. Mol Ther 2006; 14(3): 316-27.

[127] Briggs JA, Simon MN, Gross I, et al. The stoichiometry of Gag protein in HIV-1. Nat Struct Mol Biol 2004; 11(7): 672-5.

[128] Fuller SD, Wilk T, Gowen BE, Krausslich HG, Vogt VM. Cryo-electron microscopy reveals ordered domains in the immature HIV-1 particle. Curr Biol 1997; 7(10): 729-38.

[129] Kingston RL, Olson NH, Vogt VM. The organization of mature Rous sarcoma virus as studied by cryoelectron microscopy. J Struct Biol 2001; 136(1): 67-80.

[130] Yeager M, Wilson-Kubalek EM, Weiner SG, Brown PO, Rein A. Supramolecular organization of immature and mature murine leukemia virus revealed by electron cryo-microscopy: implications for retroviral assembly mechanisms. Proc Natl Acad Sci U S A 1998; 95(13): 7299-304.

[131] Milone MC, O'Doherty U. Clinical use of lentiviral vectors. Leukemia 2018; 32(7): 1529-41.

[132] Maetzig T, Galla M, Baum C, Schambach A. Gammaretroviral vectors: biology, technology and application. Viruses 2011; 3(6): 677-713.

[133] Zhang W, Cao S, Martin JL, Mueller JD, Mansky LM. Morphology and ultrastructure of retrovirus particles. AIMS Biophys 2015; 2(3): 343-69.

[134] Wirth T, Parker N, Yla-Herttuala S. History of gene therapy. Gene 2013; 525(2): 162-9.

[135] Vargas JE, Chicaybam L, Stein RT, et al. Retroviral vectors and transposons for stable gene therapy: advances, current challenges and perspectives. J Transl Med 2016; 14(1): 288.

[136] Howe SJ, Mansour MR, Schwarzwaelder K, et al. Insertional mutagenesis combined with acquired somatic mutations causes leukemogenesis following gene therapy of SCID-X1 patients. J Clin Invest 2008; 118(9): 3143-50.

[137] Hacein-Bey-Abina S, Le Deist F, Carlier F, et al. Sustained correction of X-linked severe combined immunodeficiency by ex vivo gene therapy. N Engl J Med 2002; 346(16): 1185-93.

[138] Gaspar HB, Bjorkegren E, Parsley K, et al. Successful reconstitution of immunity in ADA-SCID by stem cell gene therapy following cessation of PEG-ADA and use of mild preconditioning. Mol Ther 2006; 14(4): 505-13.

[139] Hacein-Bey-Abina S, Garrigue A, Wang GP, et al. Insertional oncogenesis in 4 patients after retrovirus-mediated gene therapy of SCID-X1. J Clin Invest 2008; 118(9): 3132-42.

[140] Gaspar HB, Parsley KL, Howe S, et al. Gene therapy of X-linked severe combined immunodeficiency by use of a pseudotyped gammaretroviral vector. Lancet 2004; 364(9452): 2181-7.

[141] Mavilio F, Pellegrini G, Ferrari S, et al. Correction of junctional epidermolysis bullosa by transplantation of genetically modified epidermal stem cells. Nat Med 2006; 12(12): 1397-402.

[142] Dudley ME, Wunderlich JR, Robbins PF, et al. Cancer regression and autoimmunity in patients after clonal repopulation with antitumor lymphocytes. Science 2002; 298(5594): 850-4.

[143] Morgan RA, Dudley ME, Wunderlich JR, et al. Cancer regression in patients after transfer of genetically engineered lymphocytes. Science 2006; 314(5796): 126-9.

[144] McGarrity GJ, Hoyah G, Winemiller A, et al. Patient monitoring and follow-up in lentiviral clinical trials. J Gene Med 2013; 15(2): 78-82.

[145] Dull T, Zufferey R, Kelly M, et al. A third-generation lentivirus vector with a conditional packaging system. J Virol 1998; 72(11): 8463-71.

[146] Escors D, Breckpot K. Lentiviral vectors in gene therapy: their current status and future potential. Arch Immunol Ther Exp (Warsz) 2010; 58(2): 107-19.

[147] Buchschacher GL, Jr., Wong-Staal F. Development of lentiviral vectors for gene therapy for human diseases. Blood 2000; 95(8): 2499-504.

[148] Dishart KL, Denby L, George SJ, et al. Third-generation lentivirus vectors efficiently transduce and phenotypically modify vascular cells: implications for gene therapy. J Mol Cell Cardiol 2003; 35(7): 739-48.

[149] Barde I, Laurenti E, Verp S, et al. Lineage- and stage-restricted lentiviral vectors for the gene therapy of chronic granulomatous disease. Gene Ther 2011; 18(11): 1087-97.

[150] Zhang KX, Moussavi M, Kim C, et al. Lentiviruses with trastuzumab bound to their envelopes can target and kill prostate cancer cells. Cancer Gene Ther 2009; 16(11): 820-31.

[151] Shi Q, Wilcox DA, Fahs SA, et al. Lentivirus-mediated platelet-derived factor VIII gene therapy in murine haemophilia A. J Thromb Haemost 2007; 5(2): 352-61.

[152] Biffi A, Montini E, Lorioli L, et al. Lentiviral hematopoietic stem cell gene therapy benefits metachromatic leukodystrophy. Science 2013; 341(6148): 1233158.

[153] Sessa M, Lorioli L, Fumagalli F, et al. Lentiviral haemopoietic stem-cell gene therapy in early-onset metachromatic leukodystrophy: an ad-hoc analysis of a non-randomised, open-label, phase 1/2 trial. Lancet 2016; 388(10043): 476-87.

[154] Urnov FD, Rebar EJ, Holmes MC, Zhang HS, Gregory PD. Genome editing with engineered zinc finger nucleases. Nat Rev Genet 2010; 11(9): 636-46.

[155] Carroll D. Progress and prospects: zinc-finger nucleases as gene therapy agents. Gene Ther 2008; 15(22): 1463-8.

[156] Lampreht Tratar U, Horvat S, Cemazar M. Transgenic Mouse Models in Cancer Research. Front Oncol 2018; 8: 268.

[157] Doudna JA, Charpentier E. Genome editing. The new frontier of genome engineering with CRISPR-Cas9. Science 2014; 346(6213): 1258096.

[158] Sander JD, Dahlborg EJ, Goodwin MJ, et al. Selection-free zinc-finger-nuclease engineering by context-dependent assembly (CoDA). Nat Methods 2011; 8(1): 67-9.

[159] Reyon D, Tsai SQ, Khayter C, et al. FLASH assembly of TALENs for high-throughput genome editing. Nat Biotechnol 2012; 30(5): 460-5.

[160] Kim H, Kim JS. A guide to genome engineering with programmable nucleases. Nat Rev Genet 2014; 15(5): 321-34.

[161] Kim YG, Cha J, Chandrasegaran S. Hybrid restriction enzymes: zinc finger fusions to Fok I cleavage domain. Proc Natl Acad Sci U S A 1996; 93(3): 1156-60.

[162] Wolfe SA, Nekludova L, Pabo CO. DNA recognition by Cys2His2 zinc finger proteins. Annu Rev Biophys Biomol Struct 2000; 29: 183-212.

[163] Laity JH, Lee BM, Wright PE. Zinc finger proteins: new insights into structural and functional diversity. Curr Opin Struct Biol 2001; 11(1): 39-46.

[164] Gaj T, Gersbach CA, Barbas CF, 3rd. ZFN, TALEN, and CRISPR/Cas-based methods for genome engineering. Trends Biotechnol 2013; 31(7): 397-405.

[165] Lino CA, Harper JC, Carney JP, Timlin JA. Delivering CRISPR: a review of the challenges and approaches. Drug Deliv 2018; 25(1): 1234-57.

[166] Cornu TI, Thibodeau-Beganny S, Guhl E, et al. DNA-binding Specificity Is a Major Determinant of the Activity and Toxicity of Zinc-finger Nucleases. Mol Ther 2008; 16(2): 352-8.

[167] Gupta RM, Musunuru K. Expanding the genetic editing tool kit: ZFNs, TALENs, and CRISPR-Cas9. J Clin Invest 2014; 124(10): 4154-61.

[168] Joung JK, Sander JD. TALENs: a widely applicable technology for targeted genome editing. Nat Rev Mol Cell Biol 2013; 14(1): 49-55.

[169] Dunbar CE, High KA, Joung JK, et al. Gene therapy comes of age. Science 2018; 359(6372).

[170] Christian M, Cermak T, Doyle EL, et al. Targeting DNA double-strand breaks with TAL effector nucleases. Genetics 2010; 186(2): 757-61.

[171] Nemudryi AA, Valetdinova KR, Medvedev SP, Zakian SM. TALEN and CRISPR/Cas Genome Editing Systems: Tools of Discovery. Acta Naturae 2014; 6(3): 19-40.

[172] Ishino Y, Shinagawa H, Makino K, Amemura M, Nakata A. Nucleotide sequence of the iap gene, responsible for alkaline phosphatase isozyme conversion in Escherichia coli, and identification of the gene product. J Bacteriol 1987; 169(12): 5429-33.

[173] Jansen R, Embden JD, Gaastra W, Schouls LM. Identification of genes that are associated with DNA repeats in prokaryotes. Mol Microbiol 2002; 43(6): 1565-75.

[174] Perez Rojo F, Nyman RKM, Johnson AAT, et al. CRISPR-Cas systems: ushering in the new genome editing era. Bioengineered 2018; 9(1): 214-21.

[175] Razzouk S. CRISPR-Cas9: A cornerstone for the evolution of precision medicine. Ann Hum Genet 2018; 82(6): 331-57.

[176] Jinek M, Chylinski K, Fonfara I, et al. A programmable dual-RNA-guided DNA endonuclease in adaptive bacterial immunity. Science 2012; 337(6096): 816-21.

[177] Cong L, Ran FA, Cox D, et al. Multiplex genome engineering using CRISPR/Cas systems. Science 2013; 339(6121): 819-23.

[178] Tang Prize Foundation. Biopharmaceutical Science [Online] 2016 [cited 2020]. Available at: https://www.tang-prize.org/en/owner.php?cat=11&y=3

[179] Yang H, Jaeger M, Walker A, et al. Break Breast Cancer Addiction by CRISPR/Cas9 Genome Editing. J Cancer 2018; 9(2): 219-31.

[180] Barman A, Deb B, Chakraborty S. A glance at genome editing with CRISPR-Cas9 technology. Curr Genet 2020; 66(3): 447-62.

[181] Li K, Wang G, Andersen T, Zhou P, Pu WT. Optimization of genome engineering approaches with the CRISPR/Cas9 system. PLoS One 2014; 9(8): e105779.

[182] Qi LS, Larson MH, Gilbert LA, et al. Repurposing CRISPR as an RNA-guided platform for sequence-specific control of gene expression. Cell 2013; 152(5): 1173-83.

[183] Makarova KS, Wolf YI, Iranzo J, et al. Evolutionary classification of CRISPR-Cas systems: a burst of class 2 and derived variants. Nat Rev Microbiol 2020; 18(2): 67-83.

[184] Anzalone AV, Randolph PB, Davis JR, et al. Search-and-replace genome editing without double-strand breaks or donor DNA. Nature 2019; 576(7785): 149-57.

[185] Watters KE, Shivram H, Fellmann C, et al. Potent CRISPR-Cas9 inhibitors from Staphylococcus genomes. Proc Natl Acad Sci U S A 2020; 117(12): 6531-9.

[186] Komor AC, Kim YB, Packer MS, Zuris JA, Liu DR. Programmable editing of a target base in genomic DNA without double-stranded DNA cleavage. Nature 2016; 533(7603): 420-4.

[187] Konermann S, Lotfy P, Brideau NJ, et al. Transcriptome Engineering with RNA-Targeting Type VI-D CRISPR Effectors. Cell 2018; 173(3): 665-76 e14.

[188] Cornu TI, Mussolino C, Cathomen T. Refining strategies to translate genome editing to the clinic. Nat Med 2017; 23(4): 415-23.

[189] Carroll D. Genome Editing: Past, Present, and Future. Yale J Biol Med 2017; 90(4): 653-9.

[190] Cyranoski D. Chinese scientists to pioneer first human CRISPR trial. Nature 2016; 535(7613): 476-7.

[191] Hudacsek V, Gyorffy B. Genome engineering using the CRISPR-Cas9 system and applications in cancer research. Magy Onkol 2018; 62(2): 119-27.

[192] Montano A, Forero-Castro M, Hernandez-Rivas JM, Garcia-Tunon I, Benito R. Targeted genome editing in acute lymphoblastic leukemia: a review. BMC Biotechnol 2018; 18(1): 45.

[193] GP-write [Online] 2019 [cited 2020]. Available at: https://engineeringbiologycenter.org/

[194] Doudna JA. The promise and challenge of therapeutic genome editing. Nature 2020; 578(7794): 229-36.

[195] ClinicalTrials.gov [Online] [cited 2020]. Available at: https://clinicaltrials.gov/

[196] Wang D, Zhang F, Gao G. CRISPR-Based Therapeutic Genome Editing: Strategies and In Vivo Delivery by AAV Vectors. Cell 2020; 181(1): 136-50.

[197] Haridy R. FDA hits pause on one of the first US human clinical trials to use CRISPR [Online] 2018 [cited 2020]. Available at: https://newatlas.com/us-crispr-human-trial-hold-fda/54862/

[198] Censorship hinders development? Should we be more cautious about human trials of gene editing, or should we give it a go? [Online] 2018 [cited 2020]. Available at: https://theinitium.com/roundtable/20180124-roundtable-global-Crispr-Cas9/

[199] China uses gene editing to treat chronic human diseases [Online] 2018 [cited 2020]. Available at: http://big5.sputniknews.cn/china/201802051024637731/

[200] Normile D. Shock greets claim of CRISPR-edited babies. Science 2018; 362(6418): 978-9.

[201] Abduljalil JM. Laboratory diagnosis of SARS-CoV-2: available approaches and limitations. New Microbes New Infect 2020; 36: 100713.

[202] Broughton JP, Deng X, Yu G, et al. CRISPR-Cas12-based detection of SARS-CoV-2. Nat Biotechnol 2020; 38(7): 870-4.

[203] Abbott TR, Dhamdhere G, Liu Y, et al. Development of CRISPR as an Antiviral Strategy to Combat SARS-CoV-2 and Influenza. Cell 2020; 181(4): 865-76 e12.

[204] The Lancet. Genome editing: proceed with caution. Lancet 2018; 392(10144): 253.

[205] Roy B, Zhao J, Yang C, et al. CRISPR/Cascade 9-Mediated Genome Editing-Challenges and Opportunities. Front Genet 2018; 9: 240.

[206] Fellmann C, Gowen BG, Lin PC, Doudna JA, Corn JE. Cornerstones of CRISPR-Cas in drug discovery and therapy. Nat Rev Drug Discov 2017; 16(2): 89-100.

II. DOX-LOADED DNA ORIGAMI TRIANGLE UPTAKE AND CYTOTOXIC EFFECTS IN TRIPLE NEGATIVE BREAST CANCER CELL LINES

Natalie J. Holl[1], Taryn Dewey[2], Rachel Nixon[2], Chandler Mossman[1], Risheng Wang[2], Katie B. Shannon[1], Yue-Wern Huang[1]

[1]Department of Biological Sciences, Missouri University of Science and Technology, Rolla, MO 65409, USA

[2]Department of Chemistry, Missouri University of Science and Technology, Rolla, MO 65409, USA

ABSTRACT

Breast cancer affects the lives of millions of women around the world each year. Triple negative breast cancers (TNBCs) lack therapy methods with few side-effects. Less harsh treatment options are necessary to improve the overall outcome for cancer patients. DNA origami is a promising nanocarrier system. However, the uptake mechanism of this carrier is not well understood. In this study, we describe the killing efficiency of a model DOX-loaded DNA triangle origami (DOX-DNA-T) using viability reduction and apoptosis induction in two TNBC cell lines (MDA-MB-231 and MDA-MB-453). The internalization pathway of DOX-DNA-T was elucidated by inhibiting energy-dependent, clathrin-dependent, caveolin-dependent, and macropinocytosis pathways. The subcellular localization of DOX-DNA-T was determined by co-localization with organelle-specific dyes using a confocal microscope. DOX-DNA-T was able to increase the internalized DOX concentration and altered its subcellular localization. DOX-DNA-T delayed the killing of DOX, but modulated the toxicity between cell lines. The carrier facilitated DOX entry by clathrin- and caveolin-dependent endocytosis, as well as by

macropinocytosis. Understanding the cellular fate of DOX-DNA-T can help to better design DNA nanostructures as a drug delivery system.

1. INTRODUCTION

In 2018, 18.1 million new cases of cancer were diagnosed worldwide [1]. Breast cancer contributed 11.6% of these cases and remains the second leading cause of all cancer related deaths, despite years of research and funding in the field [1]. Breast cancers are classified based on receptor upregulation and overexpression compared to normal tissue. The three most commonly upregulated and targeted receptors for treatment are the estrogen receptor (ER), the progesterone receptor (PR), and the human epidermal growth factor receptor (HER-2) [2]. However, these three receptors are absent in 15 to 20% of breast cancers, which are referred to as triple negative breast cancer (TNBC) [2]. Consequently, approximately 367 thousand new cases of TNBC are diagnosed yearly, based on global cancer statistics. Because TNBCs lack the three common breast cancer receptors, they do not respond well to frequently used targeted therapies [2]. Recurrence and metastasis are also significantly higher in patients with TNBCs [3]. Metastasis is a large concern when treating cancer patients as metastasis is the cause of 90% of all cancer deaths [4]. Aggressiveness (i.e., fast formation and growth) and invasiveness make triple negative tumors difficult to remove surgically without causing harm to the surrounding healthy tissue [5]. All these factors result in worse prognosis for patients with TNBC compared to other breast cancers.

There are few treatment options for patients with TNBCs and no FDA-approved targeted therapies against the cells of TNBC tumors [2]. Conventionally, TNBCs are treated by surgically removing the tumor mass in combination with radiation or chemotherapy [5-7]. During the course of treatment, a cancer patient is likely to receive anthracyclines (e.g., Doxorubicin, DOX), which efficiently kill cells that are actively replicating [8-10]. However, anthracyclines also destroy non-cancerous cells that quickly replicate. Even if they are not replicating, cells may be harmed as the metabolic reduction of anthracyclines results in hydroxyl free radicals [11]. Cardiomyocytes are particularly susceptible to damage by the free radicals produced by anthracyclines, resulting in side effects as severe as congestive heart failure [11]. Furthermore, resistance to DOX often develops in cancerous tissues treated with the drug [11], presenting major challenges for cancers with few treatment options or for recurring cancers. In order to decrease side effects of anticancer drugs like DOX, various carriers at the nanoscale are in development which increase drug delivery efficiency using the principle of enhanced permeability and retention. This principle is observed in tumors where vasculature is abnormally permeable and lymphatic drainage is low, leading to a buildup of compounds within the tumor [12]. Delivering drugs directly to tumors using nanocarriers can combat drug resistance by increasing retention time and can reduce overall toxicity in patients [13-15].

One promising nanoparticle being used for delivery is DNA. Using base pairing, a long single-strand of circular viral genome can be artificially folded into theoretically any desired shape with the help of short synthetic DNA strands (staple strands) to act as a carrier [13]. The resulting nanostructures, or DNA origami, have size-dependent drug-loading capacity and drug release [15]. The amount of drug loaded is tunable based on

the length of the DNA strands and on DNA helix rotation [16, 17]. The use of DNA in nanostructures allows precise geometry to be designed and easy functionalization [13, 18]. Exact control of nanostructure geometry is desirable as it influences biodistribution, movement through fluids, and cellular internalization [19]. Because DNA nanostructures have been observed to possess a high affinity for and enhanced retention within tumor masses in vivo [18, 20], they have been evaluated to deliver anti-cancer drugs.

DNA nanostructures are an excellent carrier for anthracyclines, as the drugs readily intercalate into the DNA double helix and slowly dissociate [14, 15, 21]. In a previous in vitro study by Zeng et al., drug-loaded DNA nanostructures had higher accumulation and persistence in cancer cells compared to free DOX [15]. DNA nanostructures have shown the ability to passively target and localize in tumors in vivo [18, 20]. Despite the potential success of DNA nanostructure to deliver anti-cancer drugs to tumors, their exact cellular uptake mechanism and subcellular localization are still unknown, which are influential to drug delivery efficacy. In this study, we evaluated a model DOX-loaded DNA triangle origami (DOX-DNA-T) in two different TNBC cell lines: MDA-MB-231 and MDA-MB-453. We hypothesized that 1) DOX-DNA-T nanostructures would have more effective cellular uptake and killing efficiency in triple negative breast cancer cells than DOX alone, 2) the uptake mechanism of DOX-DNA-T would be energy dependent, and 3) DOX-DNA-T would localize within cellular organelles. This study provides insight to the cellular uptake mechanisms and the subcellular fate of DNA origami, with the potential to further improve the therapeutic efficacy of DNA origami as a carrier system.

2. MATERIALS AND METHODS

2.1. DNA ORIGAMI PRODUCTION

Triangle origami were prepared from synthetic L-form M13mp18 phage single-stranded genomes (Bayou Biolabs: Metairie, LA, USA) using techniques described in our previous publications [15]. Briefly, genomes and appropriately designed staple strands (Integrated DNA Technologies: Coralville, IA, USA) were mixed, incubated at 90°C, and allowed to anneal over a slow 12-hour cool down to room temperature. Desired shape was confirmed with atomic force microscopy (AFM). DOX (Fisher BioReagents: Pittsburgh, PA, USA) was loaded into the origami by incubating the folded structures with 1.2 mM of the drug for 18 hours at 37°C. Loading efficiency was calculated based on the concentration of free DOX in solution after pelleting the loaded origami and was in the range of 85 to 95%. The concentration was determined using a fluorescence spectrophotometer set to excite at 485 nm and record at 500 to 650 nm (Nanodrop 3300, ThermoFisher Scientific: Waltham, MA, USA), with the final concertation loaded being approximately 1 mM per 5 nM of origami. The stability of complexes was confirmed by incubation with different concentrations (2, 5, and 10%) of HyClone fetal clone serum (FCS, GE Healthcare Life Sciences: Marlborough, MA, USA), which is rich in proteases and DNases normally found in the blood. After incubation for various time periods, origami was run on 0.8% agarose gels containing ethidium bromide and imaged. Unless otherwise noted, the range of concentrations used to treat cells were 0, 0.0025, 0.005, 0.01, 0.025, and 0.05 nM of naked origami; 0, 0.5, 1, 2, 5, and 10 μM of free DOX; or the equivalent concentrations of each component combined in DOX-DNA-T.

2.2. CELL MAINTENANCE

MDA-MB-231 and MDA-MB-453 cell lines were purchased from the American Type Culture Collection (ATCC: Manassas, VA, USA) and were cultured in RPMI-1640 medium supplemented with 5% HyClone FCS and 1% antibiotics (50 units/mL penicillin and 50 μg/mL streptomycin). Cells were maintained in tissue culture dishes in a humidified incubator at 37°C and 5% CO2. Both cell lines were harvested upon reaching 80 to 90% confluency using trypsin for experiments or were split 1:2 to 1:4 every 2 to 4 days. Cultures were replaced with cells from liquid nitrogen storage before exceeding 30 passages. The pH of cultures was analyzed 24 and 48 hours after cells were established for 24 hours in order to determine if there were additional differences between the physiological conditions of the cells.

2.3. CELL VIABILITY

The viability of MDA-MB-231 and MDA-MB-453 cells was determined by seeding 50,000 cells for 48-hour and 100,000 cells for 24-hour experiments into 24-well cell culture plates with equal cell density per well. A lower starting density was used for longer incubations to prevent overcrowding in controls. Cells were allowed to adhere to the plates for 24 hours and then dosed with a concentration range of each component of the triangle origami. Viability was compared between naked origami, free DOX, and DOX-DNA-T. Viability was accessed using a standard sulforhodamine B (SRB) protein dye assay [22]. Briefly, after exposure for 24 or 48 hours, cells were fixed in 500 μL of 10% trichloroacetic acid for 1 hour at 4°C. Cells were rinsed with distilled water three times, excess water was removed by pipet, and plates were allowed to dry completely in a

refrigerator (at least overnight). Following drying, cells were stained with 500 μL of 0.2% SRB in 1% acetic acid for 30 minutes on a rocker. Cells were then washed three times with 1% acetic acid, with each wash sitting for 20 minutes on the rocker. Excess acetic acid was removed from the wells and plates were air dried for 30 minutes. Tris-HCl (300 μL, 10 mM) was used to dissociate the dye from cellular proteins, 250 μL of the dye solution was transferred to a 96-well microplate, and color intensity was measured using a FLUOstar Omega microplate reader set to read absorbance at 510 nm (BMG Labtechnologies: Cary, NC, USA). Wells with no cultured cells that were stained and washed served as blanks. Cell viability was calculated as the sample well intensity as a percentage of the control well intensity, with blanks subtracted from both.

Cell viability, or culture growth, was also analyzed for MDA-MB-231 cells after incubation in media with different concentrations of FCS (2, 5, and 10%) to establish the appropriate testing conditions for the DNA origami. Cells were seeded at 80,000 cells per well in 24-well cell culture plates. Cells were grown until attached, approximately 4.5 hours, and fixed to serve as a 0-time point. Other cells were grown for 24, 48, and 72 hours after the 0-time point, fixed, and analyzed using the SRB assay. Cell viability was calculated as the sample well intensity as a percentage of the highest well intensity, with appropriate blanks subtracted from both.

2.4. APOPTOSIS

Annexin V-Alexa Fluor 647 is a dye that binds with high affinity to phosphatidylserine, a cell signaling molecule expressed on the cell surface during

apoptosis [23]. Quantification of this molecule allows the portion of cells undergoing apoptosis to be determined.

For flow cytometry, MDA-MB-231 or MDA-MB-453 cells (300,000 cells per dish for 48-hour and 600,000 cells per dishfor 24-hour) were grown in 6 cm cell culture dishes for 24 hours before dosing with a concentration range of DOX or DOX-DNA-T for either 24 or 48 hours. After exposure, cells were washed with phosphate buffered saline (PBS), suspended from the plates using trypsin, and pelleted by centrifugation. The old media and PBS wash were collected and pelleted along with the trypsinized cells in order to prevent the loss of floating cells undergoing apoptosis. Cells were suspended in 1 μL of Annexin V-Alexa Fluor 647 (50 μg/mL, BioLegend: San Diego, CA, USA) in 100 μL of 1x Annexin V-binding buffer (BD Biosciences: San Jose, CA, USA), with a final dye concentration of 0.5 μg/mL. Cells were incubated with Annexin V-Alexa Fluor 647 for 30 minutes at room temperature in the dark before analysis using a CytoFLEX flow cytometer (Beckman-Coulter: Brea, CA, USA) with the far-red filter set (ex: 638 nm, em: 660/10 nm). For each experiment, 10,000 to 30,000 single cell events were captured. The population of cells undergoing apoptosis was determined using FCS Express 6 analysis software. Cells were considered apoptotic if they were positive for Annexin V staining.

For confocal microscopy, MDA-MB-231 or MDA-MB-453 cells (150,000 cells per dish for 48-hour and 300,000 cells per dish for 24-hour) were grown in 3.5 cm glass-bottomed cell culture dishes (MatTek: Ashland, MA, USA) for 24 hours before dosing with 10 μM of free DOX or an equivalent amount of DOX loaded into DNA-T. After exposure for 24 or 48 hours, old media was collected and cells were washed twice with

PBS. The first wash and old media were collected and centrifuged to harvest floating cells. The second wash was left on cells while centrifuging the media to prevent drying and was then discarded. Pelleted cells were suspended in 5 μL of Annexin V-Alexa Fluor 647 (BioLegend, 50 μg/mL) in 500 μL of Annexin V-binding buffer, with a final dye concentration of 0.5 μg/mL. Dye solution and floating cells were then pipetted back into the sample dishes and evenly distributed by tilting the dish. Dishes were incubated for 30 minutes at 37°C in the dark. Following incubation with Annexin V, cells were incubated with 1 mL of Hoechst 33342 (10 mg/mL stock, diluted 1:2000 in PBS) for 5 minutes at 37°C in the dark. Cells were then imaged using a Nikon A1R HD25 confocal microscope comparisonusing a 40x Plan Fluor objective with 1.3 NA (Nikon Instruments: Melville, NY, USA). Green (ex: 488 nm, em: 500-550 nm), far-red (ex: 640 nm, em: 663-673 nm) and blue (ex: 405, em: 425-475 nm) filter sets were used to detect DOX, Annexin V, and Hoechst, respectively. Images were obtained using Elements software and a four channel High-Sensitivity/GaAsP PMT detector unit. Confocal images were analyzed in ImageJ (National Institutes of Health).

2.5. UPTAKE

Unless otherwise noted, the following setup was used for uptake experiments. MDA-MB-231 and MBA-MB-453 cells used for flow cytometry analysis were seeded into the wells of a 24-well plate at a density of 100,000 cells per well and allowed to grow for 48 hours before treatment. Drug concentration was selected to be 2 μM in uptake studies to limit cell death and ensure cells were healthy enough for internalization. DOX intensity was measured on a flow cytometer using the green filter set (ex: 488 nm,

em: 525/40 nm), as DOX itself is fluorescent with a peak excitation wavelength of 470 nm and emission of 560 nm [24]. For each experiment, 10,000 to 30,000 single cell events were captured. For confocal microscopy, MDA-MB-231 and MBA-MB-453 cells were plated in 3.5 cm glass-bottom culture dishes at a density of 300,000 cells per dish and allowed to adhere for 48 hours. DOX intensity was also analyzed using a 488 nm laser line on the confocal. Confocal images were analyzed in ImageJ. All cells were washed twice before harvesting with trypsin or imaging. Pelleted cells were suspended in 150 μL of PBS for flow cytometry. Cells were imaged in 1 mL of warm PBS. All inhibitor solutions were sterilized by using 0.2 μm syringe filters. Concentrations for inhibitors were the same as the ones used for our previous publication [25]. Live cell fluorescence was examined within 1 hour of washing or harvesting. Confocal images were analyzed in ImageJ.

2.5.1. Subcellular Localization. DOX-DNA-T were expected to be subcellularly localized in the lysosome, mitochondria, or nuclei. Using LysoTracker (Deep Red, Invitrogen: Carlsbad, CA, USA), MitoTracker (Deep Red, Invitrogen), and Hoechst 33342, subcellular localization was revealed by co-localization with these specific markers. MDA-MB-231 and MBA-MB-453 cells were plated in 3.5 cm glass-bottom culture dishes and grown for 24 hours for microscopy. Cells were treated with 2 μM of DOX or DOX-DNA-T for 24 or 48 hours. The treated or untreated cells were incubated with specific markers following the instructions provided by the manufacturers. Briefly, LysoTracker and MitoTracker were prepared as 100x stock solutions and diluted in fresh media to 50 nM. Media was prewarmed and 2 mL of each solution was added to cells. Cells were incubated for 30 minutes at 37°C in the dark. Staining solution was discarded

and samples were then incubated with 1 mL of warm Hoechst 33342 (10 mg/mL stock, diluted 1:2000 in PBS) for 5 minutes at 37°C in the dark. The cells were washed twice with warm PBS, 1 mL of warm PBS was added to each dish to keep the cells moist, and cells were then imaged using a confocal microscope.

2.5.2. Time-Dependent Uptake. The internalization of DOX and DOX-DNA-T was determined over the course of 0 to 4 hours and after 24 and 48 hours using flow cytometry. Cells were plated in 6-well culture plates at a density of 500,000 per well and allowed to grow for 48 hours before dosing with 2 μM of DOX or DOX-DNA-T. During 0- to 4-hour experiments, cells were dosed at 0 minutes, 10 minutes, 30 minutes, 1 hour, 2 hours, and 4 hours before washing. For 24- and 48-hour experiments, cells were plated at 225,000 cells per well and 112,500 cells per well in 3.5 cm culture dishes, respectively, and allowed to grow for 48 hours before dosing. Surface area was accounted for in order to achieve the same cell density in different culture vessels. Select time points (1, 24, and 48 hours) were chosen be imaged using a confocal microscope for visual comparison.

2.5.3. Energy Inhibition. Multiple forms of endocytosis, including clathrin- and caveolin-dependent endocytosis, as well as macropinocytosis, require energy for vesicle formation at the cell surface [26]. MDA-MB-231 and MBA-MB-453 cells were plated into a 24-well plate or glass-bottomed culture dishes for flow cytometry or microscopy, respectively. An inhibitor cocktail was prepared at 100x in water and diluted to 10x in PBS. Cells were pre-incubated with the metabolic inhibitor mixture (230 μM of sodium azide, 15 μM of sodium fluoride, and 2 μg/mL antimycin A) for 1 hour, followed by incubation with 2 μM of DOX or DOX-DNA-T for 1 hour. Cells were then imagined with a Nikon confocal microscope or harvested for analysis using a flow cytometer. DOX

was expected to diffuse into cells [27-30], so further inhibition studies were carried out using only DOX-DNA-T.

2.5.4. Clathrin Inhibition. MDA-MB-231 and MBA-MB-453 cells were plated into a 24-well plate or glass-bottomed culture dishes for flow cytometry or microscopy, respectively. A 2x working solution of sucrose was prepared in water. A 1000x stock solution of chlorpromazine was prepared in water and was diluted to a 10x working solution in PBS. A 100x stock solution of monodansylcadaverine (MDC) was prepared in 100% methanol and was diluted to a 10x working solution in PBS. Cells were pre-incubated with 0.45 M sucrose, 10 μM chlorpromazine, or 25 μg/mL MDC for 30 minutes at 37°C. Cells were treated with 2 μM of DOX-DNA-T for 1 hour and then imagined with a Nikon confocal microscope or harvested for analysis using a flow cytometer.

2.5.5. Caveolae Inhibition. To inhibit lipid raft-dependent caveolin endocytosis, filipin and nystatin were used to sequester cholesterol [31]. MDA-MB-231 and MBA-MB-453 cells were plated into a 24-well plate or glass-bottomed culture dishes for flow cytometry or microscopy, respectively. A 100x stock solution of filipin was prepare in 1:4 DMSO:PBS and was diluted to a 10x working solution in PBS. A 100x stock solution of nystatin was prepare in 100% methanol and was diluted to a 10x working solution in PBS. Cells were pre-incubated with 3 μg/mL filipin or 20 μg/mL nystatin for 30 minutes before treatment with 2 μM of DOX-DNA-T for another 1 hour. Cell were then imagined with a Nikon confocal microscope or harvested for analysis using a flow cytometer.

2.5.6. Macropinocytosis Inhibition. MDA-MB-231 and MBA-MB-453 cells were plated into a 24-well plate or glass-bottomed culture dishes for flow cytometry or

microscopy, respectively. Cells were pre-treated with EIPA (5-(N-ethyl-N-isopropyl)-amiloride (30 μM) or cytochalasin D (Cyt D, 1 μg/mL) for 30 minutes before treatment with 2 μM of DOX-DNA-T for another 1 hour. EIPA was prepared as 2 mg/mL stock solution in 100% methanol and diluted to 10x in PBS. Cyt D was prepared as 1 mg/mL stock solution in 100% ethanol and diluted to 10x in PBS. Cells were then imagined with a Nikon confocal microscope or harvested for analysis using a flow cytometer.

2.6. STATISTICAL ANALYSIS

Data are expressed as the mean ± standard deviation. One-way ANOVA followed by Tukey tests were used to compare the differences between all groups. A student's t-test was used to compare differences between specific treatment groups and controls. All statistics were performed in MiniTab 19 and most graphs were produced in GraphPad Prism 4. Each in vitro experiment was carried out in at least three independent experiments. Statistical significance was set at $p < 0.05$.

3. RESULTS

3.1. DNA ORIGAMI PRODUCTION

DNA origami triangle folding and shape were confirmed using AFM (Figure 1A). DNA-T were approximately 50 nm across and their geometry was not altered by the intercalation of DOX. DNA-T showed higher stability in lower concentrations of FCS (Figure 1B), with the least band streaking observed in 2% FCS and the highest observed in 10% FCS. In 10% FCS, origami bands showed low streaking after initial mixing, but

were destabilized relatively quickly. In 5% FCS, origami bands showed similar streaking from 0 to 8 hours, but began to show increased streaking after 12 and 24 hours. In 2%, origami appear to be stable after 16 hours of incubation.

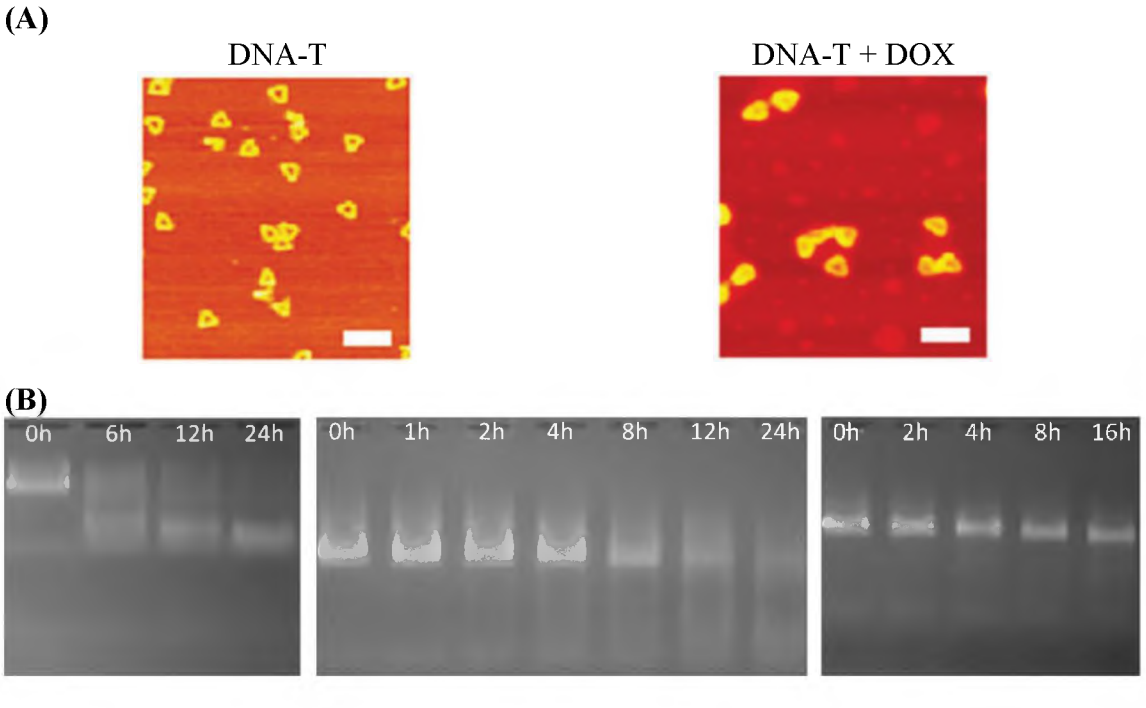

Figure 1. DNA structure and stability confirmation using AFM and agarose gels. (A) AFM images of DNA origami triangles. Scale bar is 100 nm. (B) Agarose gel showing the stability of DNA-T incubated in RPMI-1640 cell culture medium (Left 10%, middle 5%, and right 2% FCS) for the indicated time period.

3.2. CELL VIABILITY

Ideally, DNA-T would be tested in low concentrations of FCS to retain high stability. However, it was unknown if breast cancer cells would retain substantial culture growth if incubated with 2% FCS. The growth of MDA-MB-231 cells in media with different concentrations of FCS was tested using a SRB assay in order to determine the best concentration to use for DNA-T testing (Figure 2). MDA-MB-231 culture growth

was significantly different at all concentrations of FCS (N = 7, p's < 0.05). However, incubation with 5 and 10% FCS resulted in similar increasing growth at all time points. Cells did not grow nearly as well in 2% FCS and the population did not increase from 48 to 72 hours. Therefore, 5% FCS was chosen to provide stability to DNA-T and allow the breast cancer cell cultures to retain a normal amount of growth.

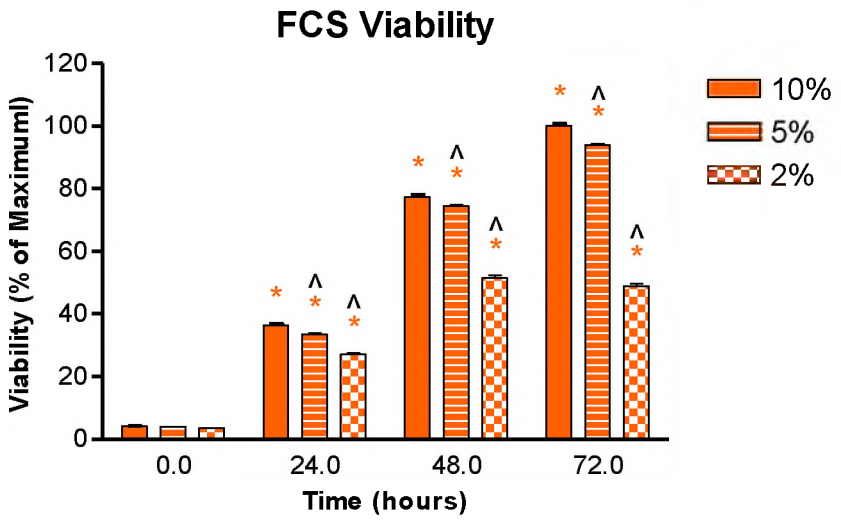

Figure 2. MDA-MB-231 population in 10, 5, and 2% FCS. The cell population after 72h in 10% FCS was the maximum and was normalized to 100%. This population was used to normalize all other treatment groups, * indicates significance vs. 0-time point and ^ indicates significance vs. 10% FCS at a given time point (p's < 0.05, ANOVA with Tukey's post hoc test). The populations between 2% FCS at 48 and 72 h FCS were not different. N = 7 per experiment, 1 experiment.

The viability of both cells lines was accessed after treatment with DNA-T, DOX, and DOX loaded into DNA-T using SRB assays (Figure 3). DNA-T alone did not affect the survival of MDA-MB-231 or MDA-MB-453 cells, which was expected (N = 9, p's > 0.5). The viability of both cell types in DOX and DOX-DNA-T was time- and concentration-dependent. Higher concentrations and longer times resulted in more death.

DOX alone killed more cells after 24 hours than DOX-DNA-T, with significant decreases at 2 through 10 μM in MDA-MB-231 and at 1 through 10 μM in MDA-MB-453 ($N = 9$, p's < 0.005). Cell viability dropped to 46 and 45% in MDA-MB-231 and MDA-MB-453 cells after 10 μM of DOX exposure for 24 hours, respectively. DOX-DNA-T only showed a significant decrease at 5 and 10 μM of DOX in MDA-MB-231 and only at 10 μM in MDA-MB-453 ($N = 9$, p's < 0.05) with 24-hour exposure. The resulting viabilities were 76 and 78% in MDA-MB-231 and MDA-MB-453, respectively, after 24-hour incubation with 10 μM of DOX-DNA-T. After 48 hours of exposure, DOX also decreased viability at lower concentrations, which both cell lines experiencing significant decreases at 0.5 through 10 μM ($N = 9$, p's < 0.005). DOX-DNA-T treatment for 48 hours showed a significant decrease in viability at 2 through 10 μM in both cell lines and additionally at 1 μM for MDA-MB-231 ($N = 9$, p's < 0.005). Both treatments reduced the viability of the cell lines down to a similar level after 48-hour 10 μM exposure, with survival being approximately 7 to 11%.

Table 1. Acidity of MDA-MB-231 and MDA-MB-453 cultures. Mean pH ± the SD.

Time	**pH**		
	231	**453**	**Media**
24h	7.12 ± 0.03	7.47 ± 0.03	7.47 ± 0.02
48h	7.04 ± 0.03	7.42 ± 0.02	

MDA-MB-453 seemed more susceptible to DOX alone than MDA-MB-231, with lower viability at 1 through 5 μM after 24 hours and at 0.5 through 2 μM after 48 hours. Loading DOX into DNA seemed to modulate the differences in viability between the two

cell lines. Differences in toxicity were not likely due to altered pH between the cell types, as cell culture media remained around neutral pH (Table 1).

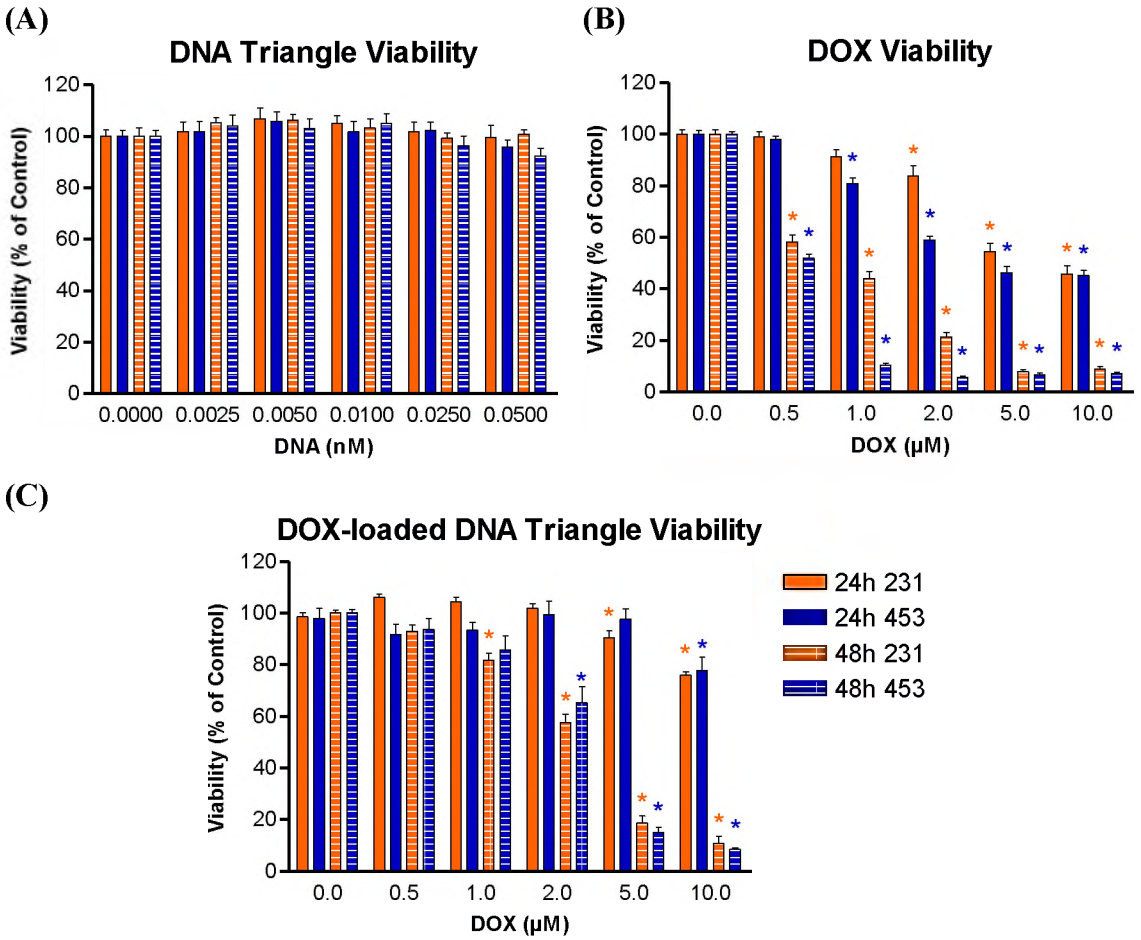

Figure 3. Viability of MDA-MB-231 and 453 cells after exposure to (A) DNA-T alone, (B) free DOX, and (C) DOX-DNA-T for 24 and 48h. Untreated cell population was considered 100% viable and used to normalize the viability of other groups. Treated cell population was calculated as a percentage of the control and compared to the control and other groups using one-way ANOVA with Tukey's post hoc test, * p's < 0.05. N = 3 per experiment, 3 experiments.

3.3. APOPTOSIS

DOX exposure produced a much higher rate of total apoptosis compared to DOX-DNA-T overall (Figure 4). After 48 hours, 10 μM of DOX resulted in 20% and 51% of

MDA-MB-231 and MDA-MB-453 cells undergoing apoptosis, respectively, while 10 μM of DOX-DNA-T after 48 hours resulted in 20% and 16% in the same cell lines. For DOX alone, apoptosis at both time points and in both cell lines was significantly increased at 5 and 10 μM ($N = 3$, p's < 0.05). At 2 μM of DOX, 24- and 48-hour MDA-MB-453, as well as 48-hour MDA-MB-231 were significantly higher ($N = 3$, p's < 0.01). MDA-MB-231 also showed significance at 1 μM of DOX after 48-hour exposure ($N = 3$, p's < 0.05). DOX-DNA-T did not induce significant apoptosis at any concentration after 24 hours, except for 2 μM in MDA-MB-453 cells, which was not substantially higher than the control. After 48 hours, MDA-MB-453 showed significantly higher apoptosis at 1 through 10 μM and MDA-MB-231 at 5 and 10 μM of DOX-DNA-T ($N = 3$, p's < 0.05). Example flow cytometry data is shown in Figure 4C and D.

Figure 5 shows confocal images of MDA-MB-231 and MDA-MB-453 cells after 24- and 48-hour exposure to 10 μM of DOX and DOX-DNA-T. Results were visually comparable to flow data, with cells exposed to DOX alone appearing to have more visible red apoptosis staining than DOX-DNA-T treated cells. Cells treated with DOX-DNA-T also appeared to have a higher concentration of DOX within them, based on the greater fluorescence intensity observed. DOX seemed to be localized in the cytoplasm in both cases. Morphological analysis of the cells with DIC imaging (Figure 6) revealed more debris in cultures treated with DOX-DNA-T and more blebbing cells in cultures treated with DOX alone. Debris in DOX-DNA-T treated cultures were dark and did not appear to have much staining. Some cells appeared to have this debris associated with the cell surface.

(A)

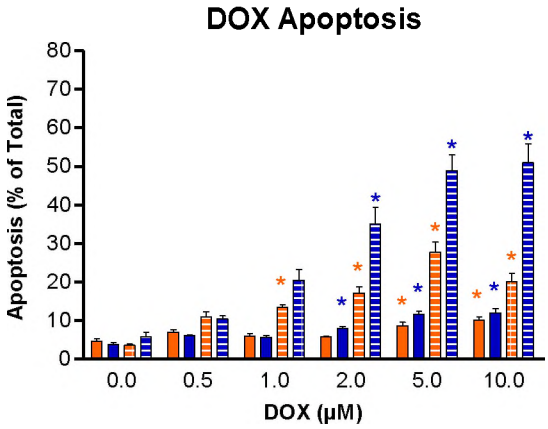

(B)

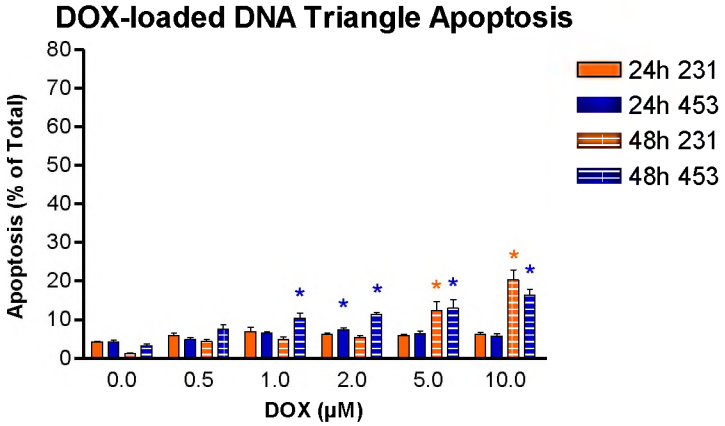

(C)

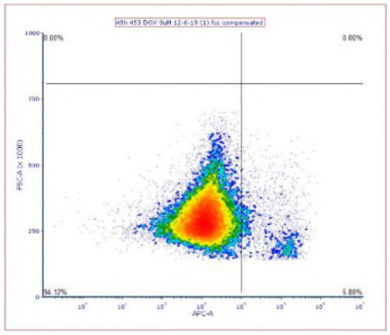

(D)

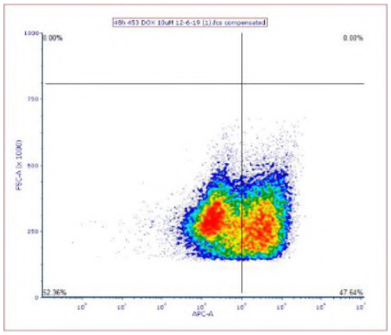

Figure 4. Total apoptosis of MDA-MB-231 and MDA-MB-453 cell lines after exposure to (A) DOX and (B) DOX-DNA-T for 24 and 48h, quantified using flow cytometry. The percentage of cells positive for Annexin V staining were considered apoptotic. Example flow cytometry data of (C) 453 cells with no drug exposure and (D) 453 cells after 48h DOX exposure. Samples were compared to the control and other groups using one-way ANOVA with Tukey's post hoc test, * p's < 0.05. N = 3 experiments, with 10-30k cells per sample.

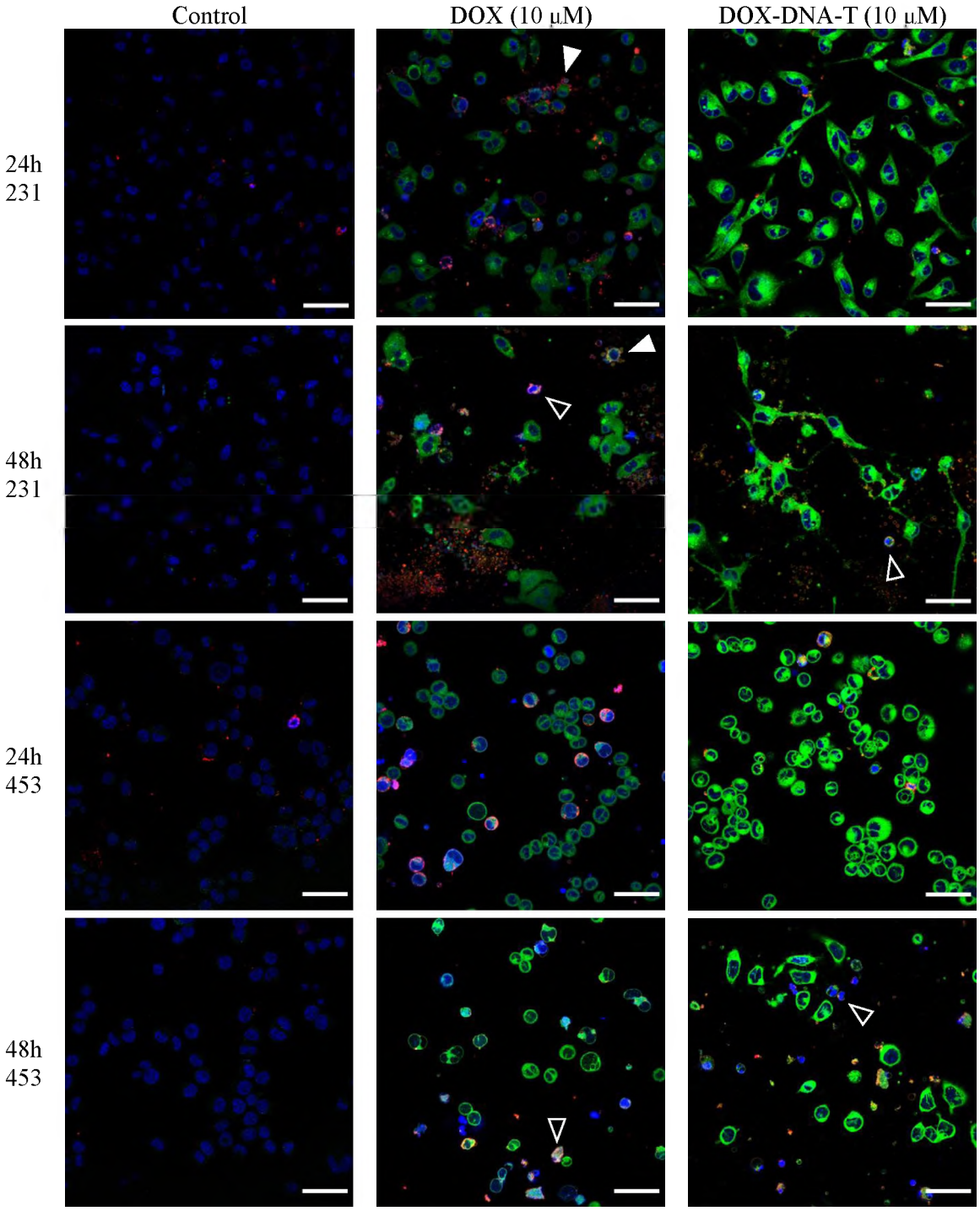

Figure 5. Confocal images of cells undergoing apoptosis after exposure to 10 μM of DOX or DOX-DNA-T. Blue is Hoechst, red is Annexin V, and green is DOX. White arrowheads indicate blebbing cells and white-outlined black arrowheads point to apoptotic bodies. Scale bar is 50 μm, 40x oil objective.

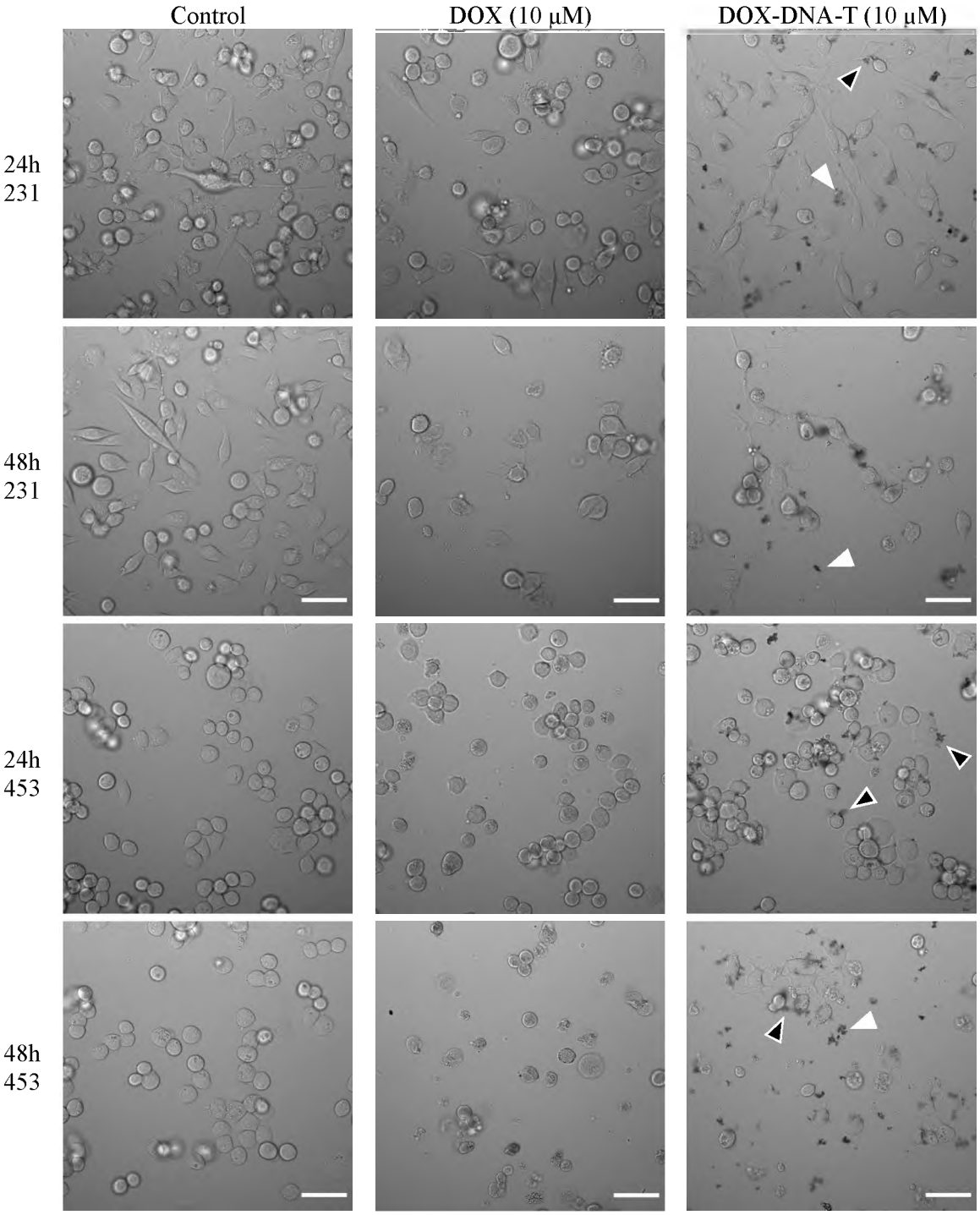

Figure 6. Morphology of cells after exposure to 10 μM of DOX and DOX-DNA-T. White arrowheads point to debris in solution and white-outlined black arrowheads point to membrane-associated debris. Scale bar is 50 μm, 40x oil objective.

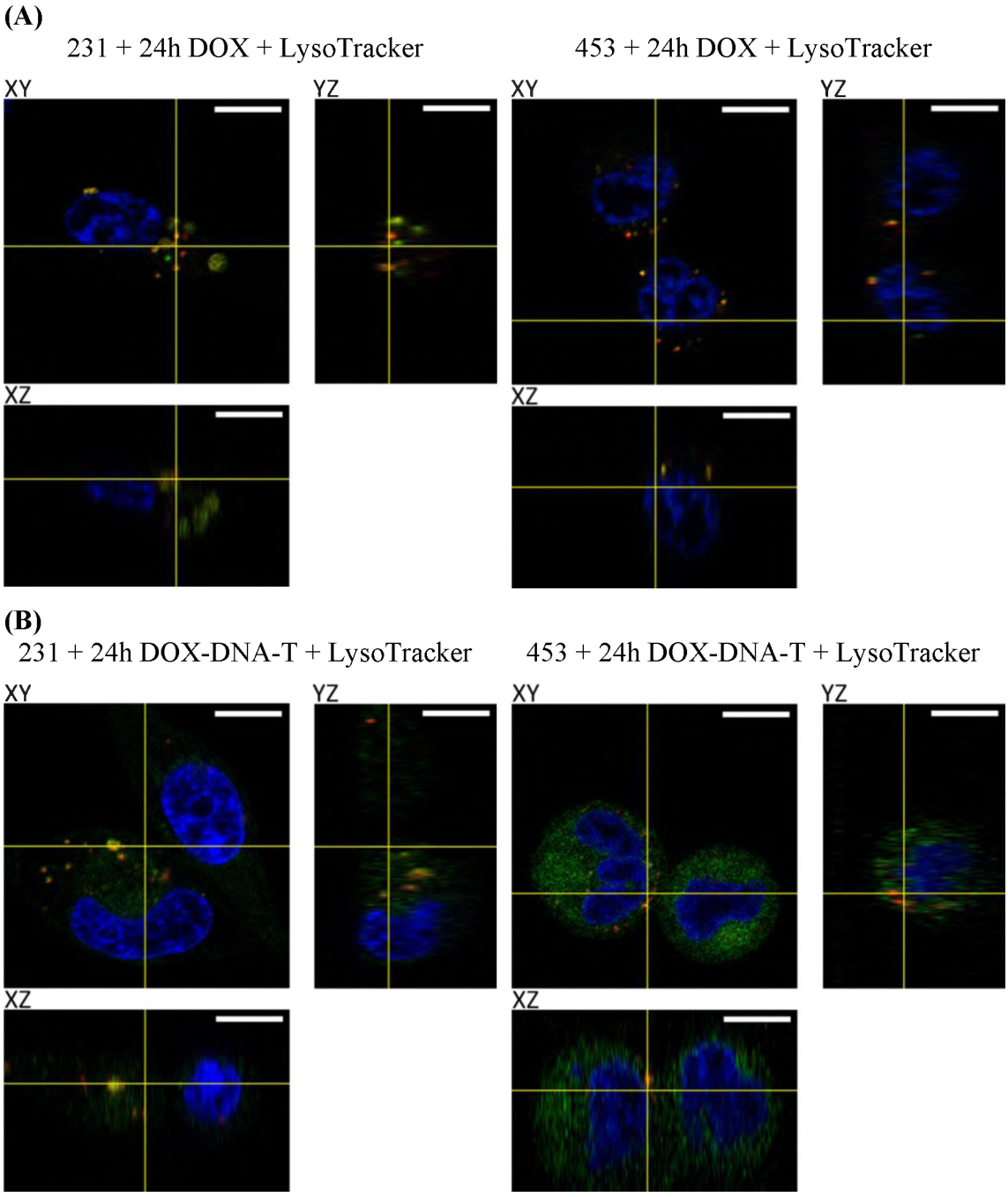

Figure 7. Localization of (A) DOX and (B) DOX-DNA-T in MDA-MB-231 (left) and MDA-MB-453 (right) after 24h. Blue is Hoechst, green is DOX, and red is LysoTracker. Cells were treated with 2 μM of either free DOX or DOX-DNA-T for 24h. Scale bar is 10 μm in XY, XZ, and YZ. Images are 5x zoomed in areas from a 60x oil objective field. Z-stacks were imaged 25 μm around the focal point, with a 1 μm step. Full field images can be found in the supplementary data.

3.4. UPTAKE

3.4.1. Subcellular Localization. DOX alone localized into the lysosome based on green DOX fluorescence co-localizing with the red LysoTracker in both cell lines (Figure 7). DOX-DNA-T were expected to be subcellularly localized in the lysosome, mitochondria, or nuclei. However, DOX-DNA-T was dispersed through the cell cytoplasm, had low nuclear localization, and had relatively low lysosomal localization compared to DOX alone. MDA-MB-453 seemed to have lower DOX-DNA-T lysosomal localization compared to MDA-MB-231, which seemed to increase from 24 to 48 hours. MDA-MB-453 had noticeably smaller lysosomes compared to MDA-MB-231. Localization did not seem to differ substantially between 24 and 48 hours and neither free DOX nor DOX-DNA-T seemed to localize within the mitochondria (Appendix Figures 1-8).

3.4.2. Time-Dependent Uptake. The internalization of DOX and DOX-DNA-T was determined over the course of 0 to 4 hours and after 24 and 48 hours using flow cytometry (Figure 8). Select time points (1, 24, and 48 hours) were chosen be imaged using a confocal microscope for visual comparison. In both cell lines, DOX uptake was significant from 1 to 4 hours and after 24 and 48 hours ($N = 3$, p's < 0.005). DOX uptake was significantly different between 24- and 48-hour incubation ($N = 3$, p's < 0.05). DOX uptake after 24 and 48 hours was not different between the two cell lines ($N = 3$, p's > 0.05). Internalization during 30 minutes to 4 hours and after 24 and 48 hours was significant after DOX-DNA-T exposure ($N = 3$, p's < 0.05). DOX-DNA-T uptake was the same in MDA-MB-453 cells between 24 and 48 hours ($N = 3$, p's > 0.5). Although the average fluorescence of MDA-MB-231 cells was higher after 48-hour DOX-DNA-T

treatment compared to 24-hour treatment, the two time points were not significantly different ($N = 3$, p's > 0.1). MDA-MB-231 cells did show significantly higher fluorescence after incubation with DOX-DNA-T compared to free DOX at both time points and to DOX-DNA-T treated MDA-MB-453 cells after 48 hours ($N = 3$, p's < 0.05). After 24- and 48-hour incubation, MDA-MB-453 cells had similar DOX-DNA-T fluorescence compared to 48-hour DOX ($N = 3$, p's > 0.5). During shorter periods of time, internalization was similar between the free drug and loaded drug in both cell lines ($N = 3$, p's > 0.1 time point vs. time point), though DNA-T averages were lower at every time point. MDA-MB-453 internalized more DOX when it was loaded into DNA-T compared to MDA-MB-231 during the shorter duration incubation, after 2 and 4 hours ($N = 3$, p's < 0.05). Confocal images confirmed that DOX-DNA-T uptake at 1 hour was similar to DOX alone and was higher than free DOX after 24 and 48 hours (Figure 9). DOX-DNA-T had a similar diffused appearance after 1, 24, and 48 hours at 2 μM. However, DOX appeared to be diffused throughout cells after 1 hour and collect into lysosomes after 24 and 48 hours in MDA-MB-231 and after 48 hours in MDA-MB-453.

3.4.3. Energy Inhibition. Inhibition studies were carried out with 1-hour drug incubations as uptake in the first 4 hours did not plateau and 1 hour was the first time point where all conditions were significantly different from the control. Cells incubated with metabolic inhibitors and DOX or DOX-DNA-T are shown in Figure 10. The mixture of metabolic inhibitors prevented energy-dependent internalization by depleting cellular ATP levels. Sodium azide and antimycin A interfere with the mitochondrial electron transport chain [32, 33], while sodium fluoride inhibits glycolysis [34]. Cells were imagined with a confocal microscope or harvested for quantitative analysis using a flow

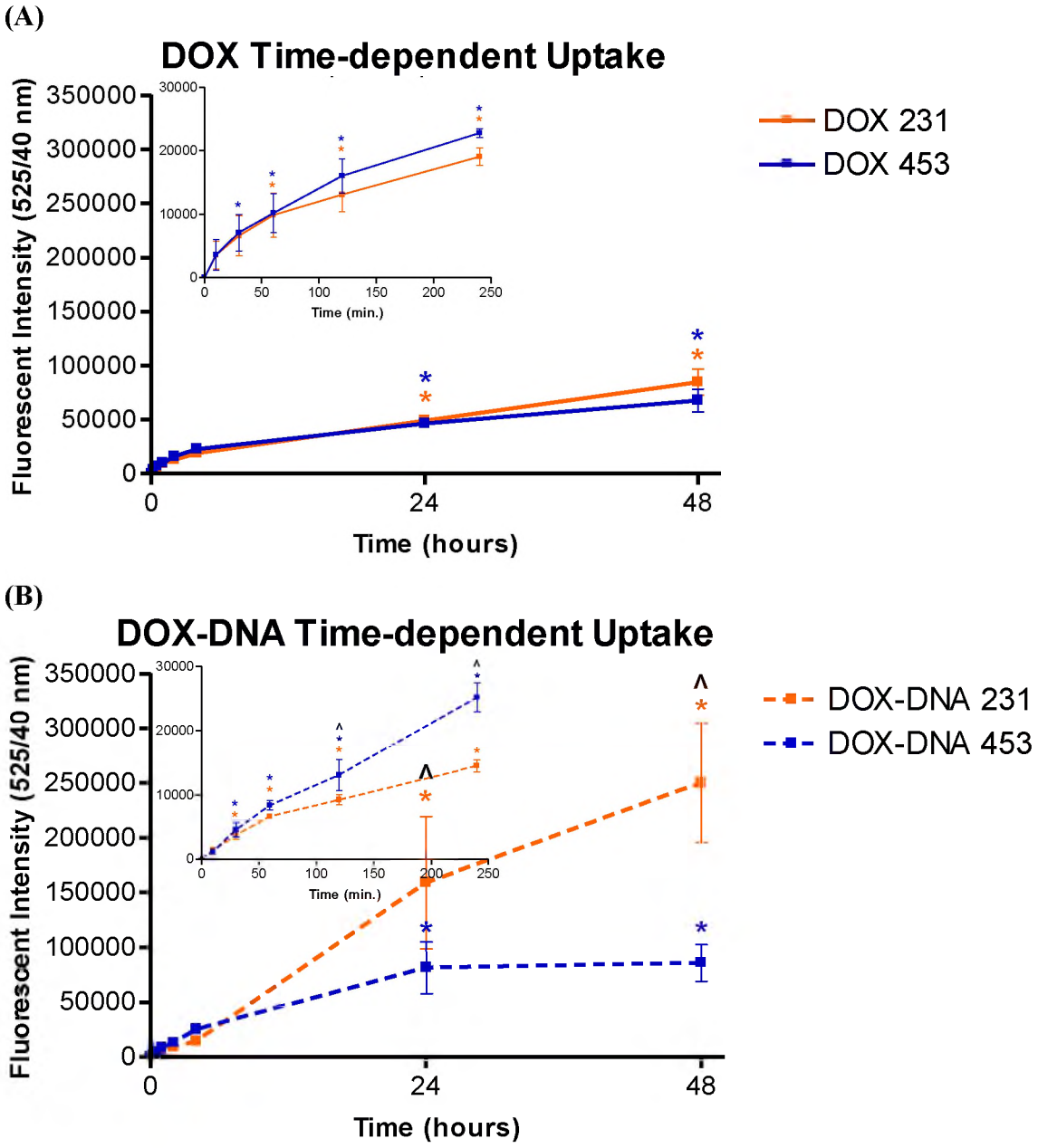

Figure 8. Time-dependent uptake of 2 μM of (A) DOX or (B) DOX-DNA-T. The small graph insert is a magnified 0 to 4h time scale. Significance vs. control is indicated with a colored *, color corresponding to the line color, p's < 0.05. A ^ indicates significance between cell lines at a given time point, p's < 0.05. Analyzed in CytExpert with 525/40 nm filter set (505-545 nm range). Significance between groups and vs. the controls were determined using one-way ANOVA with Tukey's post hoc test. N = 3 experiments, with 10-30k cells per sample.

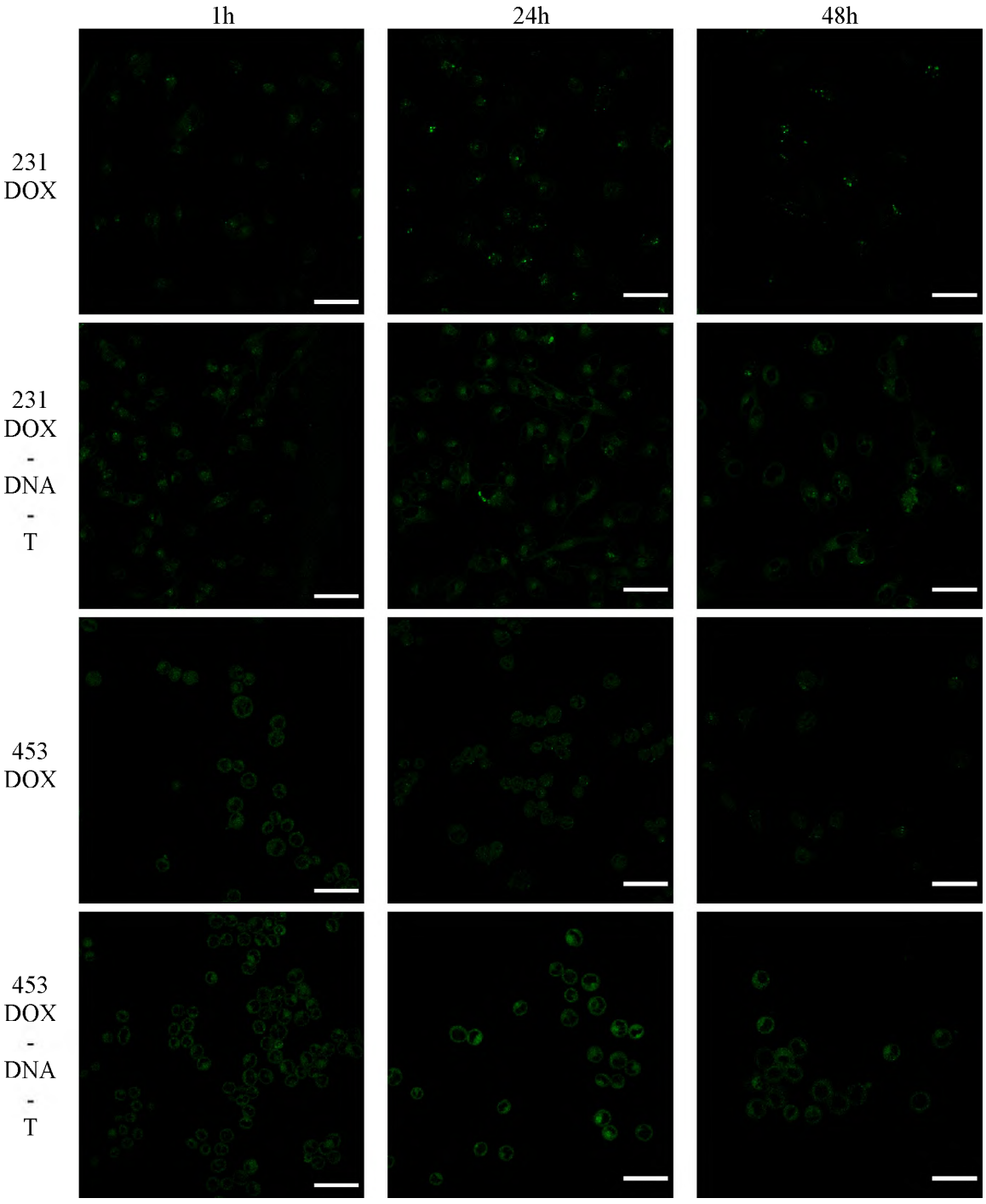

Figure 9. Time-dependent uptake microscopy of DOX or DOX-DNA-T after 1, 24, and 48h. Drug concentration was 2 μM. Scale bar is 50 μm, 40x oil objective.

cytometer. DOX fluorescence inside either cell line did not significantly differ after cells were pre-incubated with a metabolic inhibitor cocktail, indicating that DOX internalization was not energy dependent and through diffusion ($N = 3$, p's > 0.5). Cell fluorescence after treatment with the metabolic inhibitor and DOX-DNA-T was significantly lower than without inhibitor ($N = 3$, p's < 0.05). Energy inhibition reduced MDA-MB-231 fluorescence to 85% of uninhibited fluorescence and MDA-MB-453 to 75%. This indicates that DOX-DNA-T required energy to be internalized. Differences are not as apparent in confocal images for energy inhibited samples or those treated with other inhibitors, likely because fewer cells could be analyzed than with flow cytometry.

3.4.1. Clathrin Inhibition. Both MDA-MB-231 and MDA-MB-453 showed similar trends after incubation with several clathrin-dependent endocytosis inhibitors (Figure 11). The clathrin inhibitors used interfere with clathrin plasma membrane distribution and clathrin-coated pits. Sucrose causes clathrin to form microcages, rather than the normal lattice structures that are required to form endocytic vesicles [35]. Chlorpromazine causes clathrin and the AP-2 protein required for lattice assembly to relocate from the plasma membrane to internal vesicles [36]. MDC functions by stabilizing clathrin-coated pits and limits formation of new lattices [37, 38]. Sucrose and MDC decreased internalization of DOX-DNA-T to a higher degree than Chlorpromazine, though all showed significant decreases ($N = 3$, p's < 0.05). Sucrose decreased fluorescence to 31 and 35% of the uninhibited fluorescence in MDA-MB-231 and MDA-MB-453, respectively. MDC reduced fluorescence to 61% in MDA-MB-231 and 76% in MDA-MB-453, while Chlorpromazine resulted in decreases to 83% and 76% in the same

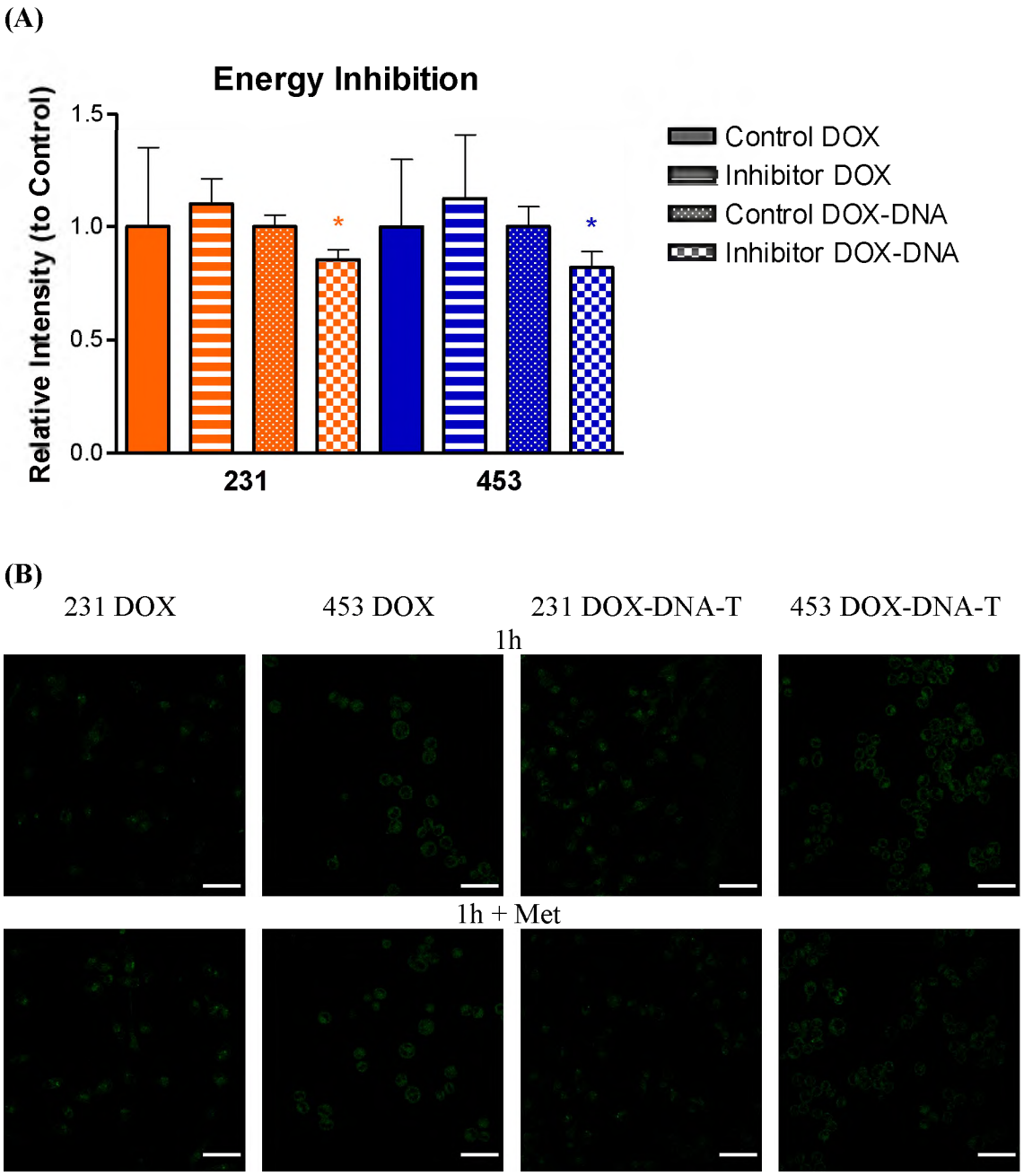

Figure 10. Energy-dependent uptake inhibition of 2 μM of DOX or DOX-DNA-T after 1h. Uninhibited controls after 1h incubation were used to normalize the data set and inhibited samples were compared to the control using one-tailed t-tests, p's < 0.05. N = 3. Scale bar is 50 μm, 40x oil objective.

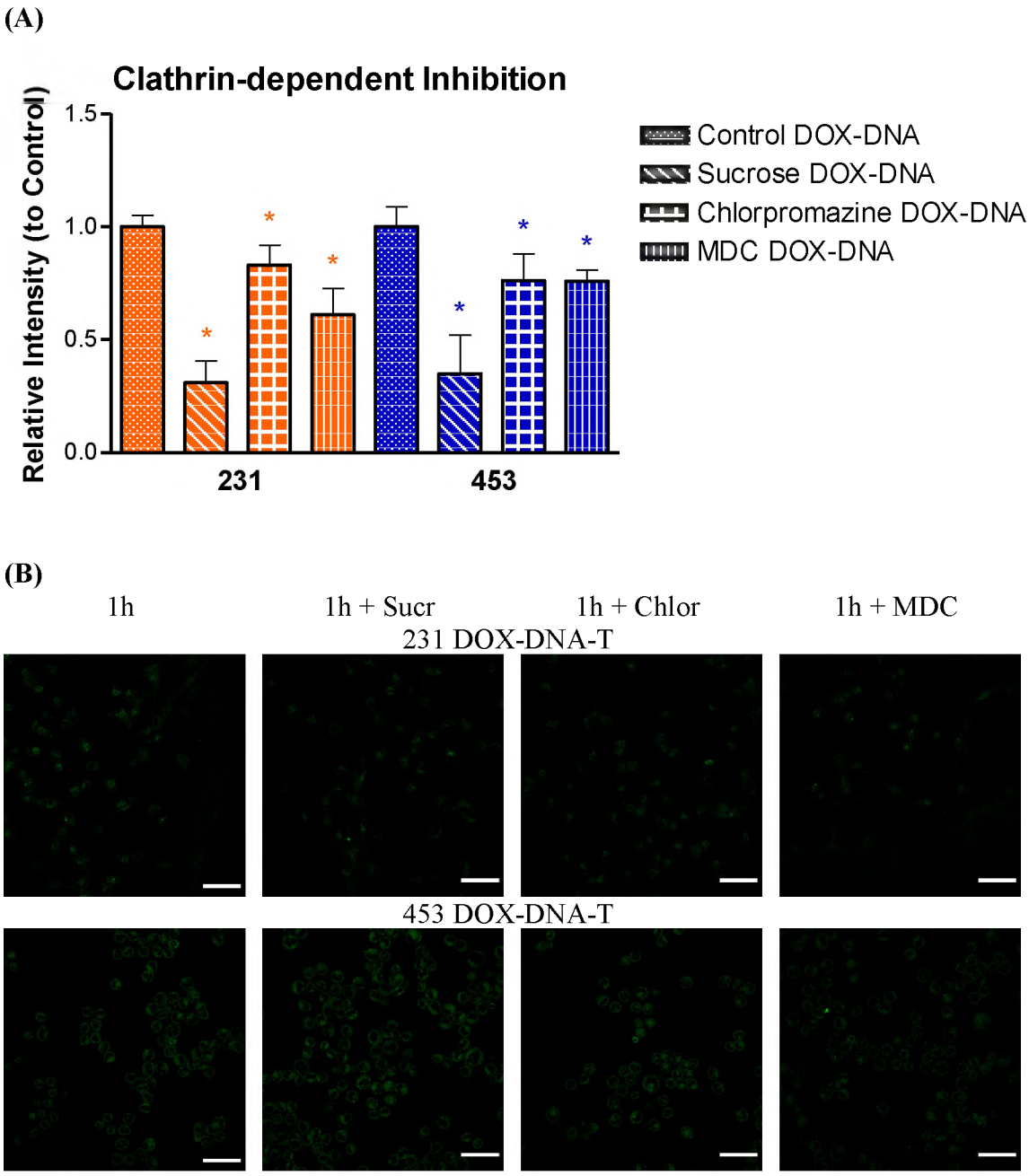

Figure 11. Clathrin-dependent uptake inhibition of 2 μM DOX-DNA-T after 1h. Uninhibited control fluorescence of DOX-DNA-T after 1h incubation was used to normalize the data set and inhibited samples were compared to the control using one-tailed t-tests, p's < 0.05. N = 3. Scale bar is 50 μm, 40x oil objective.

respective cell lines. Sucrose may have decreased fluorescence more than other inhibitors as it is not as specific [31].

3.4.2. Caveolae Inhibition. Caveolin-dependent endocytosis was inhibited with filipin and nystatin pre-incubation (Figure 12). Both sequester and deplete cholesterol from the membrane, which is required for caveolar invagination and lipid-raft-dependent internalization [31, 39]. Filipin and nystatin significantly inhibited DOX-DNA-T uptake in both cell lines ($N = 3$, p's < 0.05). MDA-MB-231 fluorescence was reduced to 83% of the control using filipin and to 71% using nystatin. MDA-MB-453 incubation with filipin reduced cell fluorescence to 63% and nystatin reduced it to 71%.

3.4.3. Macropinocytosis Inhibition. Macropinocytosis inhibitors significantly reduced the fluorescence of cells (Figure 13). Cyt D alters the polymerization of actin [40], on which macropinocytosis is dependent [41]. EIPA inhibits Na+/H+ exchange, insulting in alterations in submembrane pH that affect actin remodeling GTPases [42]. MDA-MB-231 cell fluorescence was reduced to 80% of the control using EIPA and to 73% using Cyt D. With MDA-MB-231, EIPA reduction was significant ($N = 3$, $p < 0.05$) but Cyt D was slightly out of the significance range ($N = 3$, $p = 0.07$), likely due to higher variation. Both inhibitors significantly reduced the fluorescence in MDA-MB-453 cells, with EIPA decreasing it to 83% and with Cyt D to 73% ($N = 3$, p's < 0.05).

4. DISCUSSION

The flexible shape and enhanced tumor retention, along with biocompatibility, makes DNA origami an interesting drug carrier [20]. Although DNA nanostructures have

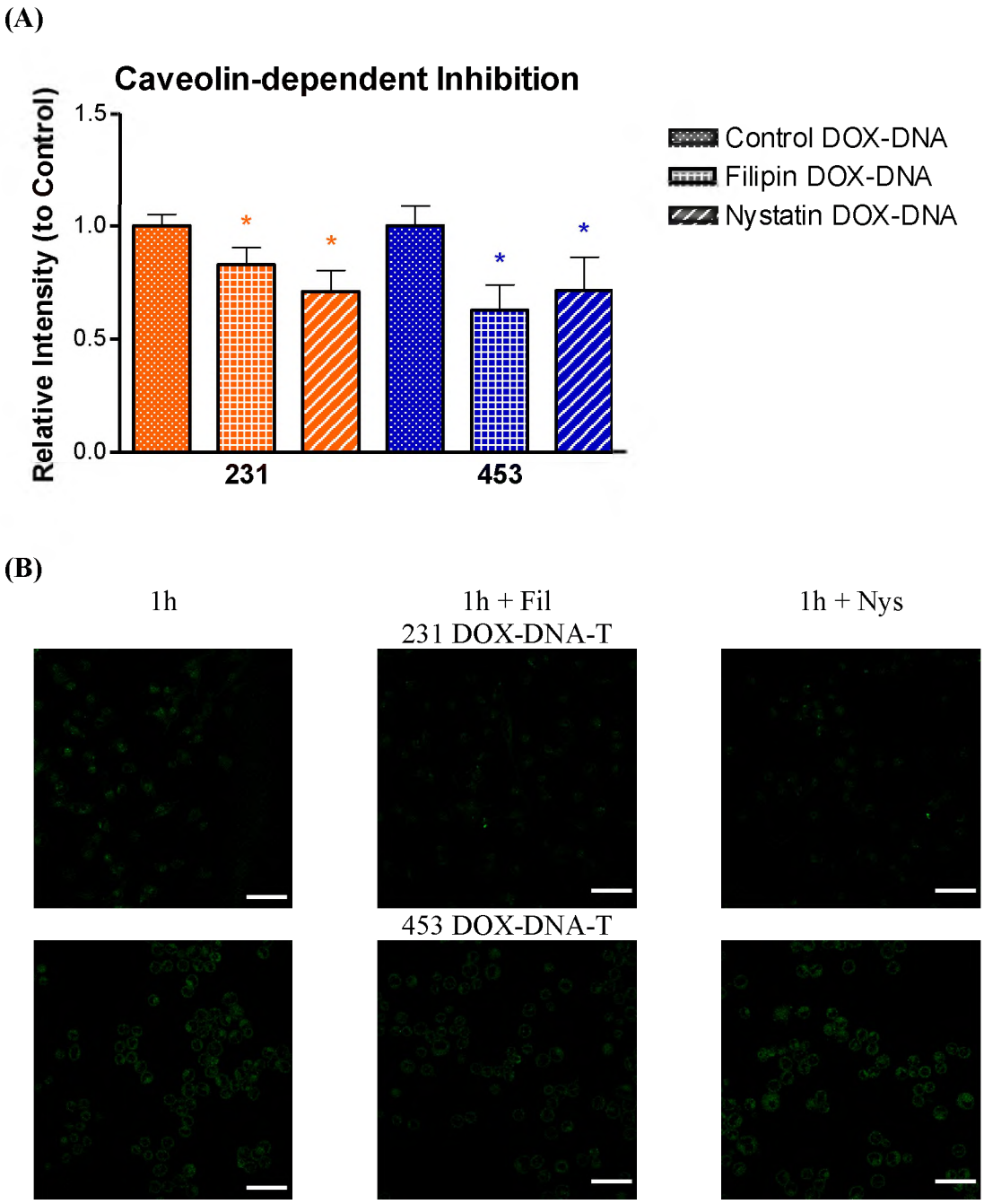

Figure 12. Caveolin-dependent uptake inhibition of 2 μM DOX-DNA-T after 1h. Uninhibited control fluorescence of DOX-DNA-T after 1h incubation was used to normalize the data set and inhibited samples were compared to the control using one-tailed t-tests, p's < 0.05. N = 3. Scale bar is 50 μm, 40x oil objective.

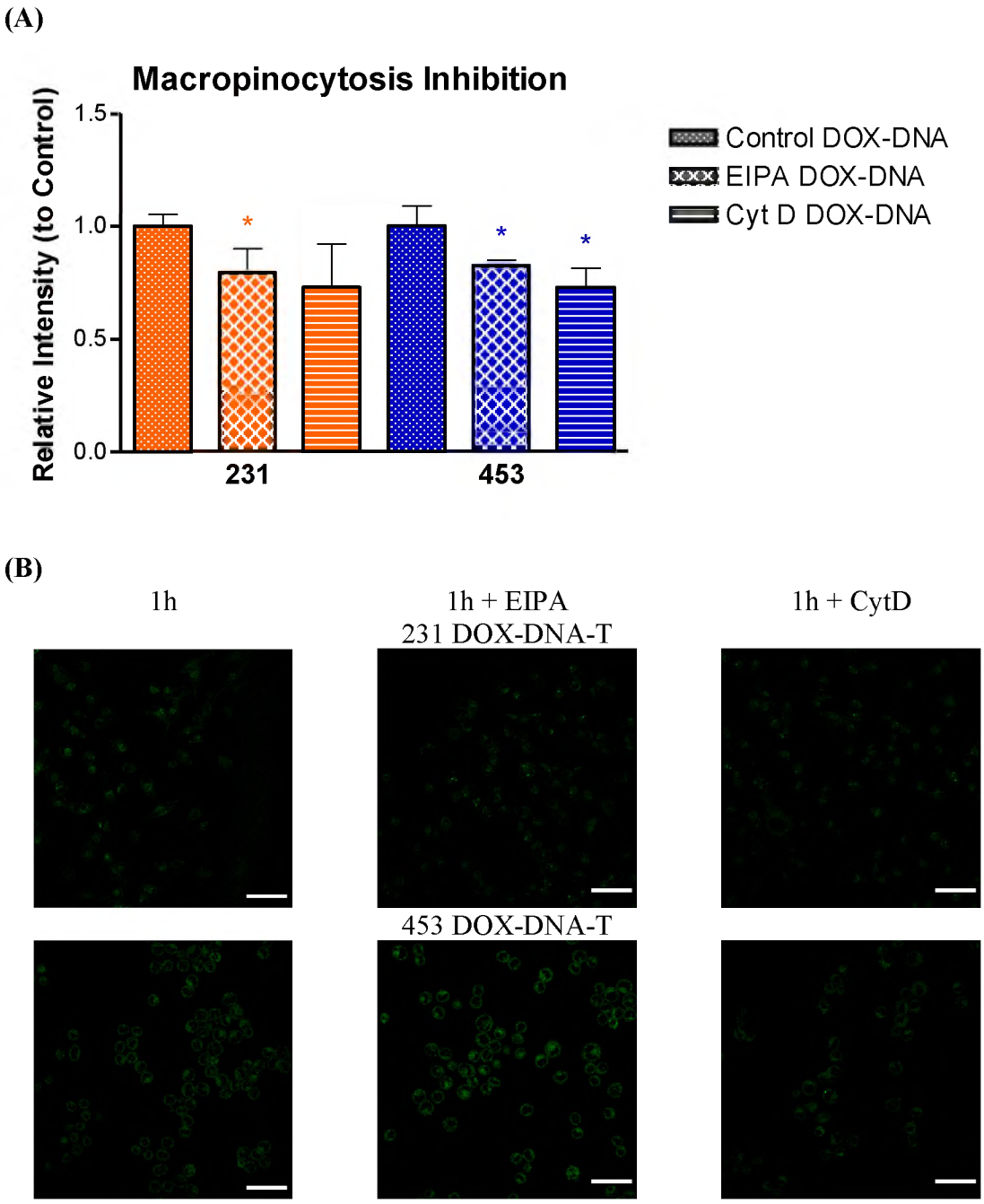

Figure 13. Macropinocytosis inhibition of 2 μM of DOX-DNA-T after 1h. Uninhibited control fluorescence of DOX-DNA-T after 1h incubation was used to normalize the data set and inhibited samples were compared to the control using one-tailed t-tests, p's < 0.05. N = 3. Scale bar is 50 μm, 40x oil objective.

the potential to overcome resistance and reduce systematic toxicity [13, 14], their exact cellular uptake mechanism was not well understood. Uptake mechanism and subcellular localization influence drug delivery efficacy and need to be considered when designing drug carriers. The stability of DNA nanostructures in physiological environments has been a concern in vivo due to endogenous nucleases [43]. Despite concerns, DNA nanostructures maintain their integrity in cell medium for up to 12 hours at the concentration of FCS tested, enough time for adequate circulation and cellular uptake [44, 45].

The anticancer efficacy of drug-loaded DNA origami has been shown to be shape-dependent in vivo [18]. In our study, the decrease in viability after exposure to DOX and DOX-DNA-T was significant and differed between time-points and concentrations. DOX alone was more toxic overall. DOX-DNA-T seemed to have a delayed toxicity in the cell lines, based on both viability and apoptosis analyses. This may have been due to the origami slowly releasing the DOX. Since DNA nanostructures sequester loaded anthracyclines and have a delayed killing effect, systemic exposure and off-targeting can be reduced as the origami have time to passively accumulate in tumors. Interestingly, DOX-DNA-T seemed to modulate the differences in DOX toxicity between the two cell lines, with both cell lines having a very similar decrease in viability. Extending the time points analyzed would likely reveal higher efficiency in DOX-DNA-T killing as cell death seemed delayed. There was a sharp decrease in viability at higher concentrations of DOX-DNA-T after 48 hours and this trend is likely to continue. Zeng et al. were able to show similar killing efficiencies in MDA-MB-231 cells between DOX and several DOX-loaded DNA origami shapes after 96 hours [15].

Induction of apoptosis at most concentrations and time points was consistent with the decreases observed in viability. DOX-DNA-T treatment resulted in less apoptosis based on flow cytometry and microscopy analysis. However, at higher concentrations and longer times, where DOX and DOX-DNA-T viability reduction was similar, the two treatments did not result in similar amounts of apoptosis. This indicates that DOX-DNA-T may be killing cells by a different mechanism, or that cells exposed to DOX-DNA-T apoptosis faster at these concentrations and were dead before the analysis occurred, resulting in lower total apoptosis recorded. It is also possible that DOX-DNA-T induced more necrosis rather than just apoptosis. Cultures had more debris after treatment with DOX-DNA-T compared to DOX alone. When cells undergo necrosis, they rapidly lose membrane integrity and cellular contents are released into the surroundings [46], which may be the cause of the debris and potential faster cell death observed. However, further experimentation is required to differentiate between death mechanisms.

Although DNA-T sequesters DOX initially, the drug slowly dissociates from the complexes. Zeng et al. showed that there was not a significant difference in DOX release from origami between 6.6 and 7.4 pH [15]. DOX release was around twice as high at 4.5 pH, the pH of lysosomes. The differences in drug release at different pH likely play a role in drug dynamics within cells, especially if the carrier interacts with lysosomes. However, the differences observed in toxicity were likely not due to differences in media pH, as all cell culture media pH was close to neutral, even after 48 hours of cell growth.

As DOX is a small molecule, it was expected that the drug would not be localized in certain areas within cells, but diffuse evenly throughout the cytoplasm. Dispersed DOX would also have a higher chance to attack the nucleus than if it were trapped in

specific areas of the cells, which would explain the higher killing. After 1-hour incubation DOX appeared to be diffused throughout the cells. However, it was found that free DOX localized into lysosomes after 24 and 48 hours. Along with time-dependent localization, DOX localization appeared to be concentration dependent. DOX was more evenly distributed in the cells at the 10 μM concentration used for apoptosis analysis compared to the 2 μM used for subcellular localization. Cells may be able to pack DOX into lysosomes to sequester the drug, if the concentration is low enough or the exposure time is shorter. This mechanism seems likely, as DOX enters into cells by diffusion and would not be localized within the lysosomes after endocytosis and endosome evolution into lysosomes. DOX being diffused in cells after 1 hour and appearing to become localized into the lysosomes overtime supports this. This is also in agreement with previous work which has shown DOX can be trapped inside synthetic liposomes that have a low internal pH (4.6) compared to the environment (7.5) [47]. It has been speculated that DOX may become trapped inside membranes with low internal pH due to DOX protonation and gaining charge [47]. Gaining charge would prevent DOX from diffusing, as charged molecules are unable to pass through lipid membranes [48].

Without a sequestering mechanism, DOX would likely just diffuse out of the lysosomes if pushed inside. MDA-MB-453 cells had noticeably smaller lysosomes, and were also more susceptible to DOX at concentrations in the middle of the tested range. At high concentrations or long periods of exposure, it may be the case that cells do not have sufficient lysosomal capacity or free lysosomal protons to sequester DOX. MDA-MB-453 cells may reach their sequestering limit before MDA-MB-231 and thus die at lower concentrations of the drug. It is unknown what the threshold concentration of DOX might

be for this mechanism in live cellular systems. A previous study has shown nuclear localization after 72 hours using the same concentration of DOX (2 μM) [15]. It is possible more DOX was able to enter cells after 72-hour incubation and avoided being sequestered. However, epifluorescent imaging or fixing cells may have produced artifacts, resulting in the appearance of nuclear localization. Epifluorescence microscopes capture light from the entire cell, so fluorescence inside the cytoplasm above the nucleus can appear as nuclear localization. Fixation can also result in artificial entry of compounds into cells [49]. Confocal microscopy utilizes lasers to take images of singular planes within cells, allowing clearer images to be captured.

The localization of DOX was altered by loading it into DNA-T. DOX-DNA-T was expected to be localized within cell lysosomes, the opposite of the expected outcome for DOX alone. However, relatively few lysosomes showed localization with DOX-DNA-T compared to DOX alone. DOX-DNA-T was instead more evenly spread throughout the cells at both time points and concentrations imaged. This may have been due to the higher concentration of internalized DOX facilitated by DNA-T. As endosomes evolve into lysosomes, they fuse with vesicles from the Golgi apparatus and become acidified [50]. During acidification and when lysosomes maintain their low pH by pumping in protons, if acidification is prevented by molecules acting as "proton sponges," lysosomes will keep transporting protons into themselves [51]. However, the lysosome will also begin to transport chloride ions inside in order to maintain their charge, which will cause water to influx to the higher concentration, leading to lysosomal swelling and bursting due to osmotic pressure [51]. High concentrations of DOX or DNA origami may act as proton sponges, as DOX becomes protonated inside lysosomes and

DNA has a negatively charged backbone. It is likely that DOX-DNA-T is originally localized in endosomes after endocytosis. DOX and DOX-DNA-T may be released from the endosomes due to bursting. Bursting lysosomes release toxic substances and may attribute to the sharp decline in cell health when treated with DOX-DNA-T, as lysosomal swelling and lysis is associated with increased cytotoxicity [51, 52]. This might explain why MDA-MB-453 seemed to have lower lysosomal localization of DOX-DNA-T, if they have smaller lysosomal capacity and their lysosomes with internalized DOX-DNA-T lyse quickly. This process may result in higher cellular DNA damage and cause the cells to die faster or necrose, preventing the total apoptotic population from being detected. Generally, necrosis is less desirable in vivo than apoptosis because of the release of inflammatory substances and wastes from unorganized cell death [46]. Nonetheless, DNA-T allows DOX to avoid sequestering by lysosomes initially. After 48 hours, DOX-DNA-T lysosomal localization appeared to increase in the cells but this fluorescence may have been DOX dissociated from the DNA-T.

Localization and apoptosis imaging studies revealed higher fluorescence of internalized DOX when loaded into DNA-T. Uptake of DOX and DOX-DNA-T was analyzed at 2 μM to reveal the differences between internalization quantity and route. Although the viability of the two cell lines differed after 24- and 48-hour DOX exposure, their DOX internalization appeared to be reaching a threshold. This may have been due to DOX diffusion eliminating the concentration gradient between the internal and external environment of the cells, allowing only so much DOX to be internalized. Binding of DOX to internal cell structures or entrapment in lysosomes would decrease the concentration of free DOX inside cells and reestablish a small concentration gradient

overtime, leading to the slight upward trend observed over long exposure periods [29]. While uptake between 0 and 4 hours was similar between the free and carried drug, DOX-DNA-T showed higher uptake at 24 and 48 hours, indicating DNA-T facilitated drug entry. Since internalized DOX was already bound in DNA-T, this may have also encouraged DOX diffusion from external DNA-T that released DOX into the culture media. Enhanced accumulation may aid in killing cancers that have developed resistance to the drug as exposure time and dose is increased [14]. MDA-MB-453 showed lower uptake of DOX-DNA-T after 24 and 48 hours compared to MDA-MB-231, even though their viability was similar after DOX-DNA-T exposure. This may have been due to MDA-MB-453 having a lower ability to localize DOX-DNA-T in lysosomes or other factors such as differences in metabolic function between the cell lines, different uptake mechanisms being damaged after longer exposure to DOX, or different methods of DOX-DNA-T expulsion.

DOX internalization by diffusion was confirmed as fluorescence was not significantly different from metabolic-inhibited internalization. Cells treated with metabolic inhibitors actually showed slightly higher DOX uptake on average. This is consistent with a proposed mechanism which states that DOX enters by diffusion and is actively pumped out of cells [28, 30]. Energy-dependent pumps would not function in the presence of metabolic inhibitors and cause DOX concentration to be increased inside cells.

DOX-DNA-T internalization appeared to be by a different mechanism than free DOX. Inhibition of all pathways studied resulted in decreased fluorescence of internalized DOX when it was carried by DNA-T. Unlike free DOX, incubation with

metabolic inhibitors reduced internalized DOX-DNA-T significantly, indicating a dependence on energy. The highest decrease in fluorescence was observed using clathrin and caveolin/lipid-raft inhibitors, indicating that DOX-DNA-T uptake is reliant on various endocytosis mechanisms. Negatively charged DNA nanostructures likely interact with positively charged membrane molecules on the cell surface and induce endocytosis. It must also be considered that many pharmacological inhibitors effect multiple pathways [31]. For instance, MDC interacts with transglutaminases, which are important for actin assembly [31, 37]. Sucrose is not very specific and can block the formation of membrane invaginations not coated with clathrin [31]. EIPA may alter endocytosis involving clathrin and it has been suggested that Cyt D may block most forms of endocytosis [31, 53]. Thus, using complementary inhibitors provides strong support for the use of various specific pathways. To confirm that DNA origami does not prefer specific pathways, siRNA inhibition of essential proteins utilized in each pathway would be necessary. It is also a possibility that DNA-T could be labeled separately from DOX to further analyze the uptake, but sources have indicated that conjugated dyes may become dissociated from DNA after internalization [54]. Uptake inhibition of DOX-DNA-T may not have been as efficient as possible due to DOX being released from DNA origami in solution and entering cells by diffusion.

Along with siRNA testing, further studies with various nanostructure shapes and sizes will enable us to identify if DNA origami is preferentially taken up by a pathway dependent on specific proteins and the optimal geometry to achieve the highest transport efficiency and cellular uptake. It would be most ideal to deploy a quantitative structure activity relationship (QSAR) analysis to test different shapes and sizes of DNA origami

for finding a relationship between structure and function. The most effective nanostructure derived from such an analysis can be used in a targeted delivery system. One such target could be the urokinase-type plasminogen activator receptor (uPAR), which is upregulated in some TNBCs [55]. The TNBC cell lines MDA-MB-231 (high uPAR expression) and MDA-MB-453 (low uPAR) were tested to further this goal in future studies. The functionalization capacity of DNA origami holds many potentials. However, despite the unknowns that still need to be elucidated, DNA origami research may lag due to concerns about its stability.

5. CONCLUSIONS

DNA-T is able to facilitate DOX internalization by an energy-dependent endocytosis mechanism. The carrier is able to circumvent differences in DOX toxicity between cell lines and DOX sequestering in lysosomes. The toxicity of DOX was delayed when loaded into DNA-T, likely due to slow release from the nanostructures. The mechanism of cell death may differ when using DNA-T as a carrier for DOX. The higher concentration of DOX internalized with DNA-T indicates therapeutic concentrations can be lowered with similar effects, as long as exposure time is sufficient.

Cancer is a devastating disease and many chemotherapies leave patients debilitated, especially in cases like TNBC where harsh treatment is the only option. Drug delivery to tumor sites can decrease the harm chemotherapies inflict on healthy tissue and decrease overall patient morbidity. More treatment options give patients and doctors alternatives which may be better suited to individual care. The mechanism of DNA

nanostructure uptake is now better understood, allowing these factors to be considered when delivering drugs and developing DNA origami as a drug carrier system.

REFERENCES

[1] Bray F, Ferlay J, Soerjomataram I, et al. Global cancer statistics 2018: GLOBOCAN estimates of incidence and mortality worldwide for 36 cancers in 185 countries. CA Cancer J Clin 2018; 68(6): 394-424.

[2] Hwang SY, Park S, Kwon Y. Recent therapeutic trends and promising targets in triple negative breast cancer. Pharmacol Ther 2019.

[3] Jhan JR, Andrechek ER. Triple-negative breast cancer and the potential for targeted therapy. Pharmacogenomics 2017; 18(17): 1595-609.

[4] Mehlen P, Puisieux A. Metastasis: a question of life or death. Nat Rev Cancer 2006; 6(6): 449-58.

[5] Foulkes WD, Smith IE, Reis-Filho JS. Triple-negative breast cancer. N Engl J Med 2010; 363(20): 1938-48.

[6] Waks AG, Winer EP. Breast Cancer Treatment: A Review. JAMA 2019; 321(3): 288-300.

[7] Yagata H, Kajiura Y, Yamauchi H. Current strategy for triple-negative breast cancer: appropriate combination of surgery, radiation, and chemotherapy. Breast Cancer 2011; 18(3): 165-73.

[8] Bonadonna G, Monfardini S, De Lena M, Fossati-Bellani F. Clinical evaluation of adriamycin, a new antitumour antibiotic. Br Med J 1969; 3(5669): 503-6.

[9] Abraham R, Basser RL, Green MD. A risk-benefit assessment of anthracycline antibiotics in antineoplastic therapy. Drug Saf 1996; 15(6): 406-29.

[10] Mross K. New anthracycline derivatives: what for? European Journal of Cancer and Clinical Oncology 1991; 27(12): 1542-4.

[11] Hortobagyi GN. Anthracyclines in the treatment of cancer. An overview. Drugs 1997; 54 Suppl 4: 1-7.

[12] Greish K. Enhanced permeability and retention (EPR) effect for anticancer nanomedicine drug targeting. Methods Mol Biol 2010; 624: 25-37.

[13] Wu D, Wang L, Li W, Xu X, Jiang W. DNA nanostructure-based drug delivery nanosystems in cancer therapy. Int J Pharm 2017; 533(1): 169-78.

[14] Halley PD, Lucas CR, McWilliams EM, et al. Daunorubicin-Loaded DNA Origami Nanostructures Circumvent Drug-Resistance Mechanisms in a Leukemia Model. Small 2016; 12(3): 308-20.

[15] Zeng Y, Liu J, Yang S, et al. Time-lapse live cell imaging to monitor doxorubicin release from DNA origami nanostructures. J Mater Chem B 2018; 6(11): 1605-12.

[16] Ke Y, Bellot G, Voigt NV, Fradkov E, Shih WM. Two design strategies for enhancement of multilayer-DNA-origami folding: underwinding for specific intercalator rescue and staple-break positioning. Chem Sci 2012; 3(8): 2587-97.

[17] Zhao YX, Shaw A, Zeng X, et al. DNA origami delivery system for cancer therapy with tunable release properties. ACS Nano 2012; 6(10): 8684-91.

[18] Zhang Q, Jiang Q, Li N, et al. DNA origami as an in vivo drug delivery vehicle for cancer therapy. ACS Nano 2014; 8(7): 6633-43.

[19] Caldorera-Moore M, Guimard N, Shi L, Roy K. Designer nanoparticles: incorporating size, shape and triggered release into nanoscale drug carriers. Expert Opin Drug Deliv 2010; 7(4): 479-95.

[20] Kim KR, Kang SJ, Lee AY, et al. Highly tumor-specific DNA nanostructures discovered by in vivo screening of a nucleic acid cage library and their applications in tumor-targeted drug delivery. Biomaterials 2019; 195: 1-12.

[21] Agudelo D, Bourassa P, Berube G, Tajmir-Riahi HA. Intercalation of antitumor drug doxorubicin and its analogue by DNA duplex: structural features and biological implications. Int J Biol Macromol 2014; 66: 144-50.

[22] Vichai V, Kirtikara K. Sulforhodamine B colorimetric assay for cytotoxicity screening. Nat Protoc 2006; 1(3): 1112-6.

[23] Vermes I, Haanen C, Steffens-Nakken H, Reutelingsperger C. A novel assay for apoptosis. Flow cytometric detection of phosphatidylserine expression on early apoptotic cells using fluorescein labelled Annexin V. J Immunol Methods 1995; 184(1): 39-51.

[24] Kauffman MK, Kauffman ME, Zhu H, Jia Z, Li YR. Fluorescence-Based Assays for Measuring Doxorubicin in Biological Systems. React Oxyg Species (Apex) 2016; 2(6): 432-9.

[25] Xu Y, Liu BR, Lee HJ, et al. Nona-arginine facilitates delivery of quantum dots into cells via multiple pathways. J Biomed Biotechnol 2010; 2010: 948543.

[26] Foroozandeh P, Aziz AA. Insight into Cellular Uptake and Intracellular Trafficking of Nanoparticles. Nanoscale Res Lett 2018; 13(1): 339.

[27] Speelmans G, Staffhorst RW, de Kruijff B, de Wolf FA. Transport studies of doxorubicin in model membranes indicate a difference in passive diffusion across and binding at the outer and inner leaflets of the plasma membrane. Biochemistry 1994; 33(46): 13761-8.

[28] Siegfried JM, Burke TG, Tritton TR. Cellular transport of anthracyclines by passive diffusion. Implications for drug resistance. Biochem Pharmacol 1985; 34(5): 593-8.

[29] Dalmark M, Storm HH. A Fickian diffusion transport process with features of transport catalysis. Doxorubicin transport in human red blood cells. J Gen Physiol 1981; 78(4): 349-64.

[30] Dalmark M. The Physicochemical Properties and Transmembraneous Transport of Doxorubicin. In: Muggia FM, Young CW, Carter SK, Eds. Anthracycline Antibiotics in Cancer Therapy. Developments in Oncology. Springer: Dordrecht, NL 1982; pp. 165-72.

[31] Ivanov AI. Pharmacological inhibition of endocytic pathways: is it specific enough to be useful? Methods Mol Biol 2008; 440: 15-33.

[32] Harvey J, Hardy SC, Ashford ML. Dual actions of the metabolic inhibitor, sodium azide on K(ATP) channel currents in the rat CRI-G1 insulinoma cell line. Br J Pharmacol 1999; 126(1): 51-60.

[33] Huang LS, Cobessi D, Tung EY, Berry EA. Binding of the respiratory chain inhibitor antimycin to the mitochondrial bc1 complex: a new crystal structure reveals an altered intramolecular hydrogen-bonding pattern. J Mol Biol 2005; 351(3): 573-97.

[34] Guminska M, Sterkowicz J. Effect of sodium fluoride on glycolysis in human erythrocytes and Ehrlich ascites tumour cells in vitro. Acta Biochim Pol 1976; 23(4): 285-91.

[35] Heuser JE, Anderson RG. Hypertonic media inhibit receptor-mediated endocytosis by blocking clathrin-coated pit formation. J Cell Biol 1989; 108(2): 389-400.

[36] Wang LH, Rothberg KG, Anderson RG. Mis-assembly of clathrin lattices on endosomes reveals a regulatory switch for coated pit formation. J Cell Biol 1993; 123(5): 1107-17.

[37] Huang YW, Lee HJ. Cell-penetrating peptides for medical theranostics and targeted gene delivery. In: Koutsopoulos S, Ed. Peptide applications in biomedicine, biotechnology and bioengineering. Woodhead Publishing: Oxford, UK 2018; pp. 359–70.

[38] Phonphok Y, Rosenthal KS. Stabilization of clathrin coated vesicles by amantadine, tromantadine and other hydrophobic amines. FEBS Lett 1991; 281(1-2): 188-90.

[39] Nabi IR, Le PU. Caveolae/raft-dependent endocytosis. J Cell Biol 2003; 161(4): 673-7.

[40] Cooper JA. Effects of cytochalasin and phalloidin on actin. J Cell Biol 1987; 105(4): 1473-8.

[41] Lim JP, Gleeson PA. Macropinocytosis: an endocytic pathway for internalising large gulps. Immunol Cell Biol 2011; 89(8): 836-43.

[42] Koivusalo M, Welch C, Hayashi H, et al. Amiloride inhibits macropinocytosis by lowering submembranous pH and preventing Rac1 and Cdc42 signaling. J Cell Biol 2010; 188(4): 547-63.

[43] Ramakrishnan S, Ijas H, Linko V, Keller A. Structural stability of DNA origami nanostructures under application-specific conditions. Comput Struct Biotechnol J 2018; 16: 342-9.

[44] Douglas SM, Bachelet I, Church GM. A logic-gated nanorobot for targeted transport of molecular payloads. Science 2012; 335(6070): 831-4.

[45] Mei Q, Wei X, Su F, et al. Stability of DNA Origami Nanoarrays in Cell Lysate. Nano Letters 2011; 11: 1477-82.

[46] Rock KL, Kono H. The inflammatory response to cell death. Annu Rev Pathol 2008; 3: 99-126.

[47] Mayer LD, Bally MB, Cullis PR. Uptake of adriamycin into large unilamellar vesicles in response to a pH gradient. Biochim Biophys Acta 1986; 857(1): 123-6.

[48] Lodish H, Berk A, Matsudaira P, et al. Transport of ions and small molecules across cell membranes. In: Molecular cell biology. 5th ed. W. H. Freeman and Company: New York, NY 2003; pp. 245-300.

[49] Huang YW, Lee HJ, Tolliver LM, Aronstam RS. Delivery of nucleic acids and nanomaterials by cell-penetrating peptides: opportunities and challenges. Biomed Res Int 2015; 2015: 834079.

[50] Cooper GM. Protein Sorting and Transport: The Endoplasmic Reticulum, Golgi Apparatus, and Lysosomes. In: The Cell: A Molecular Approach. 2nd ed. Sinauer Associates: Sunderland, MA 2000.

[51] Pei D, Buyanova M. Overcoming Endosomal Entrapment in Drug Delivery. Bioconjug Chem 2019; 30(2): 273-83.

[52] Lee DU, Park JY, Kwon S, et al. Apoptotic lysosomal proton sponge effect in tumor tissue by cationic gold nanorods. Nanoscale 2019; 11(42): 19980-93.

[53] Dutta D, Donaldson JG. Search for inhibitors of endocytosis: Intended specificity and unintended consequences. Cell Logist 2012; 2(4): 203-8.

[54] Lacroix A, Vengut-Climent E, de Rochambeau D, Sleiman HF. Uptake and Fate of Fluorescently Labeled DNA Nanostructures in Cellular Environments: A Cautionary Tale. ACS Cent Sci 2019; 5(5): 882-91.

[55] Sliutz G, Eder H, Koelbl H, et al. Quantification of uPA receptor expression in human breast cancer cell lines by cRT-PCR. Breast Cancer Res Treat 1996; 40(3): 257-63.

SECTION

2. CONCLUSIONS

DNA is a highly therapeutic molecule, with the potential to alter cell protein expression and carry drugs into cells. A large number of DNA delivery tools have been explored and it is apparent that delivery technologies will continue to develop in order to improve overall patient outcome. DNA nanostructures are a promising delivery method due to programmability and modification. They facilitate drug delivery into cells, showed a delayed toxicity that allows cells to uptake ample amounts of the complex, and require energy to be internalized most efficiently. Loading DOX into DNA origami can reduce systemic exposure by sequestering the drug. Facilitation of DOX entry using DNA origami may allow therapeutic doses to be lowered with adequate exposure time. However, the optimal size and shape of origami has yet to be determined. Further studies need to be conducted in order to discover the optimal geometry for drug delivery and to increase origami stability for use in vivo. Full understanding of the uptake mechanism will allow better design of DNA origami as a drug carrier system.

APPENDIX

PAPER II SUPPLEMENTARY FIGURES

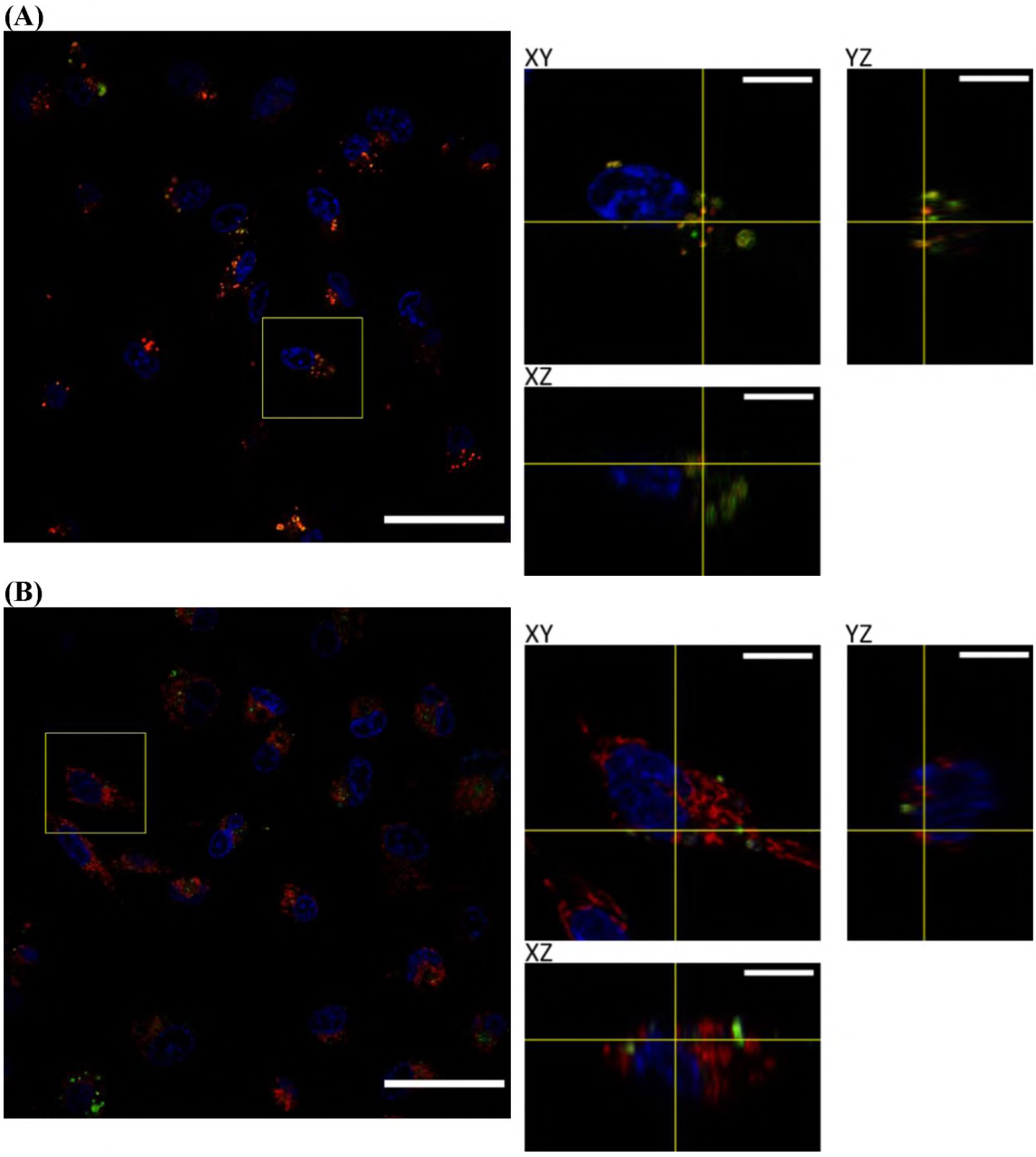

Supplementary Figure 1. 24h DOX localization in MDA-MB-231. Blue is Hoechst, green is DOX, and red is (A) LysoTracker or (B) MitoTracker. Scale bar is 50 µm in images of field. XY, YZ, and XZ images are the area in the yellow box, 5x, Scale bar is 10 µm.

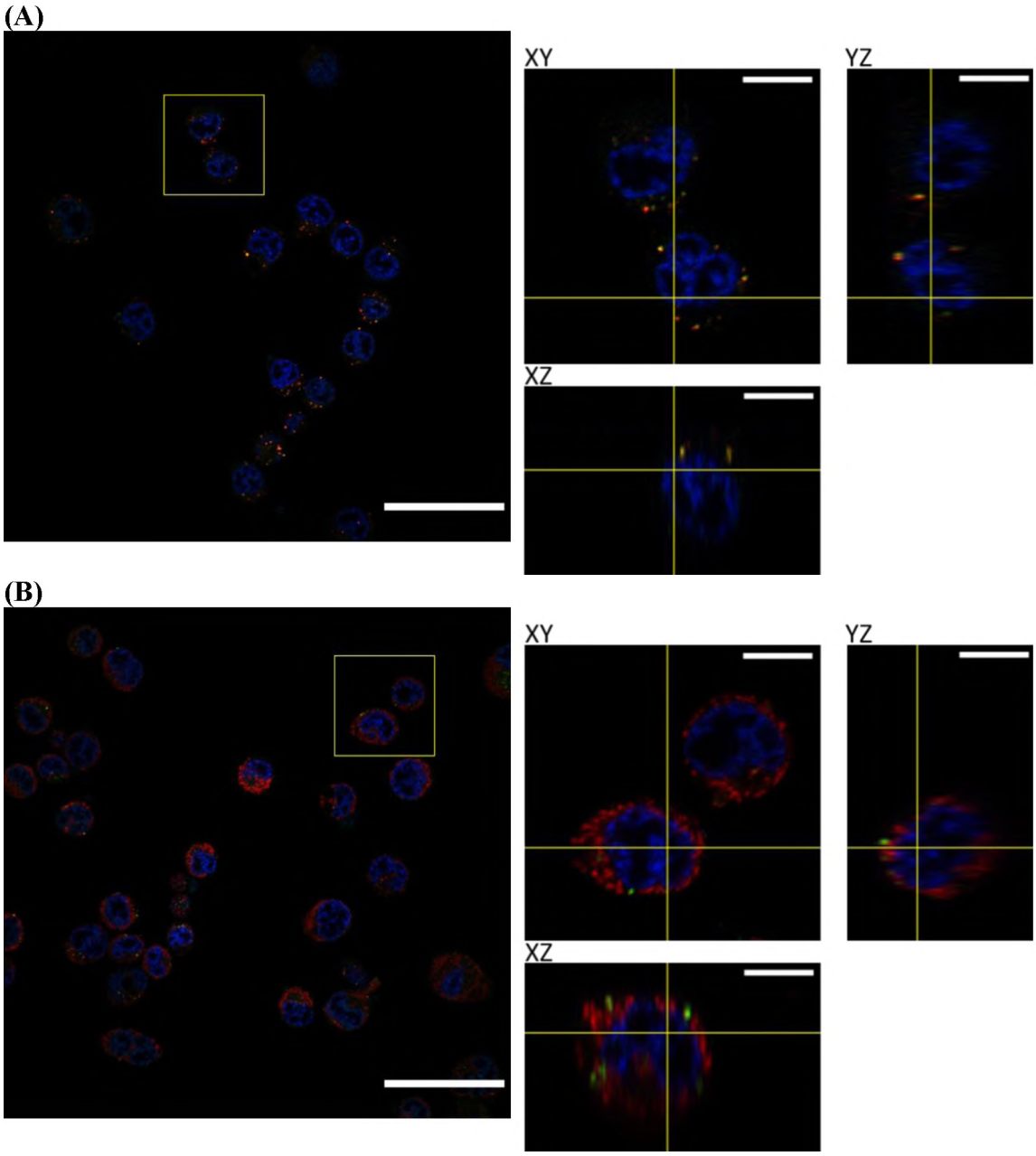

Supplementary Figure 2. 24h DOX localization in MDA-MB-453. Blue is Hoechst, green is DOX, and red is (A) LysoTracker or (B) MitoTracker. Scale bar is 50 μm in images of field. XY, YZ, and XZ images are the area in the yellow box, 5x, Scale bar is 10 μm.

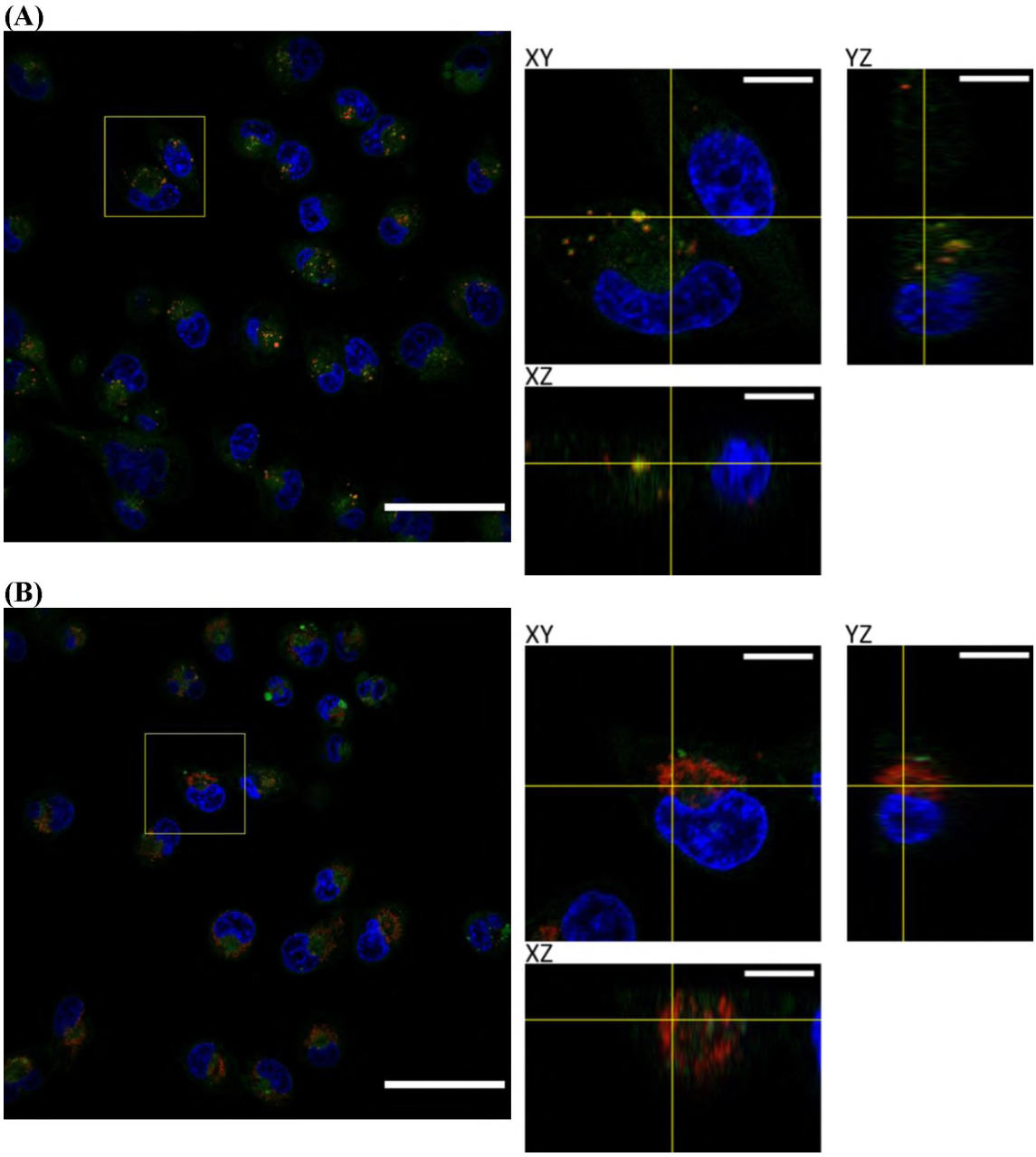

Supplementary Figure 3. 24h DOX-DNA-T localization in MDA-MB-231. Blue is Hoechst, green is DOX, and red is (A) LysoTracker or (B) MitoTracker. Scale bar is 50 μm in images of field. XY, YZ, and XZ images are the area in the yellow box, 5x, Scale bar is 10 μm.

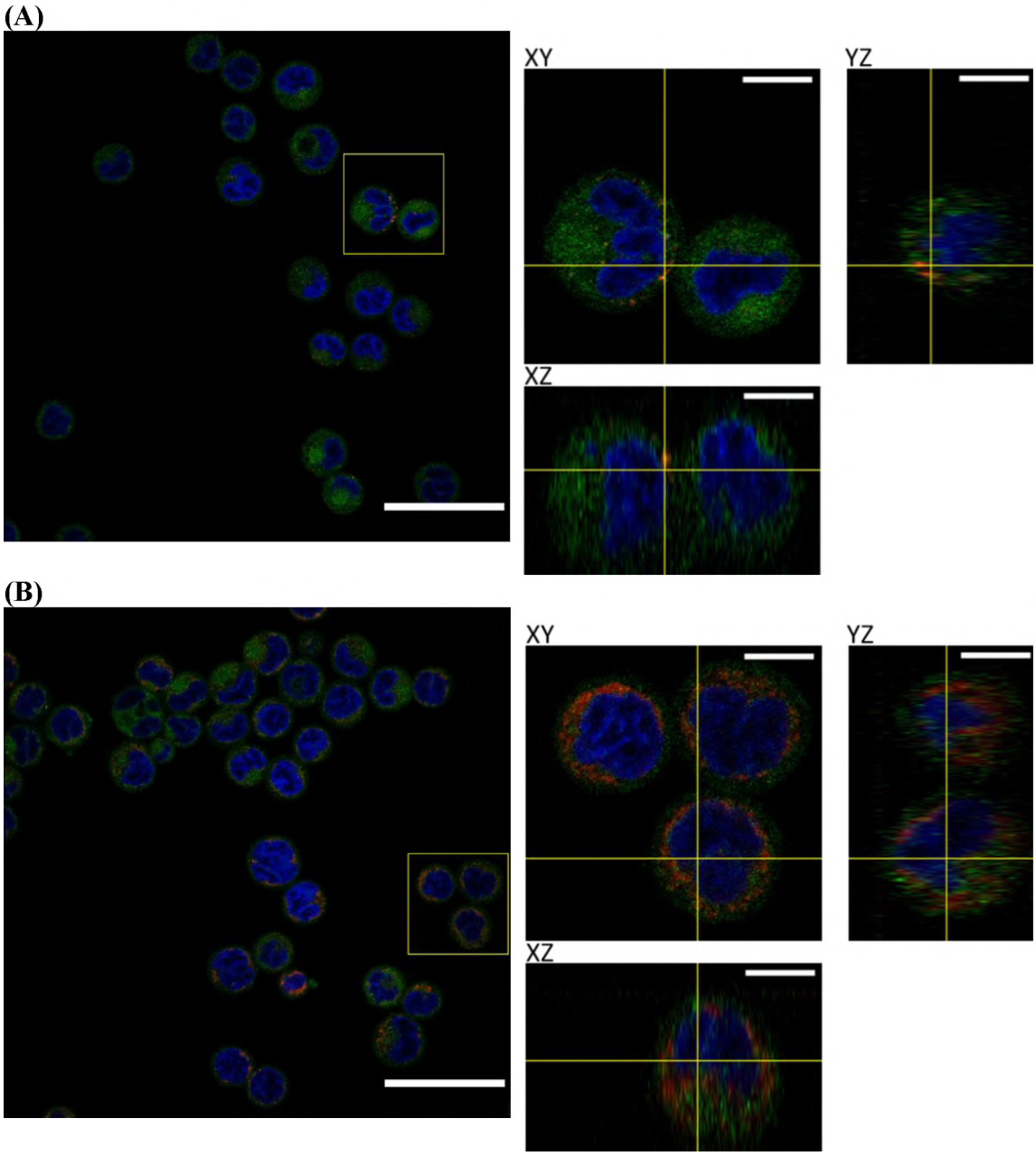

Supplementary Figure 4. 24h DOX-DNA-T localization in MDA-MB-453. Blue is Hoechst, green is DOX, and red is (A) LysoTracker or (B) MitoTracker. Scale bar is 50 μm in images of field. XY, YZ, and XZ images are the area in the yellow box, 5x, Scale bar is 10 μm.

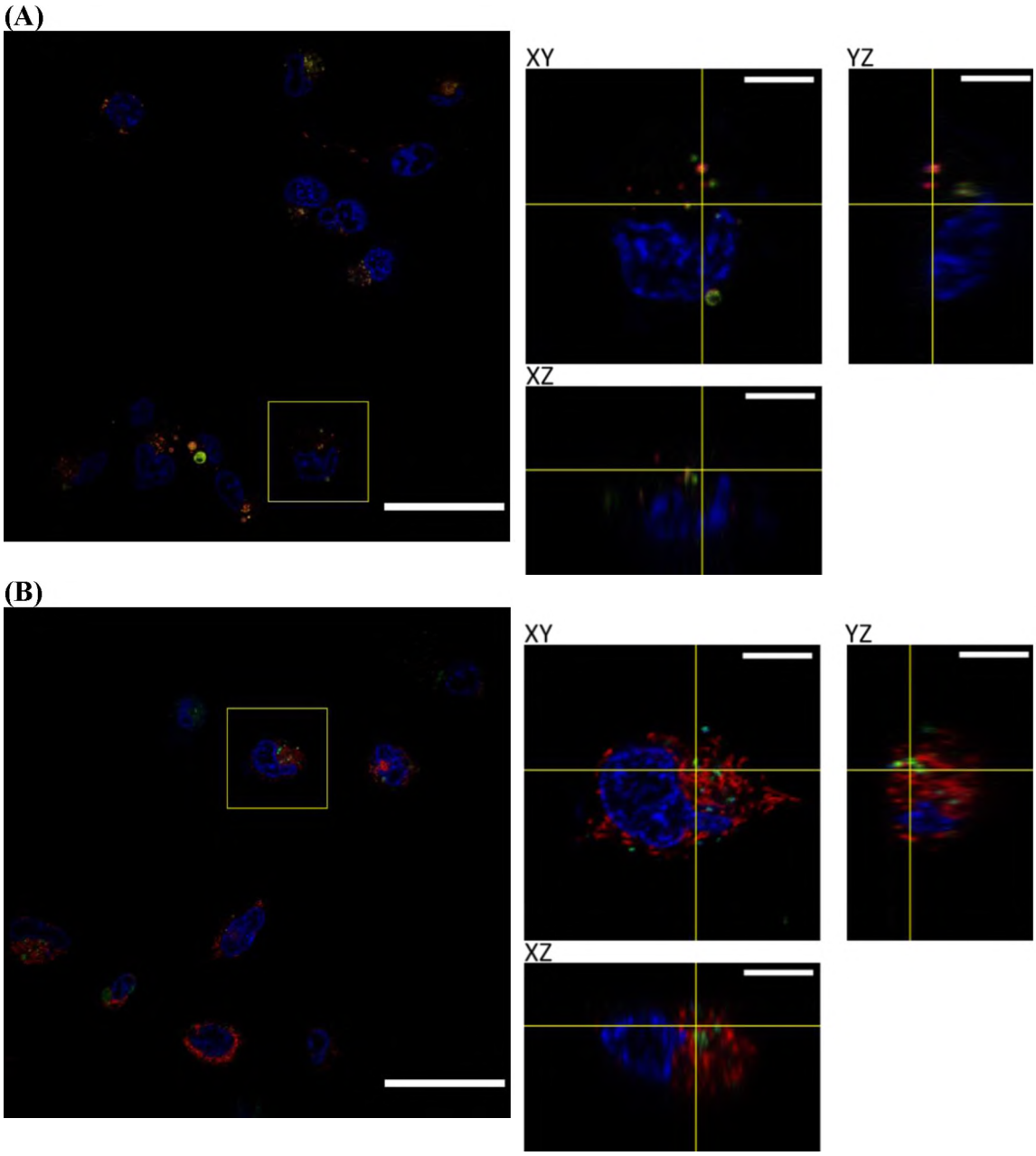

Supplementary Figure 5. 48h DOX localization in MDA-MB-231. Blue is Hoechst, green is DOX, and red is (A) LysoTracker or (B) MitoTracker. Scale bar is 50 μm in images of field. XY, YZ, and XZ images are the area in the yellow box, 5x, Scale bar is 10 μm.

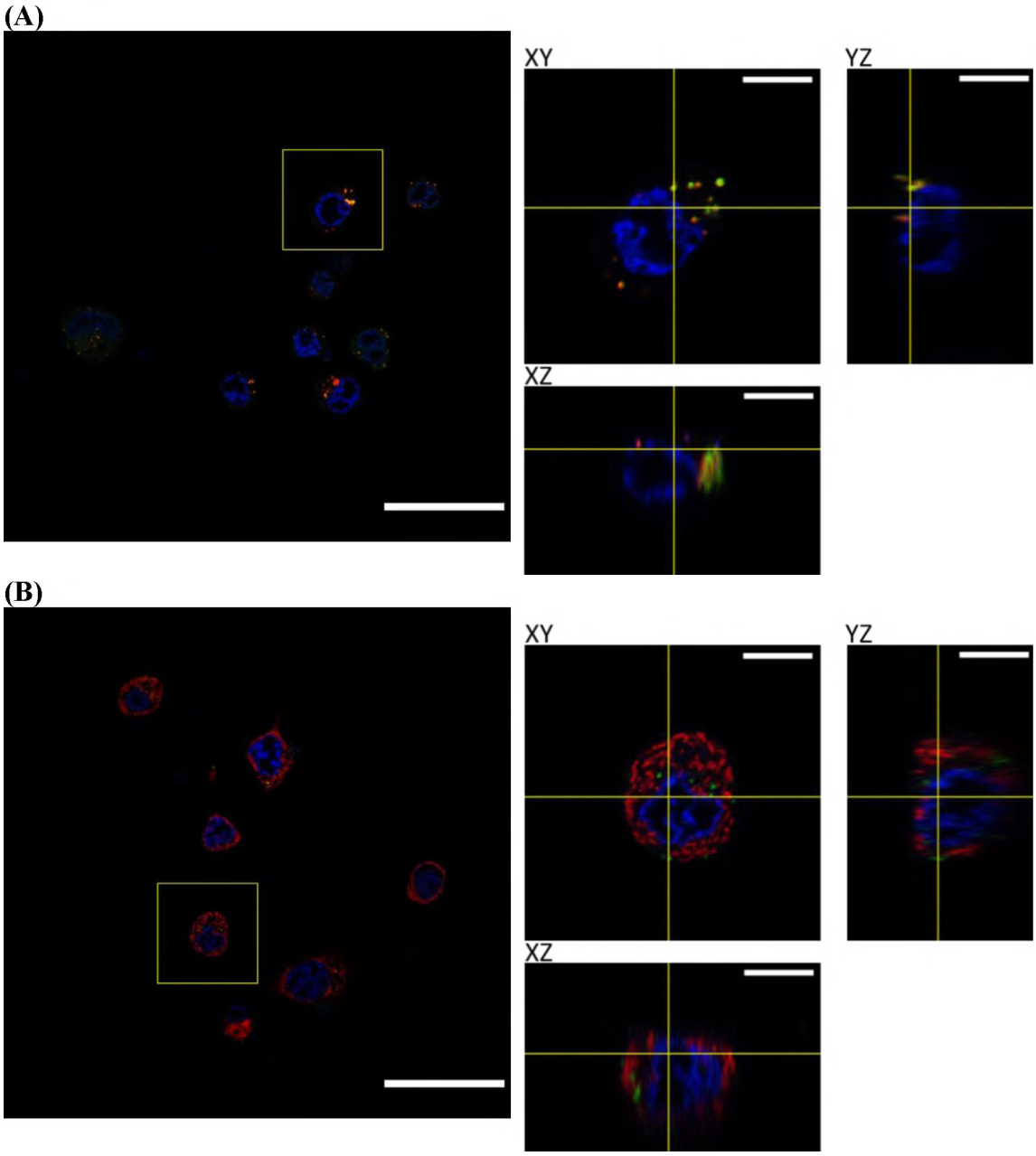

Supplementary Figure 6. 48h DOX localization in MDA-MB-453. Blue is Hoechst, green is DOX, and red is (A) LysoTracker or (B) MitoTracker. Scale bar is 50 μm in images of field. XY, YZ, and XZ images are the area in the yellow box, 5x, Scale bar is 10 μm.

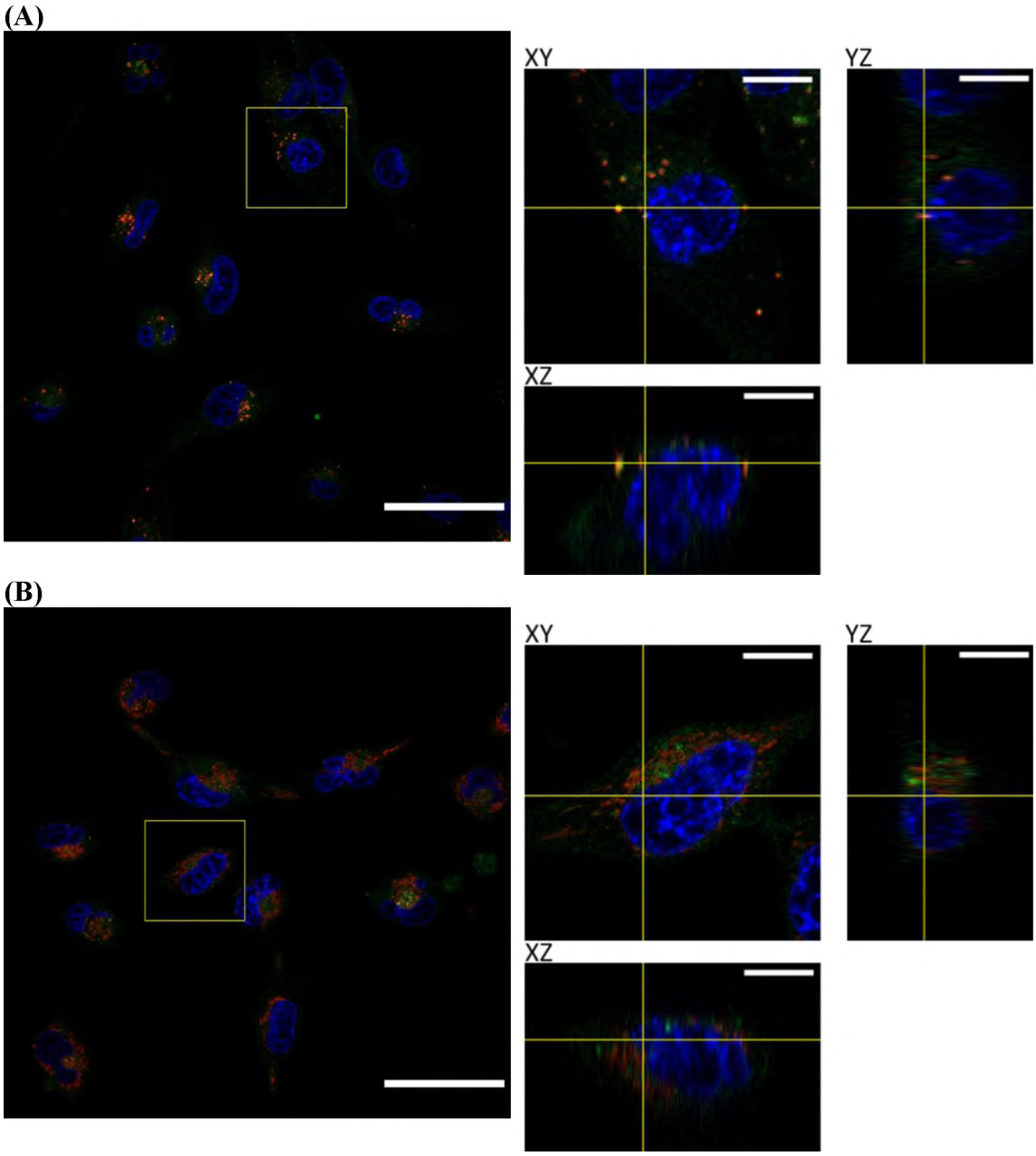

Supplementary Figure 7. 48h DOX-DNA-T localization in MDA-MB-231. Blue is Hoechst, green is DOX, and red is (A) LysoTracker or (B) MitoTracker. Scale bar is 50 μm in images of field. XY, YZ, and XZ images are the area in the yellow box, 5x, Scale bar is 10 μm.

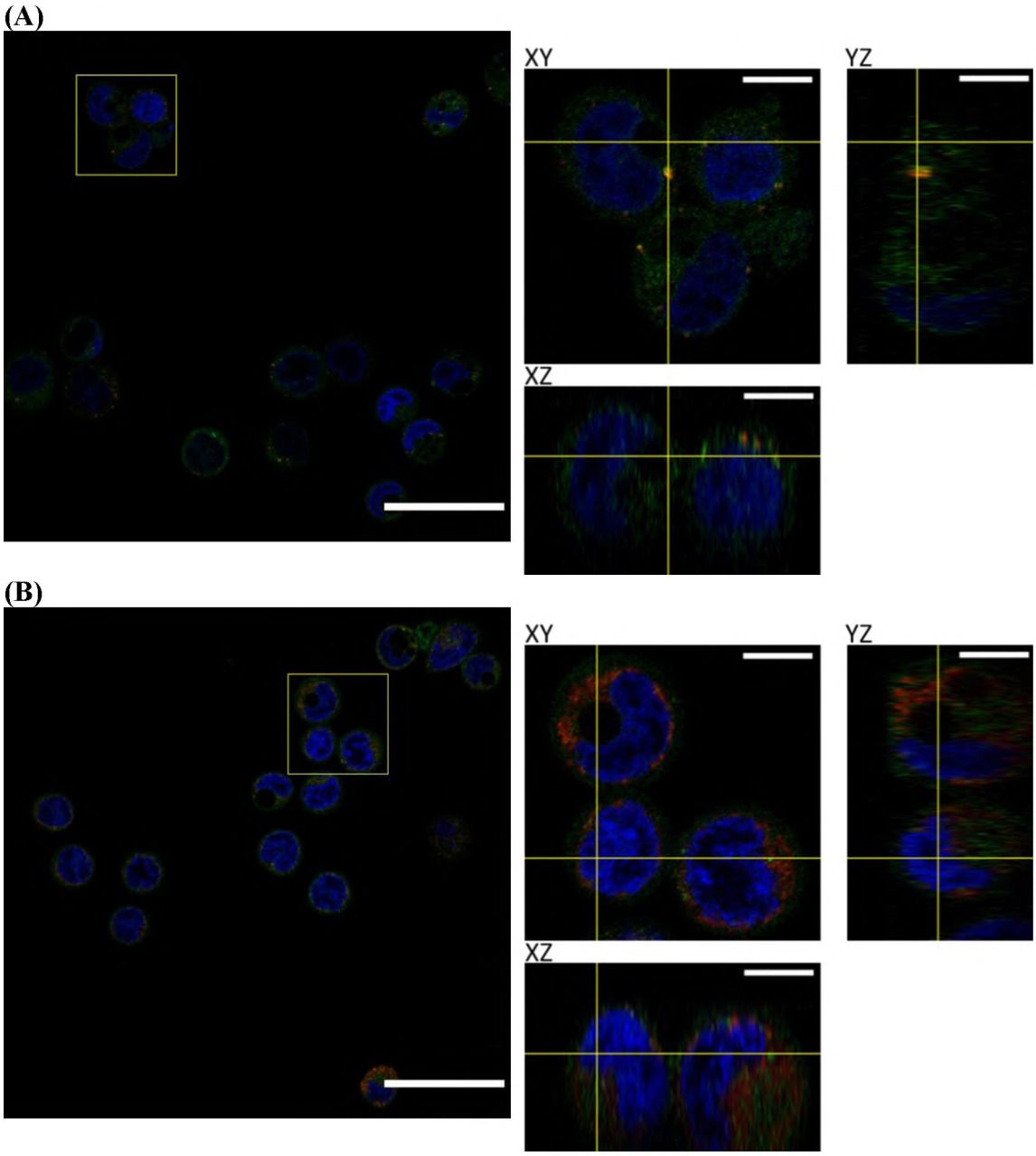

Supplementary Figure 8. 48h DOX-DNA-T localization in MDA-MB-453. Blue is Hoechst, green is DOX, and red is (A) LysoTracker or (B) MitoTracker. Scale bar is 50 μm in images of field. XY, YZ, and XZ images are the area in the yellow box, 5x, Scale bar is 10 μm.

BIBLIOGRAPHY

[1] Yin H, Kauffman KJ, Anderson DG. Delivery technologies for genome editing. Nat Rev Drug Discov 2017; 16(6): 387-99.

[2] Burney TJ, Davies JC. Gene therapy for the treatment of cystic fibrosis. Appl Clin Genet 2012; 5: 29-36.

[3] Hoban MD, Orkin SH, Bauer DE. Genetic treatment of a molecular disorder: gene therapy approaches to sickle cell disease. Blood 2016; 127(7): 839-48.

[4] Dickey AS, La Spada AR. Therapy development in Huntington disease: From current strategies to emerging opportunities. Am J Med Genet A 2018; 176(4): 842-61.

[5] Al-Dosari MS, Gao X. Nonviral gene delivery: principle, limitations, and recent progress. AAPS J 2009; 11(4): 671-81.

[6] Korzh V, Strahle U. Marshall Barber and the century of microinjection: from cloning of bacteria to cloning of everything. Differentiation 2002; 70(6): 221-6.

[7] Xia J, Martinez A, Daniell H, Ebert SN. Evaluation of biolistic gene transfer methods in vivo using non-invasive bioluminescent imaging techniques. BMC Biotechnol 2011; 11: 62.

[8] Tomizawa M, Shinozaki F, Motoyoshi Y, et al. Sonoporation: Gene transfer using ultrasound. World J Methodol 2013; 3(4): 39-44.

[9] Kim HJ, Greenleaf JF, Kinnick RR, Bronk JT, Bolander ME. Ultrasound-mediated transfection of mammalian cells. Hum Gene Ther 1996; 7(11): 1339-46.

[10] Luft C, Ketteler R. Electroporation Knows No Boundaries: The Use of Electrostimulation for siRNA Delivery in Cells and Tissues. J Biomol Screen 2015; 20(8): 932-42.

[11] Roy I, Mitra S, Maitra A, Mozumdar S. Calcium phosphate nanoparticles as novel non-viral vectors for targeted gene delivery. Int J Pharm 2003; 250(1): 25-33.

[12] Felgner PL, Gadek TR, Holm M, et al. Lipofection: a highly efficient, lipid-mediated DNA-transfection procedure. Proc Natl Acad Sci U S A 1987; 84(21): 7413-7.

[13] Heitz F, Morris MC, Divita G. Twenty years of cell-penetrating peptides: from molecular mechanisms to therapeutics. Br J Pharmacol 2009; 157(2): 195-206.

[14] Merten OW, Gaillet B. Viral vectors for gene therapy and gene modification approaches. Biochem Eng J 2016; 108: 98-115.

[15] Wu D, Wang L, Li W, Xu X, Jiang W. DNA nanostructure-based drug delivery nanosystems in cancer therapy. Int J Pharm 2017; 533(1): 169-78.

[16] Ramakrishnan S, Ijas H, Linko V, Keller A. Structural stability of DNA origami nanostructures under application-specific conditions. Comput Struct Biotechnol J 2018; 16: 342-9.

[17] Caldorera-Moore M, Guimard N, Shi L, Roy K. Designer nanoparticles: incorporating size, shape and triggered release into nanoscale drug carriers. Expert Opin Drug Deliv 2010; 7(4): 479-95.

[18] Zhang Q, Jiang Q, Li N, et al. DNA origami as an in vivo drug delivery vehicle for cancer therapy. ACS Nano 2014; 8(7): 6633-43.

[19] Bray F, Ferlay J, Soerjomataram I, et al. Global cancer statistics 2018: GLOBOCAN estimates of incidence and mortality worldwide for 36 cancers in 185 countries. CA Cancer J Clin 2018; 68(6): 394-424.

[20] Jhan JR, Andrechek ER. Triple-negative breast cancer and the potential for targeted therapy. Pharmacogenomics 2017; 18(17): 1595-609.

[21] Foulkes WD, Smith IE, Reis-Filho JS. Triple-negative breast cancer. N Engl J Med 2010; 363(20): 1938-48.

[22] Hwang SY, Park S, Kwon Y. Recent therapeutic trends and promising targets in triple negative breast cancer. Pharmacol Ther 2019.

[23] Waks AG, Winer EP. Breast Cancer Treatment: A Review. JAMA 2019; 321(3): 288-300.

[24] Yagata H, Kajiura Y, Yamauchi H. Current strategy for triple-negative breast cancer: appropriate combination of surgery, radiation, and chemotherapy. Breast Cancer 2011; 18(3): 165-73.

[25] Hortobagyi GN. Anthracyclines in the treatment of cancer. An overview. Drugs 1997; 54 Suppl 4: 1-7.

[26] Agudelo D, Bourassa P, Berube G, Tajmir-Riahi HA. Intercalation of antitumor drug doxorubicin and its analogue by DNA duplex: structural features and biological implications. Int J Biol Macromol 2014; 66: 144-50.

[27] Kim KR, Kang SJ, Lee AY, et al. Highly tumor-specific DNA nanostructures discovered by in vivo screening of a nucleic acid cage library and their applications in tumor-targeted drug delivery. Biomaterials 2019; 195: 1-12.

[28] Halley PD, Lucas CR, McWilliams EM, et al. Daunorubicin-Loaded DNA Origami Nanostructures Circumvent Drug-Resistance Mechanisms in a Leukemia Model. Small 2016; 12(3): 308-20.

[29] Zeng Y, Liu J, Yang S, et al. Time-lapse live cell imaging to monitor doxorubicin release from DNA origami nanostructures. J Mater Chem B 2018; 6(11): 1605-12.

VITA

Natalie Jordan Holl graduated from Lone Jack High School and received her Associate of Science degree from Northwest Missouri State University in May 2016. She received a Bachelor of Science in Biological Sciences from the Missouri University of Sicence and Technology in December 2018. During her final semester of her undergraduate degree, she was dual-enrolled as a graduate student and worked in Dr. Yue-Wern Huang's lab. The following spring, she began work as a full-time master's student. She received her master's degree in Applied and Environmental Biology from the Missouri University of Science and Technology in December 2020.